PULSED-SOURCE LUMINESCENCE MEASUREMENTS USING A COMPUTER CONTROLLED SPECTROMETER

By

ALUN TREFOR RHYS WILLIAMS, MSc. C.Chem. F.R.S.C.

A Doctoral Thesis submitted in fulfilment of the requirements for the award of the degree of Ph.D of the Loughborough University of Technology.

March 1984

Supervisors: Professor J.N. Miller — Department of Chemistry

Dr. M.A. Ford — Perkin-Elmer Limited, Post Office Lane, Beaconsfield, Bucks.

The work described in this thesis has not been submitted, in full or in part, to this or any other institution for an award.

ACKNOWLEDGEMENTS

I wish to thank my supervisors, Professor J.N. Miller and Dr. M.A. Ford, for many helpful discussions and advice during the period of research and in the preparation of this thesis.

I am grateful to Perkin-Elmer Limited for their support and provision of laboratory facilities, to the R&D Department, to Dr. M. Barnard and Dr. S.A.Winfield for their invaluable assistance and to Mrs. S.J. Crowe for deciphering my writing.

I thank M.Fuller at Thorn EMI Limited for providing advice and the donation of rare earth phosphors and P.E. Croft at Robertson Research International Limited for background information on the analysis of uranium.

CONTENTS

ABSTRACT

Traditionally fluorescence and phosphorescence measurements are made on fluorescence spectrometers using a DC source such as a 150 watt xenon lamp. Differentiation between the fast decaying fluorescence signal and the relatively long lived phosphorescence is temporally obtained using a mechanical phosphoroscope. By periodically interrupting the exciting light measurements are made at the instant of excitation (fluorescence) or during the periods of darkness (phosphorescence).

Recent advances in the design and construction of pulsed xenon lamps, together with the use of modern microprocessor controlled digital electronics, have led to the development of a pulsed xenon source luminescence spectrometer.

A conduction cooling device operating at 77°K enables the rapid and quantitative measurement of low temperature fluorescence and phosphorescence data.

Relative fluorescence and phosphorescence quantum yield measurements were made on a variety of organic compounds including aromatic hydrocarbons and amino acids. A desk top computer was used to control the spectrometer, to generate corrected emission spectra, to measure phosphorescence lifetimes and calculate relative quantum yields.

The errors associated with using a UV absorbance spectrometer to measure absorbance values were overcome by using the fluorescence spectrometer for both excitation and absorbance measurements.

The ability to discriminate between phosphors on a time basis was used in the investigation of Tb^{3+} bound to transferrin and for the spectral resolution of the various transitions from Eu^{3+} in yttrium oxide.

The combination of a solvent extraction procedure and the time delayed measurement of uranyl ion emission was found to give a sensitive and quantitative analysis of uranyl ion in aqueous samples.

CHAPTER ONE

INTRODUCTION

1.1 General

The basic components of instruments designed to measure luminescence, i.e. fluorescence and phosphorescence, are well documented in the literature for example, Parker (1962, 1968), Udenfriend (1966), Chen (1967A),(1972),Winefordner (1972), Melhuish (1972), Guilbault (1973) and West (1979). A standard form of nomenclature has been proposed by Melhuish and Zander (1981).

The essential elements are a light source, a means of isolating the excitation and emission radiation and a detector rotated at 90° to the incident light path, Figure 1. Several types of light sources have been used including tungsten incandescence, mercury, hydrogen and deuterium discharge lamps. The vast majority of instruments use a xenon lamp, normally a 150 watt source, although 300 watts and 450 watts have been used. The performance of the xenon lamp is influenced by the regulation of the power supply which directly affects the stability and life of the lamp. Short term fluctuations of the light intensity and long term drift are generally compensated for by ratioing the signal from the detector with that of a reference detector monitoring either white light directly from the lamp, or a monochromatic light at the exit slit of the excitation monochromator. Several designs of monochromator mountings have been used commercially, including those of Gillieson, Ebert-Fastie and Czerny-Turner. Monochromators are generally scanned linearily with respect to wavelength from low to high wavelength.

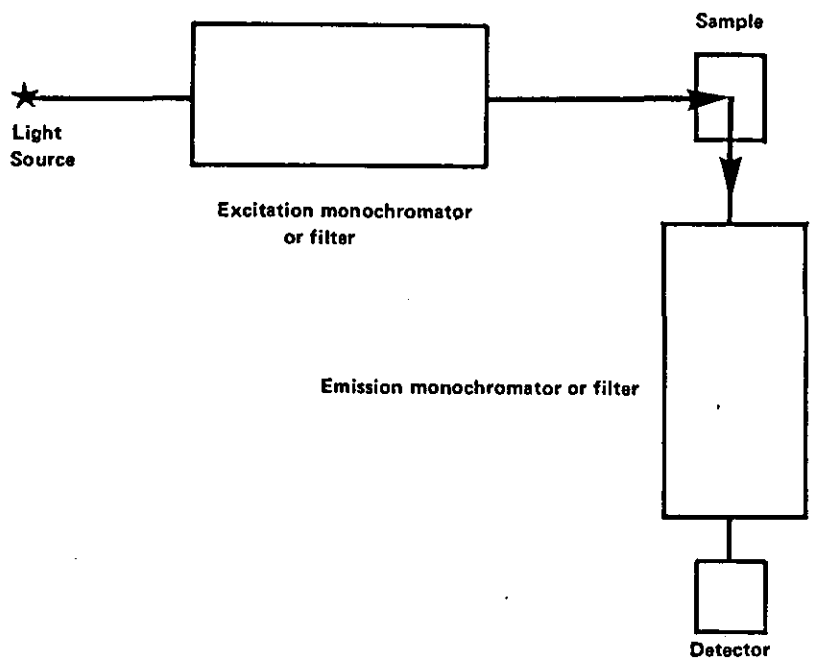

Figure 1. Essential components of a fluorescence spectrometer

Photomultipliers are the detectors used on the luminescence spectrometers and are traditionally a side-on tube with either an S-5 response (200 - 650nm) or an S-20 (220 - 900nm). The photomultiplier signals are amplified either by analogue electronics or more commonly by digital microprocessor controlled electronics following an analogue preamplifier.

1.1.1 Phosphorescence

The essential difference between phosphorescence and fluorescence is in the duration of the emission after the excitation light is cut off. Fluorescence decays almost instantaneously (within 10^{-8} s), whereas phosphorescence may have a lifetime from 10^{-4} second up to tens of seconds. A means is therefore required to discriminate between these two forms by periodically interrupting the exciting light and measuring the radiation from the sample during the periods of darkness. Becquerel (1871) placed the sample between two rotating discs mounted in a straight line. Holes cut in the circumference were offset with respect to each other such that when they were rotated the sample was intermittently illuminated and viewed in periods of darkness.

Lewis and Kasha (1944) described an alternative arrangement suited to the traditional 90° optical system consisting of a hollow cylindrical can with a slot cut in the circumference. The sample was placed inside the can which when rotated, alternately excited the sample and allowed the measurement of phosphorescence radiation during the periods of darkness. Variations in this design, Bauer and Baczinski (1958), Parker and Hatchard (1962), form the basis of many commercial phosphoroscopes.

The influence of the phosphoroscope design on the measured phosphorescence intensity has been reviewed by O'Haver and Winefordner (1966 A/B). All mechanical phosphorescence spectrometers entail certain disadvantages. In particular they are expensive to construct; it is almost impossible to independently vary the delay or dead time t_d and/or the viewing gate time t_g; short lived phosphors (0.5 - 50 msec) are difficult to measure. The rotating phosphoroscope also has the disadvantage that a substantial fraction of the phosphorescence is lost because of interruption of the cylinder (the fraction depending upon the number of slots and slot size). For these reasons Winefordner (1969) and Fisher and Winefordner (1972) proposed the use of a pulsed source and gated detector.

Two methods were used for measuring fast phosphorescence emission. In one method the photomultiplier is operated continuously and an electronic gate examines the integrated phosphorescence intensity after a delay time t_d over a gate time of t_g. In the second method the entire decay curve was presented to a fast multi-channel readout device.

These two methods were preferred to the alternative of turning the photomultiplier on and off (by applying the high voltage to the dynode chain) after the delay time t_d. However, Hamilton and Naqvi (1973) proposed a means of pulsing the photomultiplier which overcame the difficulties experienced by Fisher and Winefordner (1972). Numerous techniques for gating photomultipliers have been published including those by Hendee and Brown (1957), Peterson and Bridenbaugh (1963), Baumik et al (1965), Strambini and Galley (1976). Araki et al (1976) and Haugen and Lytle (1981).

Pulsed xenon sources have been greatly refined since they were developed in the 1930's. The peak optical power is in the kilowatt region whilst the average power can be one thousand times less. A further advantage of pulsed sources is that specific parts of the continuum can be emphasised by controlling the current, Buck et al (1963), Baker and King (1975). Generally, as the current is increased the output shifts towards the blue and ultraviolet. The maximum efficiency for a pulsed xenon source is about 60%, i.e. 60% of the input electrical energy can be converted to optical energy in the 200 - 1100 nm region. The maximum photometric efficiency for xenon is about 40 lumens per watt. Thus a major advantage over conventional continuously operating sources is the possibility of achieving higher peak intensities during the measurement period, hence better sensitivities, assuming a gated detector.

Boutilier et al (1977) has theoretically compared a pulsed source-gated detection system versus a continuously operated source and conventional electronics with respect to signal to noise ratios. Calculation showed that the pulsed system gave substantially better signal to noise for phosphorescence measurements. For fluorescence no real improvement is obtained since it is more difficult to discriminate temporally against source induced background (the decay time of source induced background is similar to the analyte fluorescence).

Mousa et al (1974) have proposed the use of a phase resolved luminescence spectrometry using a continuously operated excitation source whose intensity is modulated sinusoidally at high frequency. This is similar in principle to the phase fluor-

imeter used for calculating fluorescence lifetimes. Some degree of success was obtained in the quantitative analysis of synthetic binary mixtures.

In the following work, a xenon source is pulsed at line frequency, with an average power of 9 watts and a pulse width at half peak height of < 10 µs .The source is used in conjunction with a microprocessor controlled gated detection system in the measurement of both fluorescence and phosphorescence data.

A desk top computer is used to control the spectrometer and to store and manipulate the data. The various functions performed include correcting emission spectra, calculating areas and phosphorescence decay times.

1.2 Low Temperature Cooling

At room temperature radiationless deactivation of the triplet state is the dominant route and several methods have been used to try and restrict collisional deactivation. The most common technique is to supercool solutions to a rigid glass state - usually at the temperature of liquid nitrogen (77 K). Phosphorescence can also be observed by immobilizing the samples in rigid matrices such as polymethylmethacrylate (PMMA).

Recent investigations have shown that phosphorescence emission can be observed at room temperature from molecules adsorbed on solid surfaces such as filter paper, Schulman and Walling (1973). Two major requirements are the absence of water molecules and the presence of sodium hydroxide (with or without sodium iodide). Turro et al (1978) have also observed phosphorescence in nitrogen purged detergent solutions above the critical miscelle concentration.

The commonest type of low temperature cooling device consists of a partially silvered silica Dewar flask whose unsilvered stem is placed at the sample position. The sample is contained in a synthetic fused silica cell (typical dimensions 4mm OD, 2mm ID with a sample volume of 0.2 - 0.4 mL). This is mounted in the Dewar as shown in Figure 2A. A second type of cooling device is shown in Figure 2B in which the sample is cooled by conduction using a metal cold finger and a liquid nitrogen reservoir.

In the following work a modification of a conduction cooling device is described and used for low temperature measurements.

1.3 Luminescence Quantum Yields

The luminescence quantum yield of a compound is defined as the fraction of excited molecules that luminesce after direct excitation by a light source. The quantum yield, ϕ, is the ratio of the probabilities of radiative transition, A_i^r, to the sum of the probabilities of radiative and non-radiative transitions, A_i^{nr}, defined as

$$\phi = \frac{\text{number of photons emitted}}{\text{number of photons adsorbed}} = \frac{A_i^r}{A_i^r + A_i^{nr}} \quad .. \quad [1]$$

The quantum yield would be unity if there were no non-radiative transitions.

Quantum yields are either measured on a relative basis with reference to a standard or by absolute methods, Forster (1951), Crosby et al (1972). Both procedures have been reviewed by Demas and Crosby (1971) and Bridges (1981). Lipsett (1967) reviewed the procedures used for measuring solids and powders whilst Bril and

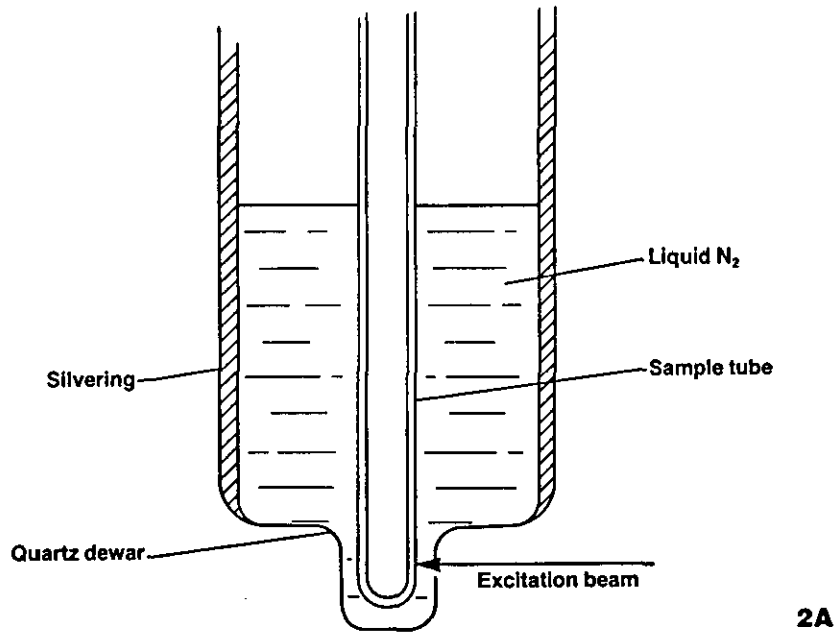

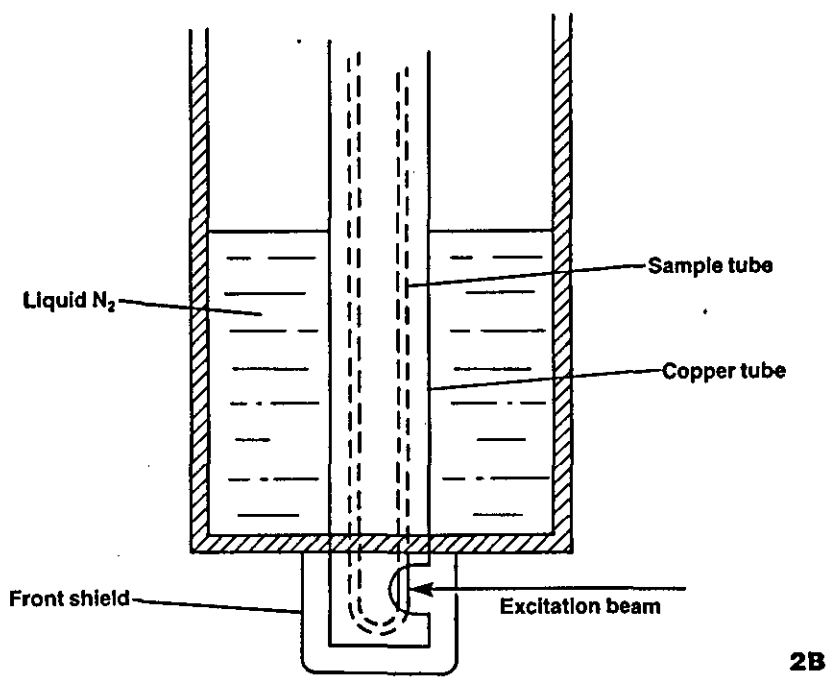

Figure 2A. Dewar flask accessory

Figure 2B. Cold finger accessory

deJagar-Veenis (1976 A/B) reviewed methods for UV, VIS, cathode-ray and X-ray excitation.

As many quantum yield measurements are made relative to a luminescent standard, the latter must be accurately calibrated. Absolute quantum yields were measured by Weber and Teale (1957) by using the dipolar scattering of monochromatic light from glycogen solution used as a standard unit of quantum yield. A comparison was then made with the fluorescence from a solution with the same apparent absorbance for the exciting light. This equation is valid when the exciting light is unpolarised and contains a correction factor which takes into account the polarisation of the sample as the standard.

1.3.1 Calorimetry

Calorimetric methods of measuring quantum yields, Callis (1976), are based on the assumption that the energy absorbed from the excitation radiation is either lost through reemitted photons or converted to heat energy by radiationless processes. By measuring the ratio of the heating of a fluorescing substance to that of a non fluorescing substance, the energy yield, Y_h, of the radiationless process is obtained. Assuming no photo-decomposition takes place, the fluorescence energy yield is the complement of Y_h and the fluorescence quantum yield is related to it by the following:

$$\Phi_f = (\bar{V}_o/V_f)(1 - Y_h) \qquad \ldots [2]$$

or

$$Y_h = 1 - \Phi_f + \Phi_f \left(\frac{\bar{V}_o - \bar{V}_f}{\bar{V}_o} \right) \qquad \ldots [3]$$

where $\bar{\nu}_o$ and $\bar{\nu}_f$ are the average frequencies of the desorbed and emitted photons respectively. Calorimetric quantum yields determined by this method are precise and accurate and have been measured in a wide range of solvents of varying refractive index, Seybold et al (1969), Gelernt et al (1974) and Olmsted (1979). Mardelle and Olmsted (1977) used a 75 W Hg lamp for excitation in a calorimetric method to determine Φ_f for 9,10-diphenylanthracene, DPA, and found a value of 0.955 in cyclohexane. Branon and Magde (1978) described the technique of thermal blooming for measuring very small temperature gradients induced by absorption of light energy. The method was used to measure exceptionally weak absorption spectra.

1.3.2 Photoacoustic Spectrometry

The heating effect within the sample is commonly measured using thermocouples or thermistors by modified versions of Bodo's technique (1963). Adams et al (1977, 1980, 1981) have described photoacoustic spectroscopy as a calorimetric method. The temperature of the sample contained within a sealed cell is monitored with the aid of a microphone transducer via the periodic pressure wave produced in the gaseous atmosphere surrounding the sample. The amplitude A of the photoacoustic signal is given by the equation;

$$A = K P_{abs} Y_h \qquad \ldots [4]$$

where P_{abs} is the absorbed radiant power and K is a constant given by the thermal transfer characteristics of the sample. Combining equation [3] and [4] we obtain:

$$A_f = K_f P_{abs(f)} \left[1 - \phi_f + \phi_f \left(\frac{(\bar{V}_o - \bar{V}_f)}{V_o} \right) \right] \quad \ldots [5]$$

and for a non-fluorescent material:

$$A_{nf} = K_{nf} P_{abs} \quad \ldots [6]$$

Combining equations [5] and [6] to give:

$$\phi_f = \frac{\lambda_f}{\lambda_o} \left(1 - \frac{A_f}{A_{nf}} \cdot \frac{K_{nf}}{K_f} \cdot \frac{P_{abs\ (nf)}}{P_{abs(f)}} \right) \quad \ldots [7]$$

and rearranging equation [7] to give:

$$\frac{A_f}{A_{nf}} = \frac{K_f}{K_{nf}} \cdot \frac{P_{abs(f)}}{P_{abs(nf)}} \cdot \left(1 - \frac{\lambda_o}{\lambda} \cdot \phi \right) \quad \ldots [8]$$

It has been shown that the photoacoustic signal is directly proportional to the absorption coefficient. However, at high absorbances, for example as are obtained in solid materials and powders, the signal becomes independent to the absorption and is then said to be saturated. If the latter signals are measured on identical instruments then:

$$P_{absf} = P_{abs(nf)} \quad \ldots [9]$$

and equation [7] reduces to:

$$\frac{A_f}{A_{nf}} = \frac{K_f}{K_{nf}} \cdot \left(1 - \frac{\lambda_o}{\lambda_f} \cdot \phi_f \right) \quad \ldots [10]$$

A plot of A_f/A_{nf} versus λ_o yields a straight line with a slope and an intercept at $\lambda_o = 0$, of K_f/K_{nf} where:

$$m = \frac{-K_f}{K_{nf}} \cdot \frac{\phi}{\lambda_f} \qquad \ldots[11]$$

Thus the quantum efficiency may be calculated from equation [11]. When applied to quinine sulphate a value of 0.53 ± 0.02 agrees well with the literature, Adams (1981). In a recent paper Ohba et al (1983) reported the use of photoacoustic spectroscopy for the determination of the luminescence quantum yields of inorganic phosphors such as Mn^{2+} in ZnS. The major deficiency of the photoacoustic method is the inability to completely quench the fluorescence of many substances.

1.3.3 Actinometry

The principle of actinometric methods, Demas and Blumenthal (1976) is the measurement of the excitation and emission intensity by chemical actinometry. The ratio of the emission to excitation intensity corrected for the function of the excitation energy absorbed is the absolute quantum yield. The method has not been widely used, as actinometers such as ferrioxalate, Reinecke's salt and uranium acetate have quantum yields which vary with wavelength. For wavelengths less than 436 nm the photochemical yield, $\phi_{Fe^{2+}}$, for Fe^{2+} production exceeds unity. In a recent paper, Demas (1981) used amplitude stabilised laser sources and electrically calibrated radiometers to calibrate the absolute value of $\phi_{Fe^{2+}}$ for the ferrioxalate actinometer. Improved accuracy and precision

were obtained over previous methods and doubts were cast on the values previously reported by Hatchard for the $\phi_{Fe^{2+}}$ yield.

1.3.4 Relative Quantum Yields

The majority of quantum yield measurements are made on a relative basis and this is discussed in the following work. It will be shown that many of the errors associated with this type of measurement can be overcome by using a fluorescence spectrometer for both absorbance and luminescence measurements. Whilst many papers have been published on the determination of fluorescent quantum yields, relatively few have appeared for phosphorescence. This work will describe the use of a conduction cooling device and a pulsed xenon source for measuring phosphorescence quantum yields at 77K, together with fluorescence quantum yields at 77K and at room temperature.

1.4 Amino Acid Luminescence

Three aromatic amino acids commonly occur in proteins. They are phenylalanine, tyrosine and tryptophan. The proteins containing only the first two are called Class A, whilst those containing the latter are Class B. The luminescence of the latter is dominated by the emission of tryptophan regardless of tyrosine content. The loss of tyrosine luminescence is almost entirely due to energy transfer between the first excited singlet states of tyrosine and tryptophan. In addition, tryptophanyl absorption and emission dominate and tyrosine contribution is small.

The room temperature luminescence studies of proteins and amino acids began in earnest after the mid-fifties. For example, Duggan and Udenfriend (1956) showed that human serum exhibited a tryptophan-like emission. Teale and Weber (1956) reported in detail on the fluorescence characteristics of aromatic amino acids including quantum yield determinations. Extensive reviews on room temperature fluorescence have been compiled by Longworth (1971), Eisinger (1969) and Chen (1967 A).

Low temperature studies of amino acids and proteins were carried out by Longworth (1961) who observed both tyrosine and tryptophan-like phosphorescence decays in the emission of human serum albumin. Earlier workers such as Freed et al (1958) and Vladimirov and Litvin (1960) could not detect the presence of the tyrosine component of human serum albumin. Konev and Bobrovich (1965) reported the presence of a tyrosine-like shoulder on the main tryptophan phosphorescence spectrum of several Class B proteins. It is only recently that more thorough investigations of protein luminescence at 77°K have been carried out.

Some of the environmental factors which determine the nature of the observed luminescence from proteins were studied in this later work. For example, Truong (1967) has reported on the pH dependence of phosphorescence of tryptophan and tyrosine in free solution and when present in a protein macromolecule. Edelhoch et al (1967), Steiner and Kolinski (1968) have discussed various aspects of the low temperature emission of peptides containing both tyrosine and tryptophan, whilst Weinryb and Steiner (1968) compared the luminescence of tryptophan derivatives at 298 K and 91 K.

In this study both room temperature and low temperature characteristics of tyrosine and tryptophan are studied, together with the low temperature luminescence of phenylalanine.

1.5 Luminescence Probes of Macromolecules

Electronic excitation energy can be transferred between chromophores by three recognised paths; singlet-singlet, triplet-singlet and triplet-triplet. The first two can occur over distances of the order of 40Å. The mechanism for this long range coupling was first put forward by Forster (1951). Triplet-triplet transfer requires a much closer approach of the donor and acceptor groups, Ermolaev and Svitashev (1959), Galley and Stryer (1968).

Fluorescence techniques using singlet-singlet transfer have been used to study the binding of ligands to proteins, Weber and Daniel (1966). Triplet-singlet transfer in proteins was demonstrated by Galley and Stryer (1969). The system studied was a complex of proflavin and α-chymotrypsin. The tryptophan residues of the latter were the triplet energy donors, while the proflavin bound at the active site served as the singlet acceptor.

Triplet-triplet energy transfer is a short range effect, less than 15 Å and the mechanism differs from that involving singlet state and is based on electron exchange interactions between the orbitals of the chromophores, Dexter (1953), McCarville and Hauxwell (1971). The properties of phosphorescent probes make them potentially more sensitive for determining short distances or changes in distances between interacting chromophores on a protein molecule.

The use of lanthanide ions as probes was demonstrated by Weissman (1942) who showed that excitation energy transfer from organic ligands to the ions leads to the characteristic line emissions (intra-4f-transitions) of the lanthanides. The efficiency varies with the nature of the ligand, temperature and solvent. Eisinger (1971) and Lamola (1971) used Eu^{3+} ions as probes for excited molecules such as nucleic acids in aqueous solutions at pH 5.0 or less. Estimates were made of donor excited state lifetimes and intersystem crossing yields. Similar experiments were performed by Filipescu et al (1968) who used Eu^{3+} and Tb^{3+} as sensitive probes in photochemical transformations. Eu^{3+} concentrations ranged from 0.025M to 0.1M for sensitiser concentrations of 0.05M. Yonuschot and Mushrush (1975) showed that Tb^{3+} could be used as a fluorescent probe with DNA and Chromatin.

In a recent paper Mushrush and Yonuschot (1983) used trivalent lanthanides Eu^{3+}, Sm^{3+}, Tb^{3+} and Dy^{3+} as sensitive fluorescent probes in the solid state with nucleotides. At neutral or slightly acidic pH's the lanthanides will precipitate the nucleotides. By measuring the narrow line emission of the lanthanides when a nucleotide is selectively excited, the quantum yield and the relative amount of lanthanide ion bound to the nucleotide can be calculated.

Crosby and Whan (1961) and Crosby (1966) showed that rare earth line emission will occur from a particular chelate only if the lowest molecular (donor) triplet state energy level is nearly the same or lies above the atomic level from which the line emission of the lanthanide ion originates. The conclusions were that the principal path of energy transfer to the ion is through the lowest triplet state of the complexed ligand and that energy transfer from the excited singlet state does not occur.

Energy transfer is highly efficient with quantum yields of 0.5 to 1.0 found by Charles and Riedel (1966). A schematic of the events prepared by Crosby is as follows:

$$S_o + h_v \longrightarrow S^* \qquad \text{(absorption)} \qquad \ldots[12]$$

$$S^* \xrightarrow{k_{st}} T \qquad \text{(intersystem crossing)} k_{st}[S^*] \qquad \ldots[13]$$

$$T + {}^7F \longrightarrow So + {}^5D \qquad \text{(intermolecular transfer)} k_{tr}[T][{}^7F] \qquad \ldots[14]$$

$${}^5D \xrightarrow{k_t} {}^7F + hv \qquad \text{(fluorescence)} k_f[{}^5D] \qquad \ldots[15]$$

Radiationless deactivation may also occur

$$T \xrightarrow{k_t} So \qquad k_t,[T] \qquad \ldots[16]$$

$${}^5D \xrightarrow{k_d} {}^7F \qquad k_d[{}^5D] \qquad \ldots[17]$$

where So, S* and T are the ground singlet, excited singlet and lowest triplet of the donor respectively. ^7F and ^5D refer to the ground and excited levels of Tb^{3+}.

Energy transfer to unchelated lanthanide ions has been demonstrated by Heller and Wasserman (1965) who showed that triplet excitation can be transferred from many aromatic carbonyl compounds to Eu^{3+} and Tb^{3+} in glacial acetic acid.

The advantages of lanthanides as probes are summarised as follows:

a) They emit characteristic and quantitatively measurable fluorescence.

b) Interaction of the rare earth ion and its environment can be studied separately both in the presence and absence of the

donor by light absorbed by the lanthanide ion.

c) Fluorescence of ions such as Eu^{3+} and Tb^{3+} is not quenched by donors and is unaffected by the presence of oxygen.

d) For Eu^{3+} and Tb^{3+} the competition between luminescence and radiationless deactivation is dominated by the former.

An investigation will be made in this work to characterise the excitation and emission spectra of the probe Tb^{3+} with a macromolecule such as transferrin. Earlier work by Luk (1971) suggested that tyrosinate ion was involved in energy transfer to the Tb^{3+}. Results for this work indicate that tryptophan is also involved in energy transfer to the lanthanide.

1.6 Luminescence of Europium (III) in Yttrium Oxide

The luminescence of Eu^{3+} essentially consists of transitions between the ^5D and ^7F levels with the magnitude and wavelength of the transition governed by the nature of the host lattice. The luminescence of Eu^{3+} has been studied in yttrium oxide by Chang (1963) and Chang and Gruber (1964), Axe and Weller (1964) and Weber (1968), among others; in yttrium oxysulphide by Ozawa (1979) and in thorium oxide by Breysse and Faure (1981).

The majority of the emission spectra presented in these papers were obtained using a 150W Xe lamp operating in the continuous mode. However, the mean lifetimes of the different $^5D_5$ transitions show an increase with decreasing J number. For example, experimental work showed that the $^5D_1$ - $^7F_1$ transition at 533nm has a mean lifetime of 0.12 ms and the $^5D_0$ - $^7F_2$ transition at 611nm has a mean lifetime of

0.92 ms. Thus, when a pulsed source Xe lamp is used for excitation of Eu^{3+} in Y_2O_3, the emission spectrum differs from that obtained using a continuous source, the difference depending on:

a) the delay between the end of the excitation and the beginning of the measurement

b) the time over which the measurement is taken.

It will be shown that the isolation of the various transitions can be made on a time basis as opposed to direct excitation into the appropriate level.

1.7 Uranyl Ion Analysis in Aqueous Samples

Several luminescence methods for uranium have been reported in the literature, the most common of these being based upon the sodium fluoride/lithium fluoride fusion technique, Adamas and Maeck (1954), Centanni et al (1956) and Thatcher and Baker (1957). Typically, the uranium is extracted with ethylacetate from a solution salted with aluminium nitrate. An aliquot of the organic phase is then transferred to a pellet of sodium fluoride containing 2% lithium fluoride. After evaporation of the solvent the pellet is fused at 1075C for 15 minutes and the luminescence of the button, when exposed to UV radiation, measured. The limit of detection of this method is approximately 10 ng on the button.

The luminescence of the uranyl ion is very susceptible to quenching both by organic molecules and by inorganic ions such as Fe^{3+}, Mn^{2+} and Cl^{1-}, Veselsky (1979) and Yokoyama and Ikeda (1976). Two approaches have been made to try and reduce this interference.

For example, the uranyl luminescence can be studied after precipitation of the sample from a solution containing calcium fluoride. After calcination of the precipitate an argon ion laser is used to excite the uranyl luminescence, Perry et al (1981).

In the second approach, solvent extraction methods have been proposed to isolate the uranium before measurement. These include ethylacetate, tributylphosphate in iso-octane, UKAEA (1962), Francois (1958); trioctylphosphine oxide (TOPO) in cyclohexane, Horton and White (1958); TOPO in Varsol, McElhaney (1978), and TOPO with biphenyl, Kohima et al (1982).

Since the luminescence from acidic uranyl solutions has a lifetime in the submillisecond region, Pant and Tripathi (1974), time discrimination has been used as a means of reducing the background fluorescence signal and hence improving the detection limit, Kaminski et al (1981), Robbins and Kinrade (1979), Hinton and White (1981), Whitkop (1982).

The luminescence lifetime varies as to the type and concentration of acid, ranging from 2.1 μs in 0.1M $HClO_4$ to 187 μs in 1M H_3PO_4, Moriyasu and Yokoyama (1977), Benson et al (1975) and Marcantonatos (1977). Ortho phosphoric acid has been used extensively as an enhancer of the uranyl ion emission. The effect is to prevent quenching of the excited uranyl ion by the hydroxyl ion, though the precise nature of the deactivation has not been adequately described, Burrows and Kemp (1974).

The following work will describe the development of a rapid and sensitive assay for uranyl ion in the presenceof quenchers using solvent extraction and time resolved emission measurement.

CHAPTER TWO

EXPERIMENTAL

2.1 Instrumentation

A Model LS-5 Luminescence Spectrometer, Rhys Williams (1981) was used for all of the experiments. This instrument measures both fluorescence and phosphorescence signals. Two reflection grating monochromators (excitation and emission) are used in the optical system with sample and reference photomultiplier detectors, Figure 3. Ratio recording electronics process the signals from the two photomultipliers to produce an output which is proportional to the level of sample emission. A xenon lamp is pulsed at line frequency and the sample photomultiplier is gated to look at the signal at the instant of the flash (fluorescence) or at some time after the flash has decayed to zero (phosphorescence). The system diagram of the instrument is shown in Figure 4.

2.1.1 Optical System

A 9 watt pulsed xenon source with a pulse width at half peak height of < 10 µs provides a continuum of energy over the wavelength range 200 to 800nm. Energy from the source is collimated by the ellipsoidal mirror and reflected by the toroid onto the entrance slit of the excitation monochromator. The latter consists of the entrance slit 2, a 1200l mm^{-1} grating blazed at 350nm, a spherical mirror and the exit slit 1.

Energy from the exit slit passes through a quartz beam splitter. This reflects a portion of the excitation beam onto a quantum corrected reference detector, so that corrected excitation spectra can be measured by recording the ratio of the fluorescence and reference signals, Parker (1958).

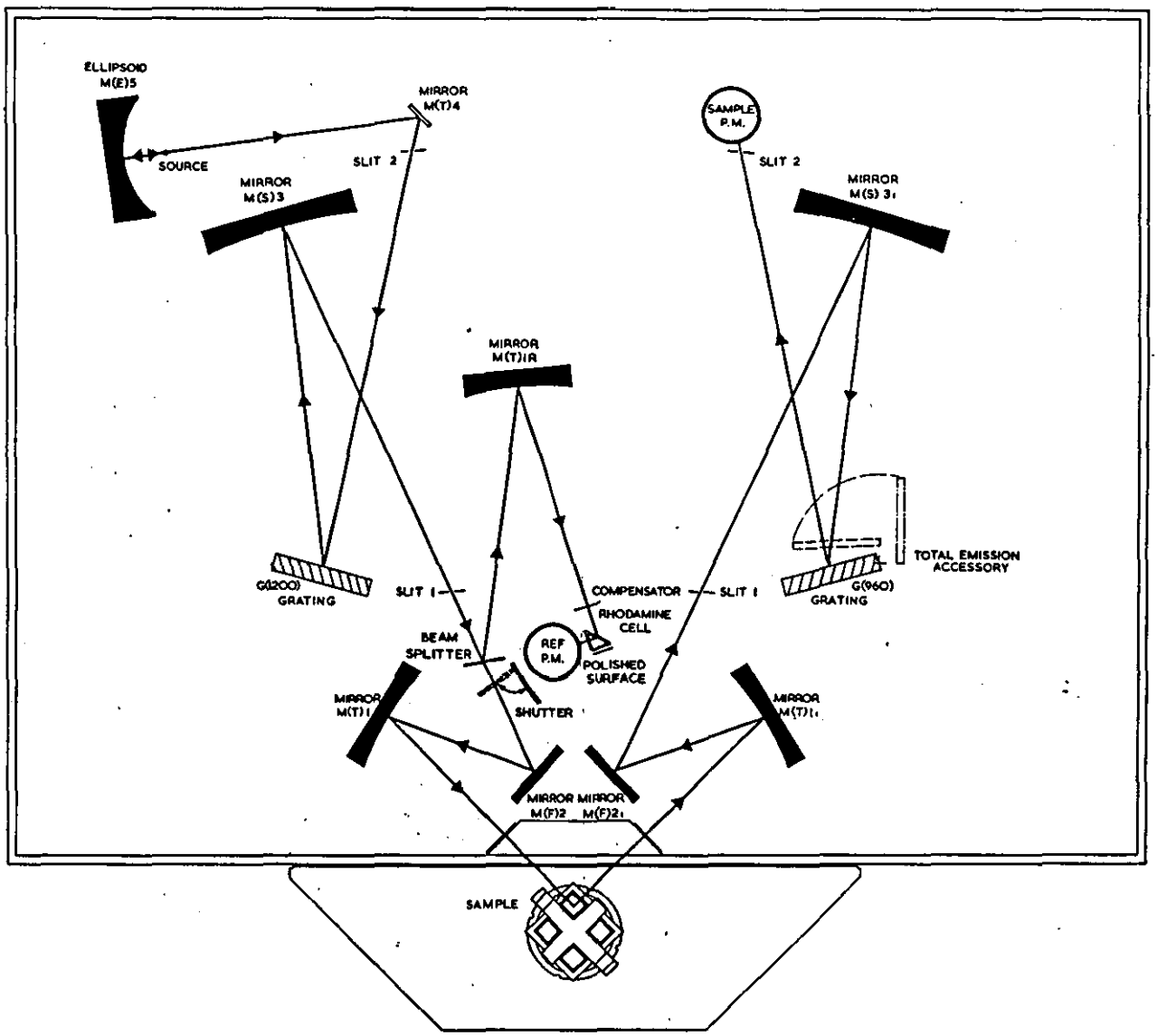

Figure 3. Model LS-5 optical diagram

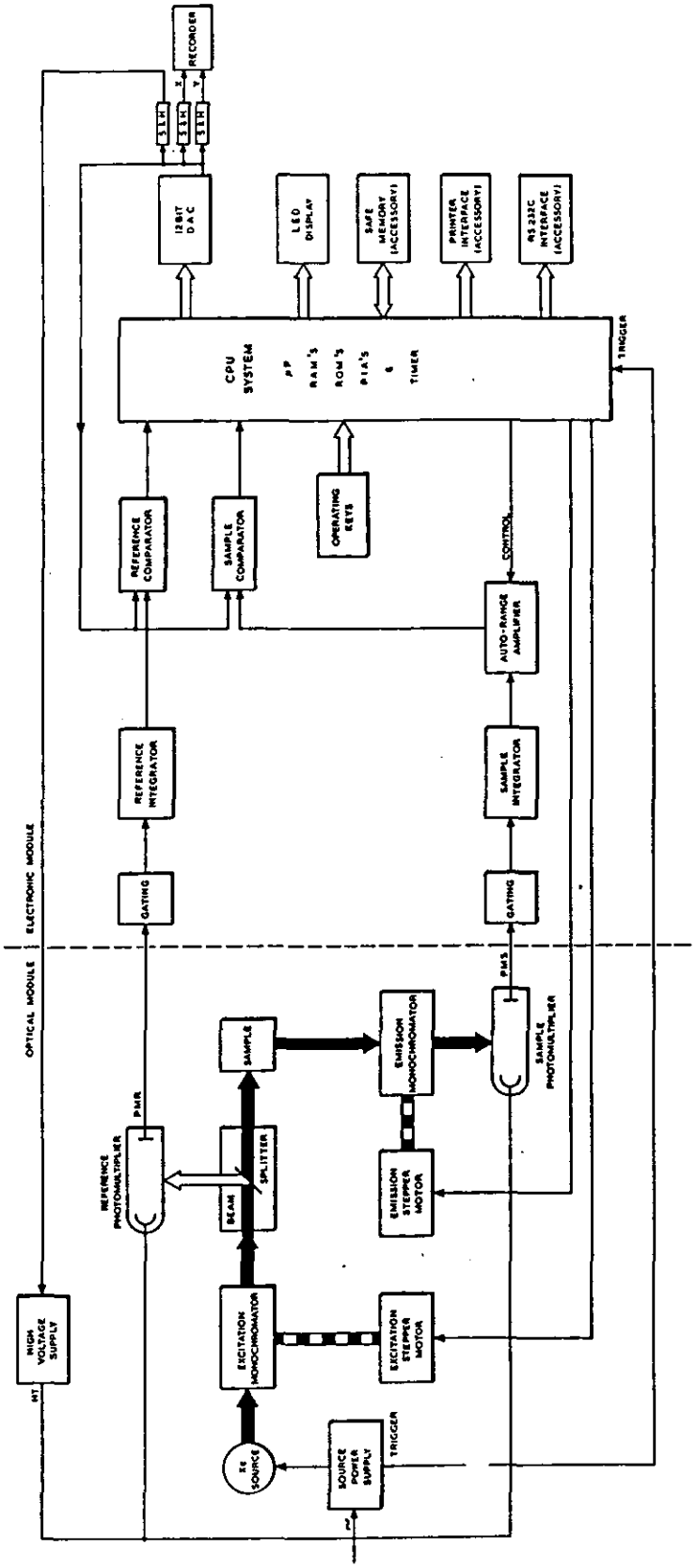

Figure 4. Model LS-5 system diagram

However, the compensated signal so obtained is proportional to the transmittance/reflectance ratio τ/P of the beam splitter and must therefore be corrected for the wavelength dependence of this ratio, Mielenz (1979). Polarisation errors are avoided by using the beam splitter at an angle of incidence of less than 15°. Most of the ratio error occurs between 200 and 400nm and Table 1 shows the normalised response (factor) experimentally obtained.

$$f = (\tau/P)/(\tau/P)_{400nm} \qquad ...[18]$$

The apparent increase in excitation energy following on the reference detector can be seen in Figures 5 A/B. These spectra were obtained by scanning the excitation monochromator with Rhodamine 101, 5 gL^{-1} in glycerol, placed in the sample holder. As the signal to the chart recorder is a ratio of sample to reference detector outputs, the apparent increase in excitation energy results in a reduction of the signal, Figure 5A.The transmittance/ reflectance characteristics of the beam splitter can be closely matched by a piece of polyethylene. The latter is placed between the rhodamine cell and beam splitter and the result is shown in Figure 5B.

Rhodamine 101 is used as the quantum counter in the reference system in preference to Rhodamine B, Taylor and Demas (1979). The fluorescence efficiency of the latter has been found to vary strongly with solvent and temperature ranging from 0.65 - 0.90, Kubin and Fletcher (1982), Drexhage (1973, 1976). Rhodamine 101 has an efficiency of 0.96 and is practically independent of

TABLE 1

Normalised response factor "f"

as obtained from Equation [18]

λ nm	f
390	1.000
370	1.005
350	1.009
330	1.014
310	1.033
290	1.062
270	1.110
250	1.196
230	1.483

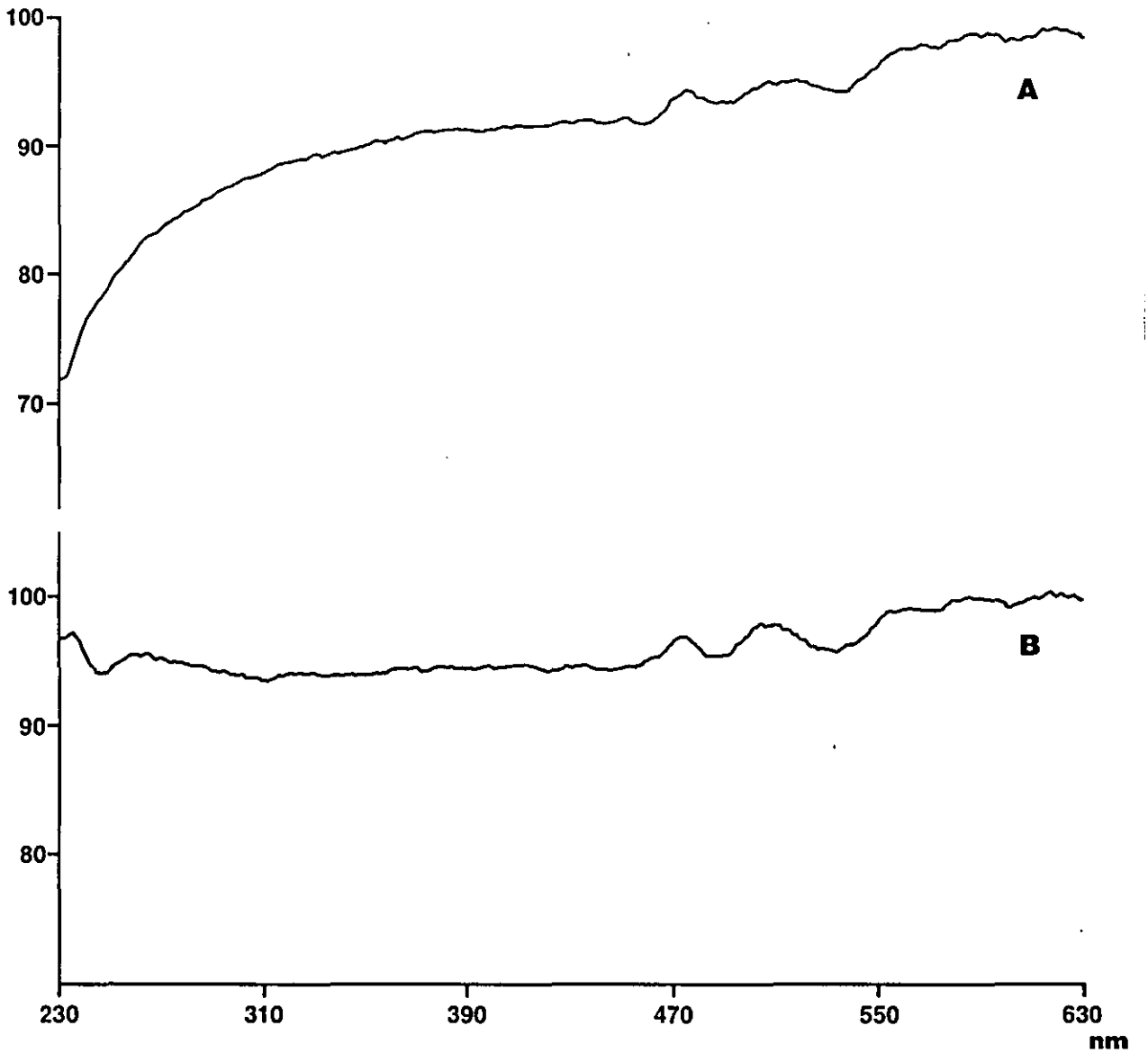

Figure 5. Rhodamine 101 excitation correction curve: a) without and b) with the beam splitter compensator

solvent and temperature. Correction is obtained between 230nm and 630nm. The geometry of the reference system is similar to that recommended by Melhuish (1972). The useable ratioing range is extended by placing a polished surface behind the rhodamine cell which reflects light with wavelengths longer than 630nm on to the reference photomultiplier.

A similar monochromator to the excitation side is used for isolating emission spectra with the exception that the emission grating has 960 l mm^{-1} and is blazed at 450nm. Both monochromators are stepper-motor driven and can be run independently to obtain the normal excitation and emission spectra, or synchronously either at the same wavelength or at different wavelengths. The excitation monochromator covers the range 200 - 720nm, whilst the emission monochromator covers the range 200 - 800nm.

The standard sample and reference photomultipliers have an S5 response (EMI 97SIR). For extended operation from 650nm to 800nm the sample photomultiplier can be replaced by a red sensitive type S20 (Hamamatsu R928). By means of the two pairs of adjustable entrance and exit slits the overall resolution of the instrument can be varied in fixed steps giving 2.5, 5, 10 and 15nm for the excitation and 2.5, 5, 10 and 20nm for the emission.

2.1.2 Electronics

The signals from the sample and reference photomultiplier are processed in separate channels and are gated depending upon

the mode of operation. In fluorescence mode both channels are opened just before the source is pulsed; in phosphorescence mode, Figure 6, the opening of the sample channel is delayed by a selectable period (t_d) as is the width of the gate (t_g), in multiples of 10 μs.

Each photomultiplier output is first integrated and then digitised in a 12 bit successive approximation A-D converter, which consists of a comparator, the 12-bit DAC and control circuits in the central processing unit (CPU). The output of the sample integrator is processed by an auto range amplifier that ensures maximum resolution is maintained during the A-D conversion process. The digitised signal is accumulated for 0.1 s, that is 5 flashes of the source, and the sample accumulation divided by the reference to obtain a ratio which is virtually unaffected by variation in source intensity.

The effect of "dark current" (output from an unilluminated photomultiplier) is eliminated in fluorescence mode by gating the sample photomultiplier a second time just before the flash and subtracting the signal obtained from the total fluorescence signal. The second gating in fluorescence mode also eliminates any contribution from phosphorescence signals with a lifetime greater than 20 ms.

The discrimination between fluorescence emission and long lived phosphorescence is difficult to achieve on instruments using a DC source since both signals will always be present. Figure 7 shows the "fluorescence" emission spectrum of coronene in n-hexane at 77K obtained using a DC operated 150W xenon source. Figure 8 shows the fluorescence spectrum obtained on the Model LS-5. The difference in appearance results from the

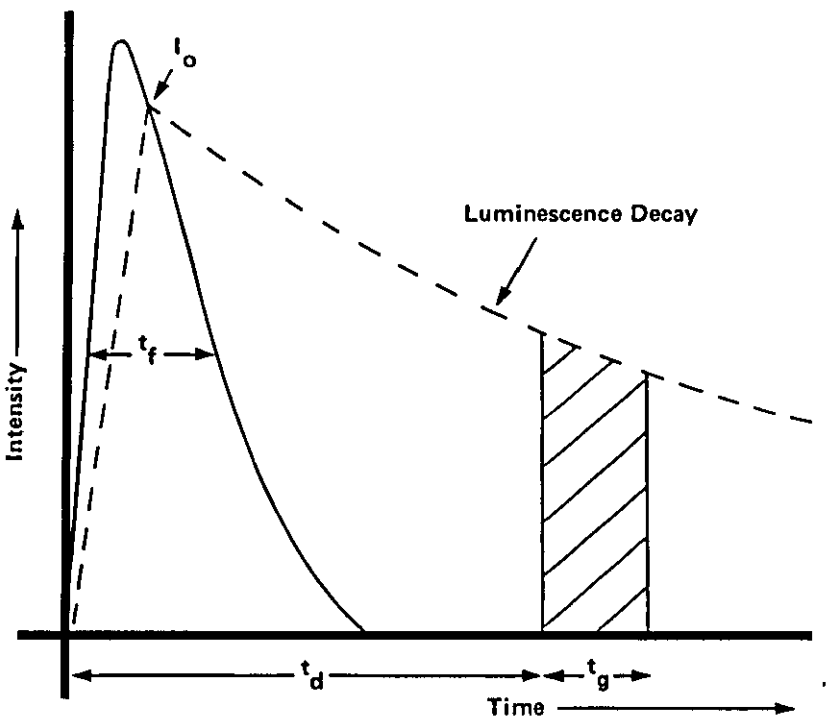

t_f = width at half peak height
t_d = delay from beginning of pulse to beginning of observation
t_g = gate width of detector

Dotted line indicates build up of luminescence signal to maximum I_o and then exponential decay

Figure 6. Schematic diagram of events occurring during excitation of a sample with a pulsed xenon sou in phosphorescence mode.

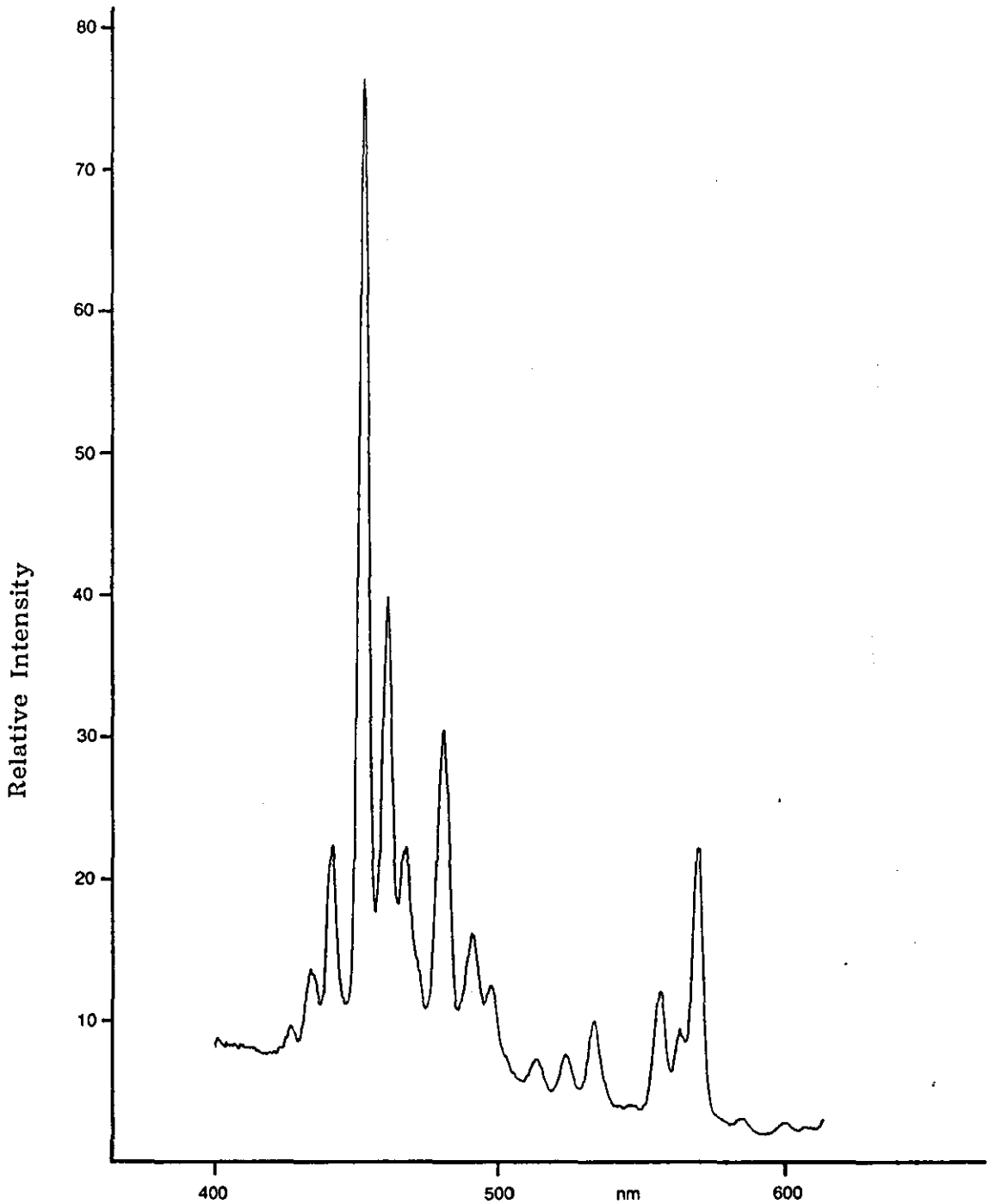

Figure 7. Low temperature "fluorescence" emission spectrum of coronene in hexane measured with a 150 watt DC xenon source

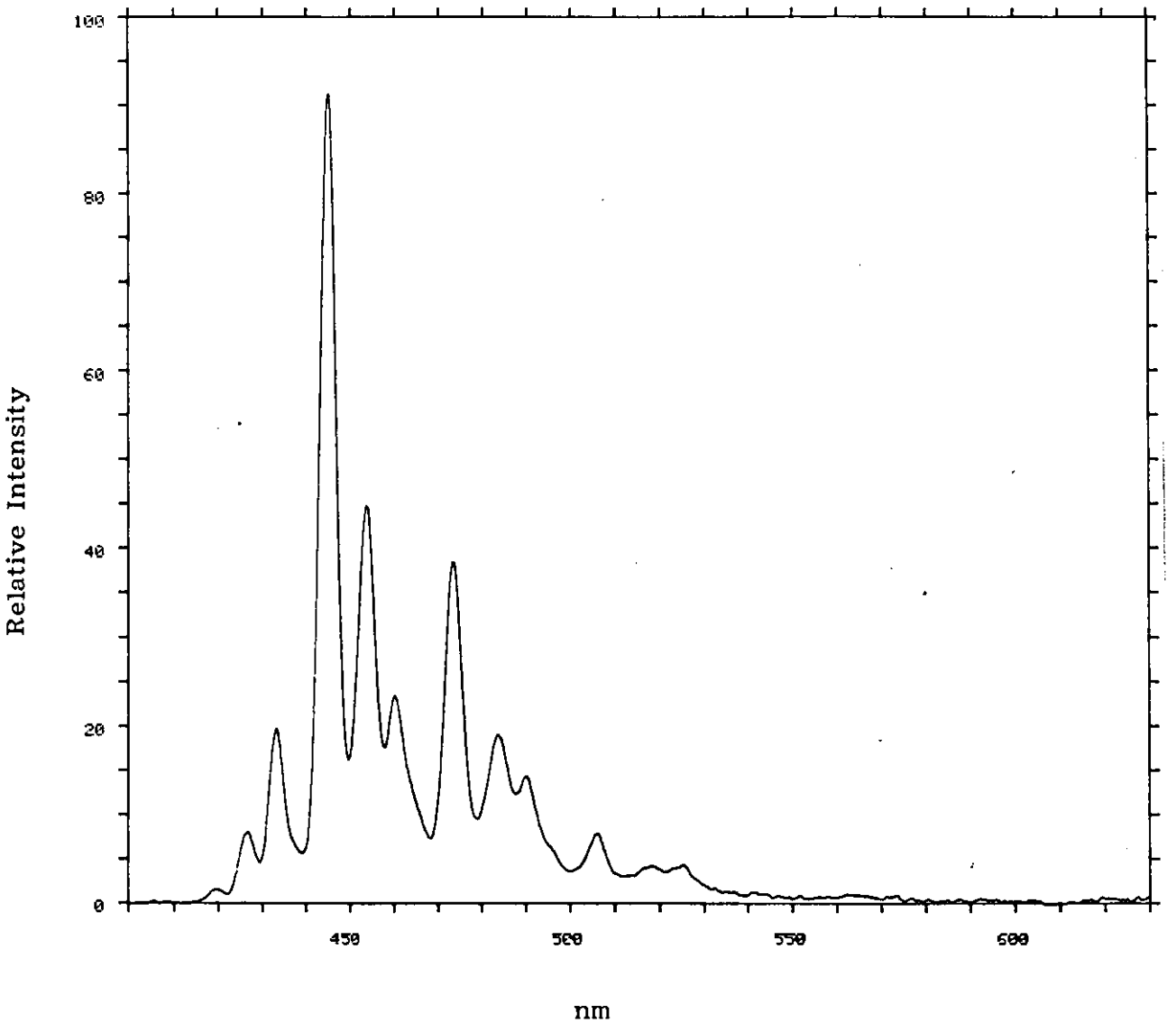

Figure 8. Low temperature fluorescence emission spectrum of coronene in hexane measured with a pulsed xenon source

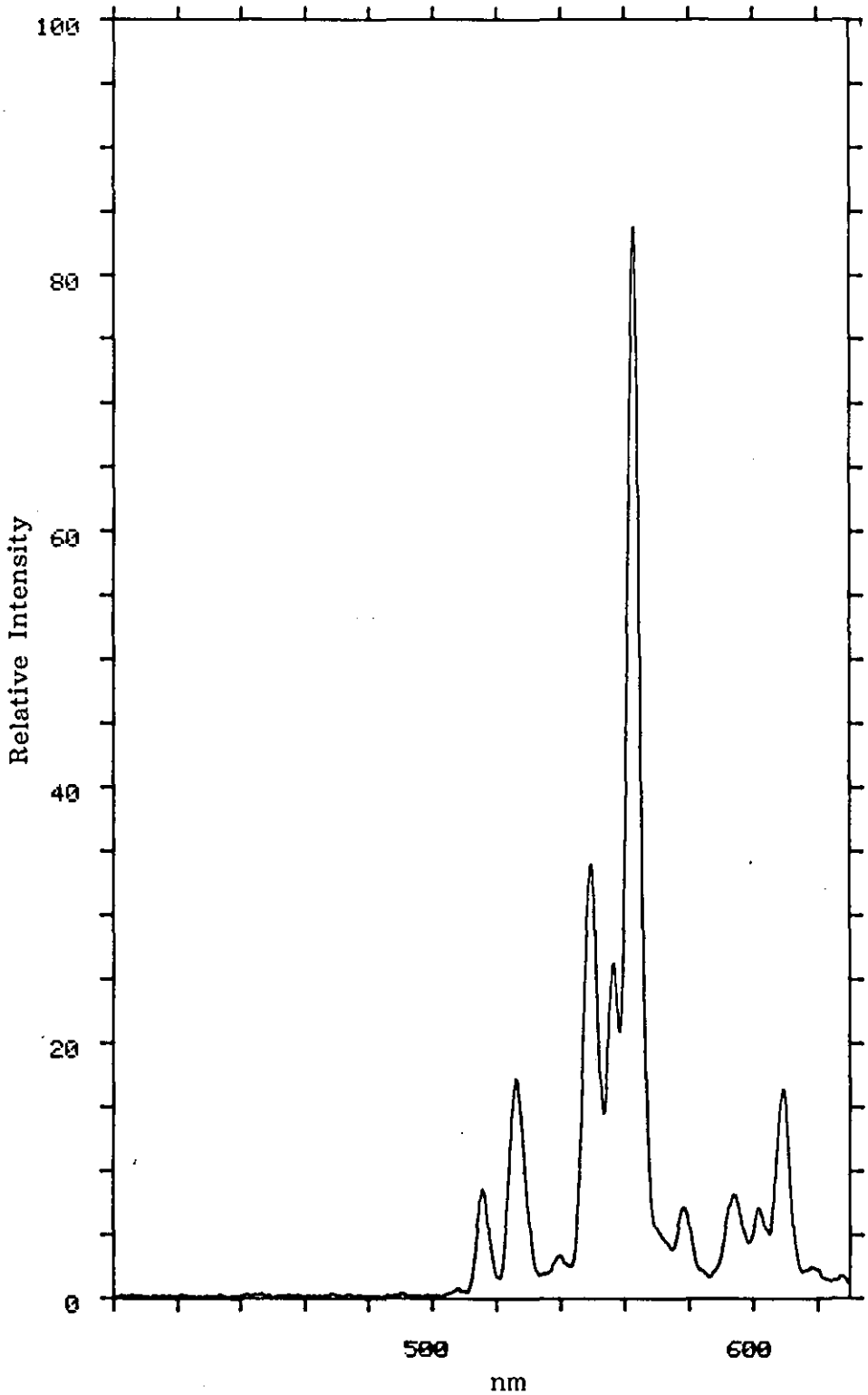

Figure 9. Low temperature phosphorescence emission spectrum of coronene in hexane as measured with a pulsed xenon source

fact that peaks above 500nm are phosphorescence transitions and are gated out by the Model LS-5. The phosphorescence emission of coronene is shown in Figure 9.

All operations such as scale expansion, filtering, integration, offsetting, are performed digitally by the microprocessor. The signals are only converted to an analogue voltage for use with an analogue input recorder. A Savitzky-Golay (1964) quadratic smoothing filter is used which provides greater reduction in noise, together with less distortion of the true signal, Bromba and Ziegler (1981).

2.1.3 Low Temperature Accessory

Conventional low temperature accessories use immersion cooling, i.e. the sample in a synthetic fused silica tube is cooled by immersion in liquid nitrogen, held in a Dewar, Chapter 1.2. Two major problems arise from this method and are:

a) poor precision resulting from non-reproducible sample positioning and erratic freezing rates

and

b) very slow sampling rates.

Additional problems can arise such as gradual fall off in signal intensity due to accretion of ice crystals in the base of the Dewar, or additionally, a build up of ice on the outside of the base of the Dewar if the accessory has not been adequately purged with dry nitrogen. In addition to the Dewar, some means of mechanically chopping the excitation and emission beams, i.e. a rotating can and its associated motor and control module, are

also required. Attempts have been made to improve the precision by rotating the sample tube, Hollifield and Winefordner (1968), Lukasiewcz et al (1972), Gifford et al (1972). This overcomes any unhomogeneity but does not overcome positioning errors.

Conduction cooling has been shown to provide an alternative to immersion cooling as a means of improving the precision and speed of analysis. Ward et al (1980A, 1980B) discussed two conduction cooling systems.

In the first, a copper rod was immersed in liquid nitrogen and the sample cooled by contact with the rod. Although the speed of analysis was improved by a factor of 3 over conventional phosphorimetry, the detection limits were similar. Measurements indicated that the operating temperature of the system was 100°K.

In the second paper, the copper rod was cooled by a flow of liquid nitrogen through the rod which resulted in the operating temperature being lowered to 85K. Generally, detection limits were lower though the main advantage was the improved precision and speed of analysis.

The conduction rod, Figure 10, used in the low temperature accessory is machined from high purity (99.99%) copper, having a thermal conductivity of 4.05 joule sec^{-1} cm^{-1} K^{-1}. Sample tubes with a 4 mm OD, 2 mm ID are inserted in a hole drilled in the top of the copper rod. A slot is milled 20 mm deep from the end to serve as the optical windows. The rod is hollowed leaving a cavity 12.2 mm in diameter extending from the open

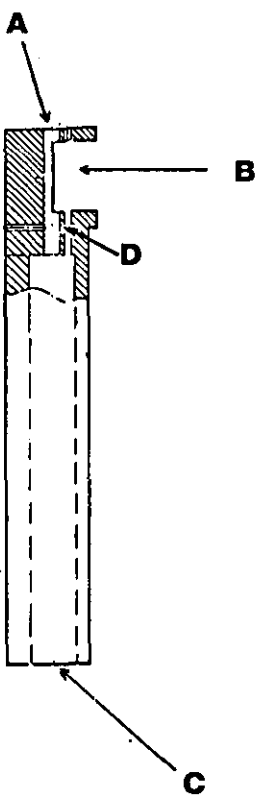

Figure 10. Schematic diagram of the conduction cooling A is the sample position, B is the optical window, C the hollow cavity and D is the hole drilled so as to allow nitrogen gas to blow over the sample.

end. A hole is drilled into the cavity allowing nitrogen gas to flow around the sample tube. Once sealed in position in the sample compartment the flow of nitrogen serves to keep the slot free of moisture from the surrounding air.

The bottom part of the copper rod is immersed in 2L of liquid nitrogen held in a box constructed of stainless steel insulated by expanded polystyrene. The accessory is enclosed by the sample compartment cover through which the sample tubes are inserted by means of a removable lid. The inside walls of the optical module are kept free of moisture by a stream of dry nitrogen at a flow rate of 1 L min^{-1}.

The performance characteristics of the conduction cooling system are described in Chapter 4.2.

2.2 Data Handling

The Model 3600 Data Station is a desk top microcomputer with keyboard, two floppy disc drives and programmable video display unit. The microprocessor data processing module has 16K of ROM operating system with 48K of RAM locations for the applications software and data storage. The modified ASCII keyboard module has 24 special functions with up to 48 functions that are software defined. A list of these functions is given in Table 2.

The two $5^1/4$ inch floppy discs each have 160K of storage capacity and the applications program, PECLS II, stored in disc 0, is written in a low level language. Disc drive 1 is used for storing data and/or OBEY programs. The latter are described later in this section.

TABLE 2

Special Function Key Commands

I. Instrument Control

1. **AUTOZ** Automatically calculates and sets the auto zero value. If auto zero is no longer needed, it cancels the command.
2. **GOTO** The excitation and emission monochromators can be driven to the specified wavelengths.
3. **INST** Reads the wavelengths, scale expansion and luminescence value.
4. **IPHOS** To make luminescence readings, the photomultiplier voltage is fixed.
5. **MANUAL** Releases the spectrometer from computer control.
6. **MODE** The scan speed and response factor are set.
7. **ORD** A scale expansion factor in fixed scale or auto concentration mode can be set or the spectrometer can be used in auto range mode.
8. **PHOS** The delay and gate times can be selected and entered.

II. Data Acquisition

1. **ACCUM** Enables up to 250 repetitively scanned spectra to be added.
2. **AVRAGE** Averages up to 250 repetitively scanned spectra.
3. **INT** Displays the ordinate value at a specified wavelength for the selected integration time set through the MODE command.
4. **PRESCN** Rapidly scans the excitation and/or the emission spectra over selected ranges to determine the maximum excitation and emission wavelengths. The ordinate value is set to 90.0.
5. **SCAN** Allows an excitation, emission, or synchronous scan to be acquired between specified wavelength limits.
6. **TDRIVE** Allows information to be acquired as a function of time to follow kinetics or to collect LC data.

III. Data Storage and Retrieval

1. **CHART** Moves the chart on Model 561 recorder forward by a specific number of centimetres.
2. **CNTENT** Reads the contents of the micro floppy disc used to store data.
3. **PLOT** Spectra can be replotted to the Model 561 recorder or the Model PP-1 printer/plotter.
4. **PRINT** Alphanumerics on screen can be printed using Model 660 or Model PR-100 printer.
5. **RETRVE** Spectra stored on disc can be recalled into memory for further manipulation.
6. **SAVE** Spectral data can be stored on micro floppy disc.
7. **VPRINT** Graphics can be printed on Model 660.

IV. Graphics Display

1. **AXIS** Annotated axes for the abscissa and ordinate are displayed.
2. **CLEAR** All the graphics screen is cleared.
3. **CLRCUR** The cursors are removed from the screen.
4. **CURSOR** Two vertical cursors can be activated to display wavelengths which can then be entered into other PECLS commands.
5. **EXPAND** The spectrum displayed between the cursors can be expanded to fill the full screen.
6. **GRID** A calibrated grid is superimposed on the displayed spectrum.
7. **INTENS** The ordinate value from the active graphics cursor position is displayed.
8. **LABEL** Allows the user to label spectra on the screen. This text is on the graphics scree and is printed with the spectrum using VPRINT.
9. **VIEW** Displays on the screen, spectra betweer specified wavelengths.

V. Mathematical manipulation and the use of OBEY programs

1. **ABEX** Expands or contracts the spectrum using either an operator selected factor or a computer calculated factor.
2. **ADD** Adds two spectra or adds a constant to a spectrum and stores the result.
3. **AREA** The area under a curve is calculated between specified wavelengths and makes a baseline correction.
4. **COPY** All or part of a spectrum can be copied from one region to another.
5. **CORR** Spectra can be corrected or the command can be used to multiply or divide spectra.
6. **DIFF** Takes the difference or scaled differenc between two spectra.
7. **DIV** A spectrum can be divided by a consta and the result stored.
8. **MERGE** Two spectra can be merged together s that excitation and emission spectra ca be combined on one scale.
9. **MULT** A spectrum can be multiplied by a constant and the result stored.
10. **OBEY** Automatic routines can be written to combine these commands.
11. **SDIFF** Two spectra can be subtracted and th result simultaneously viewed on the screen. The effect of increasing or decreasing the factor is instantly displayed on the screen.
12. **SET** SET is used to set scan, view and plot limits or to set wait off for automatic operation.
13. **SHIFT** Spectra can be shifted by up to 40 dat points.
14. **SMOOTH** Smooths a spectrum to reduce noise.
15. **STATUS** Displays the summary of the data memory.
16. **SUB** Allows one spectrum to be subtract from another.

VI. Mathematical operations and OBI programs

1. **CALC** Permits mathematical calculation and signment of stored variables V1 – 25.
2. **CHANGE** Spectral parameters or data can changed.
3. **LIST** Displays all the commands available the applications program.
4. **OUTPUT** Displays the numerical values store the variables V1 – 25.
5. **STOP** Stops PECLS the applications progra and restores the system to the opera system PETOS.
6. **TYPE** Displays the data in a spectral file.
7. **VSAVE** Transfers the numerical values of the ables V1 – 25 to a data file on disc.

The video display unit has high resolution graphics capability (720 data points horizontally, 250 data points vertically) and can also display 24 lines of 80 alphanumeric characters per line. Two asynchronous bidirectional communication ports with programmable baud rate, stop and data bits and parity are available. One is for communicating to the LS-5 via an RS232C interface and the other for connection to a graphics printer. Data is retrieved from the Model LS-5 at 0.5nm intervals.

The PECLS applications software performs five basic functions.

a) Instrument control

b) Acquisition of spectral data

c) Data storage and retrieval

d) Graphics display

e) Mathematical manipulation and the use of OBEY programs

Data is stored in one of the three data areas designated X, Y and Z which contain 3821 data points, sufficient space to store a spectrum over the whole wavelength range 200 - 800nm. The various functions can be strung together in the form of miniprograms called OBEY programs which allow the automatic collection of data, manipulation and storage. BASIC programs may also be combined with the OBEY routines. A flow diagram of an OBEY program is shown in Figure 11. This program, called DECAY.OY, is used for calculating phosphorescence lifetimes ranging from 0.060 ms to 600 ms.

The intensity $(I_p)_t$ at any time, t , after extinguishing the excitation radiation is related to the initial intensity $(I_p)_o$ by the

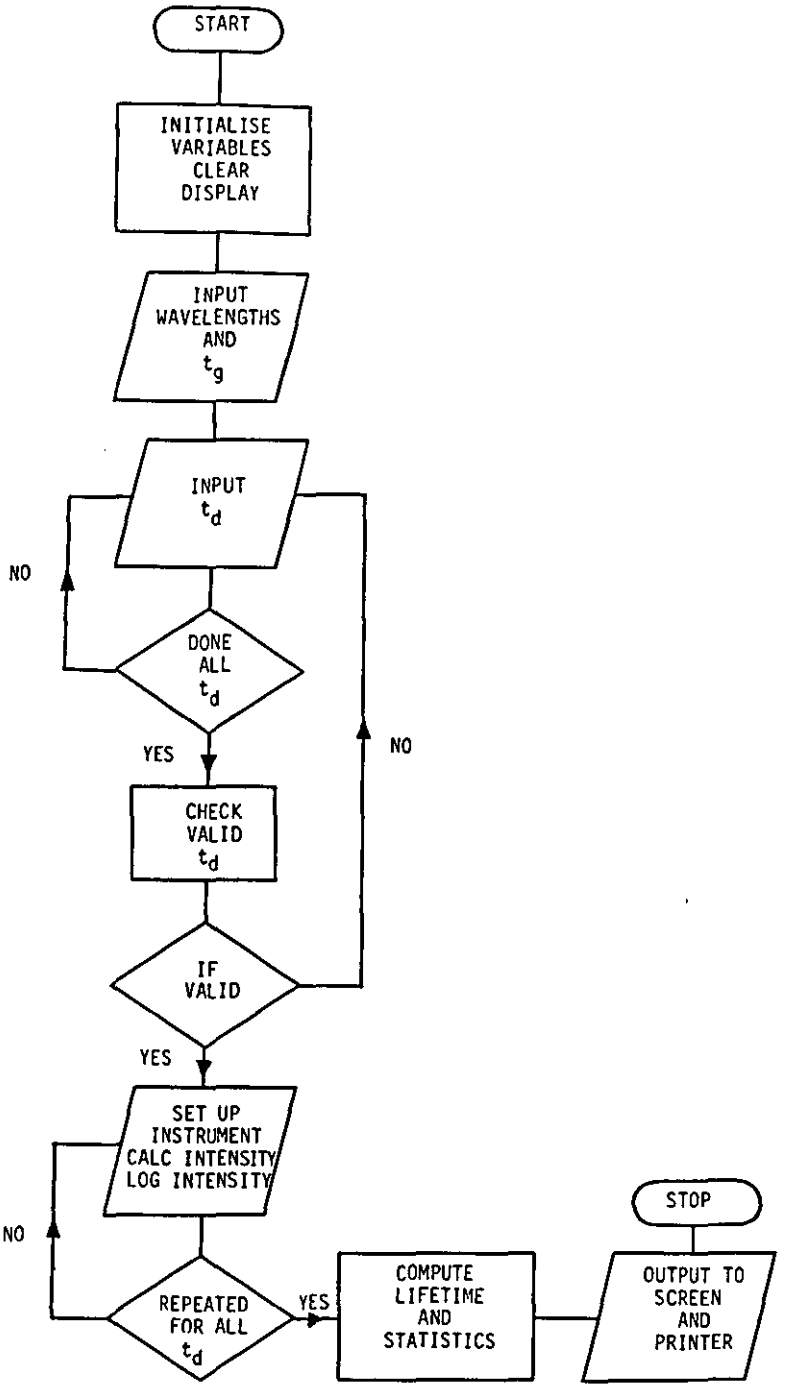

Figure 11. Flow diagram of OBEY file DECAY.OY

following equation:

$$(Ip)_t/(Ip)_o = \exp(1 - {}^{t}/\tau p) \quad \ldots[19]$$

Thus a plot of ln $(Ip)_t$ versus, t, should give a straight line with a slope of $- {}^{1}/\tau p$.

DECAY.OY controls the Model LS-5 with user defined delay times, t_d, and gate times, t_g; integrates the intensity at each delay time; calculates the log intensity; fits a straight line to the points and calculates the lifetime, together with goodness of fit and standard deviation. A typical printout is shown in Appendix I.

For longer lived species the decay curve is obtained by recording the luminescence signal after cutting off the exciting light with the shutter. The data is recorded in TDRIVE mode of the software with an instrumental response of 0.5 s and a data interval of 0.2 s. A typical decay curve is shown in Appendix II.

The fluorescence and phosphorescence quantum yields were calculated using an OBEY program called QYLDP.OY - a listing of which is shown in Appendix III. From this program the corrected excitation and emission spectra can be obtained, together with a print-out of the results; Appendix IV.

Spectra were either printed using a Model PP-1 high resolution thermal printer or using a Model 660 thermal printer for a VDU screen dump. Spectra from the latter are limited by the resolution of the VDU rather than the recorded spectra.

2.3 Materials and Reagents

2.3.1 Inorganic and Organic Materials

The inorganic and organic materials used in these studies are listed in Table 3.

2.3.2 Working Solutions

Solvents for use at room and particularly at low temperature must have a very low intrinsic luminescence. Ideally for low temperature work, the frozen solution should not form opaque 'snowed' matrices.

For aromatic hydrocarbons the most suitable solvent was methylcyclohexane. However, even spectroscopic grade was found to have an unacceptably high background. Several procedures were used to reduce the background; amongst the most successful were:

a) Fractionation; followed by storage over concentrated sulphuric acid for one week; washing with distilled water; followed by fractionation. The first quarter and last quarter were discarded and retained for further cleaning.

b) Passing spectroscopic grade or even AnalaR grade down a column consisting of 50% silica and 50% alumina. A hundredfold decrease in the background is obtained with, therefore, considerable improvements in the detectability.

TABLE 3

Inorganic and organic materials

Compound	Supplier	Purity	Batch No.
Pyrene	Applied Photo Physics	Zone Refined	-
Quinine bisulphate	BDH	AnalaR	1371090
9,10-Diphenylanthracene	Aldrich	Gold Label	052757
Rhodamine 101	Applied Photo Physics	97%	-
Anthracene	Applied Photo Physics	Zone Refined	-
Benzene	BDH	AnalaR	5623790A
Florene	Applied Photo Physics	Zone Refined	-
Pyrene	Applied Photo Physics	Zone Refined	-
9-Methylanthracene	Applied Photo Physics	Zone Refined	-
Naphthalene	BDH	Lab Grade	2316540
1 Br-naphthalene	Koch Light	Pure	6436
Tetraphenylbutadiene	Aldrich	99%	030637
Triphenylene	Aldrich	98%	30317
Sodium Salicylate	BDH	AnalaR	1809710
Lucifer yellow	Sigma	Lithium Salt	L0259
Fluorescein	BDH	Lab Grade	1981170
Benzophenone	BDH	Lab Grade	0270830
Coronene	Aldrich	99%	C8000-8
$Eu(TTA)_3$	Eastman	-	A8A
Terbium chloride	Aldrich	99.999%	1118
Gadolmium chloride	Aldrich	99.999%	0408
L-Tryptophan	Sigma	LAA-21	31F9006
L-Tyrosine	Sigma	LAA-21	31F9006
L-Phenylalanine	Sigma	LAA-21	31F9006

Table 3 Contd.

Compound	Supplier	Purity	Batch No.
Transferrin	Sigma	Iron free	12F0651
Conalbumin	Sigma	Iron free	39C-800
$Y_2O_3:Eu^{3+}$	Thorn EMI	-	-
Aluminium nitrate	HW	AnalaR	230509
Uranyl nitrate	BDH	AnalaR	6874980
Tributylphosphate	BDH	Lab Grade	5550260A
Orthophosphoric acid	BDH	AnalaR	5822200B
Trioctylphosphate	FLUKA	Lab Grade	-
Trioctylphosphine oxide	Aldrich	79%	31952
Ferric nitrate	BDH	AnalaR	5795710B
Manganous sulphate	BDH	AnalaR	230076
Sodium chloride	BDH	AnalaR	0798702
Ethanediol	Aldrich	99%+	26131
Cyclohexane	BDH	Spectroscopic	various
Methylcyclohexane	BDH	Spectroscopic	various
Hexane	BDH	Spectroscopic	various
Perchloric acid	BDH	AnalaR	10176
Sulphuric acid	BDH	AnalaR	6027150C
Nitric acid	BDH	AnalaR	6832830
Ethylacetate	BDH	Aristar	2585450

For aqueous work, for example, in the measurement of amino acids and proteins, qualitative information could be obtained from the frozen snows of the buffer solutions. However, for quantitative work a clear glass is necessary and hence 50% aqueous ethanediol was used. This solvent has been found by other workers to be best in terms of low background luminescence, unreactivity and its highly hydrophilic nature. From the work of Barel and Glazer (1969) and others it has been concluded that ethanediol has no great effect on the conformation of the protein in an aqueous solution. In addition, from the work of Kuntz (1971) and Strickland et al (1969) it can be assumed that studies on proteins at low temperature are comparable to those carried out at room temperature.

Amino acids and protein solutions were always freshly prepared prior to use, although experiments showed that solutions frozen at -7° were stable for many weeks. Stock solutions of the aromatic hydrocarbons were stable indefinitely when stored at -7° and kept in the dark. Stock solutions of terbium and gadolinium chloride were acidified with hydrochloric acid to give a 0.1M solution. Stock solutions of uranyl nitrate were similarly acidified, but with nitric acid.

A pH 8.0 buffer with 50% ethanediol was prepared from Tris buffer at 50mM, together with 5mM sodium hydrogen carbonate. The pH of the buffer was checked with an EI Ltd Model 7020 meter.

For quantum yield measurements stock solutions were made to be approximately 0.8A per cm. Solutions were diluted below 0.01A for fluorescence measurements in 1cm pathlength cuvettes. Solutions were below 0.05A for measurements in the 4 mm OD, 2 mm ID phosphorescence cells.

CHAPTER 3

RELATIVE LUMINESCENCE QUANTUM YIELDS

3.1 General

The most widely used method of determining quantum yields is the relative method. The quantum yield of the unknown, ϕ_x, is calculated according to the following equation, Parker and Rees (1960):

$$\phi_x = \phi_R \cdot \frac{A_R}{A_x} \cdot \frac{E_x}{E_R} \cdot \frac{I_R}{I_x} \cdot \frac{n^2_x}{n^2_R} \qquad \ldots[20]$$

ϕ_R is the quantum efficiency of the reference, A is the absorbance of the solution, E is the corrected emission intensity, I is the relative intensity of the exciting light and n is the refractive index of the solvent. Subscripts R and x refer to the reference and unknown respectively.

The use of equation [20] relies on using the same excitation wavelength for both reference and standard. However, assuming that the quantum yield is independent of the excitation wavelength, Vavilov (1927) then the reference and unknown may be excited at different wavelengths providing that the relative intensity of the excitation light is unity at the different wavelengths. This can be accomplished by using a Rhodamine quantum corrected reference system. Melhuish (1962). Equation [20] can then be simplified to:

$$\phi_x = \phi_R \cdot \frac{A_R}{A_x} \cdot \frac{E_x}{E_R} \cdot \frac{n^2_x}{n^2_R} \qquad \ldots[21]$$

A number of factors can affect the measurement of relative quantum yields and are:-

a) polarisation

b) refractive index changes

c) internal reflection

d) re-absorption of the emission

e) temperature

f) purity

g) radiationless deactivation by, for example, oxygen

h) variation of optical density with bandwidth

i) calibration errors between UV absorption and fluorescence spectrometers

Cehelnik et al (1975) and Poole and Findeisen (1977) reviewed the effect of polarisation on fluorescence measurements with the conclusion that four independent variables need be considered. The first is F, the polarisation of the light reaching the sample. The second is the emission anisotropy, r, of the sample. The third is G, the ratio of the sensitivities of the detection system to vertically and horizontally polarised light and which varies with wavelength. Fourth is the viewing angle, α, which the angle between the excitation and emission beams.

Almgren (1968) and Shinitzky (1972) showed that the fluorescence intensity is unaffected by the emission anisotropy if a viewing angle of $\cos^{-1}\sqrt{1/3}$ is chosen, i.e. 54.7°. Providing the emission spectra of the sample and reference do not differ greatly with respect to wavelength then the effects of G will be minimal. The effects of polarisation

are much greater when measuring quantum yields at low temperature, particularly when the viscosity of the solvent changes drastically. The emission anisotropy is strongly dependent on the viscosity. Azumi and McGlyn (1962) recommended placing polarisers in both beams to measure F, G and r to calculate the true emission. However, if polarisers are used then care should be taken to account for the wavelength dependence of the transmission of the polarisers. Paloetti and Lapecq (1969) discussed the various factors required to correct for errors in fluorescence polarisation measurements. Using non viscous solvents such as methylcyclohexane helps to produce a non-isotopic emission.

Refraction index corrections have been reviewed by Chen (1981) Busselle et al (1980) and Morris et al (1976). The conclusion was that the refractive index correction derived by Hermans and Levinson (1951) and discussed by Cundall and Pereira (1972) is very dependent upon the geometry of the source image and its relation to monochromator entrance slit and that no general correction factor can be applied.

Ware and Rothman (1976) attempted to overcome the errors associated with polarisation and refractive index changes by using an integrating sphere. Melhuish (1961) demonstrated that by using a cuvette with the sides and back painted black much of the internal reflection errors can be eliminated. Working at very dilute absorbances (less than 0.05A in a 10 mm pathlength cuvette) or extrapolating to zero absorbance eliminates re-absorption errors, Arbeloa (1980). By applying a correction for solute absorbance it is possible to produce an absorbance corrected fluorescence curve which is linear up to absorbances as high as two, Holland et al (1977).

Temperature must be constant as many fluorophores exhibit a negative temperature dependence and hence the quantum yield is affected, Mantulin and Huber (1973). High purity materials, both solutions and solvents, are essential. Traces of absorbing impurities cause problems, particularly when the sample has a low absorption. Plastic vessels should be avoided at all costs since leaching of plasticisers readily occurs. Quenching from dissolved oxygen, particularly on compounds with relatively long lived fluorescence lifetimes, may be appreciable. Oxygen quenching may be overcome by degassing with pure nitrogen prior to measurement. Quenching by halide ions on for example, quinine sulphate must be taken into account.

The errors associated with measuring the absorbance values are based upon the difference in characteristics between the UV/VIS absorption spectrophotometer and the fluorescence spectrometer. Unless two identical monochromators are used, errors may arise from two sources:

a) The effect of spectral bandwidth on the shape of the UV absorption spectrum, hence the absorbance, and the shape of the fluorescence spectrum, hence the relative fluorescence intensity. For example, the UV absorption spectrum of pyrene in n-hexane for two different slit widths is shown in Figure 12. This illustrates the change in absorbance values and peak ratios which occur as the spectral bandwidth is changed. Unless the fluorescence spectrometer has an identical monochromator the excitation spectra will also be different, Bendig et al (1980).

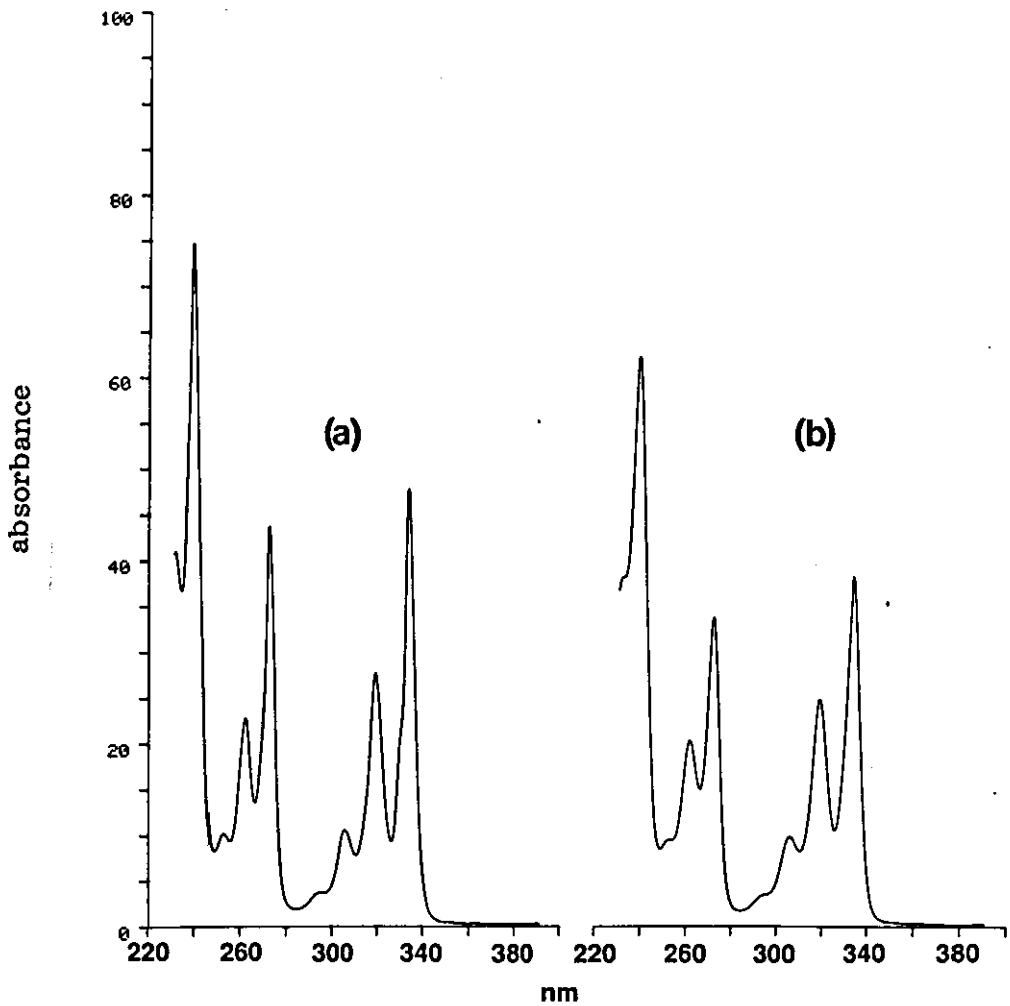

Figure 12. UV absorption spectra of pyrene in hexane measured with (a) 2nm bandwidth and (b) 4nm bandwidth

b) Wavelength accuracy is particularly important where sharp absorbance/excitation bands occur. For pyrene a 0.5 nm error in the excitation wavelength at 241 nm will result in a 7% intensity error. For a 1 nm difference the error is 15%.

Because of these likely differences in the bandwidths and spectral distributions of the light sources, several methods have been proposed to overcome the differences such as a computer controlled combination UV absorption-fluorescence spectrometer, Holland et al (1973). In a later paper (1977), the same authors proposed a means of applying corrections for solute absorbances and to produce an absorbance corrected fluorescence curve which is linear up to absorbances as high as 2.

An automated system for measuring quantum efficiencies as a function of photon energy has been described in which a standard photocell measured part of the excitation beam, Schmidt-Ott and Meier (1977). Britten et al (1978) presented a method where the absorbance of a solution was determined by measuring the fluorescent intensities at two points along the absorbance path. Gains and Dawson (1979) used absorptivity related constants derived from the apparent approximately hyperbolic relationship between fluorescence and concentration. Upton and Cline-Love (1979) used a more sophisticated technique of time correlated single photon counting.

3.2 Room Temperature Fluorescence

3.2.1 Absorbance Spectra

The errors associated with measuring absorbance values are overcome by using the same instrument to measure fluorescence

spectra as absorbance values, Rhys Williams et al (1983B). The LS-5 is effectively turned into a single beam absorption spectrometer. A mirror placed at the sample focus is used to focus excitation light into the emission monochromator. The light needs to be heavily attenuated with a wire mesh gauze to prevent overloading of the sample photomultiplier. A 10 mm pathlength cuvette is placed in the reflected beam and, by synchronously scanning both monochromators at the same wavelength, a transmission spectrum is obtained.

By dividing the sample spectrum by a reference spectrum a transmission spectrum is obtained. For example, Figure 13 shows the luminescence spectrum of a holmium oxide standard. The latter is converted to an absorbance spectrum and Figure 14 compares the absorbance spectrum of pyrene in n-hexane as measured on the Model LS-5 with the excitation spectrum. The spectra were measured with a 2.5 nm bandwidth.

Table 4 compares the ratios of the main peaks as measured on the UV absorption spectrometer and the Model LS-5. Excellent agreement between the UV absorption and fluorescence spectra is observed. In addition the values fall midway between the two values observed on the UV spectrometer run at 2 nm and 4 nm bandwidth.

A correlation plot between absorbances measured on a UV absorption spectrometer and the Model LS-5 showed excellent agreement for 0 to approximately 0.6A, Figure 15.

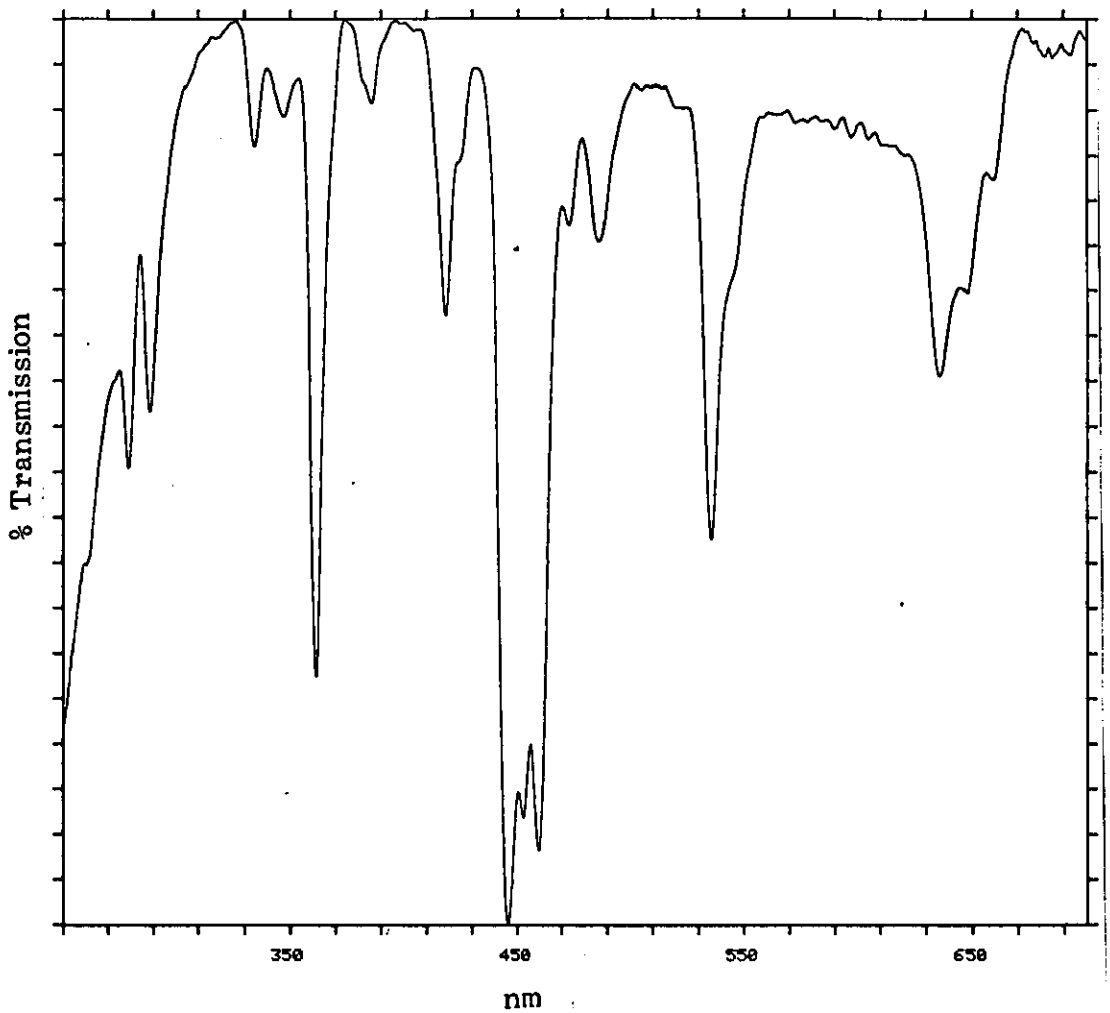

Figure 13. Transmission spectrum of a holmium oxide standard measured with a Model LS-5

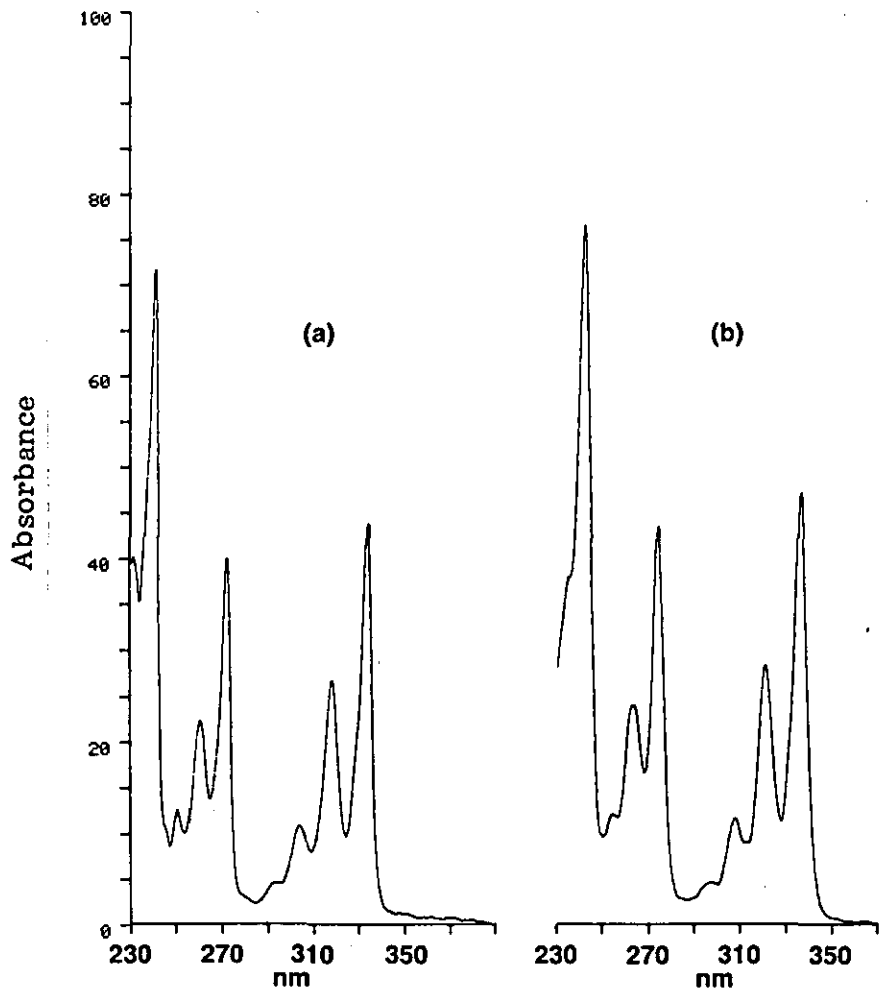

Figure 14. (a) The absorbance spectrum and (b) the excitation spectrum of pyrene in hexane as measured on the Model LS-5

TABLE 4

Comparison of peak heights of pyrene in n-hexane using a Model Lambda 5 UV absorption spectrometer and the Model LS-5

Ratio of Peaks Lambda 5	Bandwidth 2nm	4nm
241/273	1.733	1.851
241/335	1.585	1.632

Ratio of Peaks LS-5	Absorption 2.5 nm	Fluorescence 2.5 nm
241/273	1.786	1.779
241/335	1.632	1.634

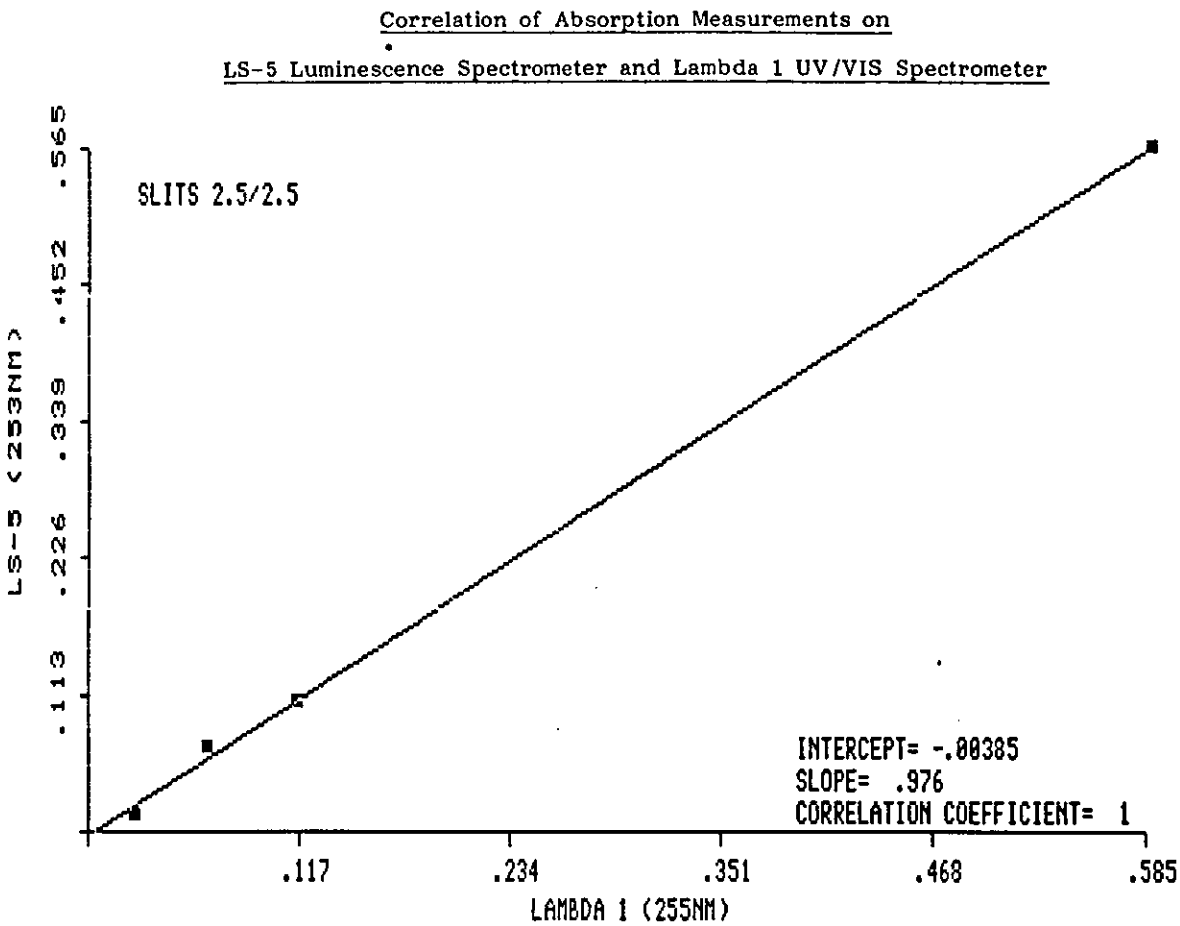

Figure 15. Correlation of absorption measurements on a Model LS-5 Luminescence Spectrometer and on a Lambda 1 UV/VIS Absorption Spectrometer using anthracene in cyclohexane

3.2.2 Quantum Yield Standard

The choice of primary quantum standard is particularly important, Velapoldi (1972), Birks (1976). Quinine sulphate is still regarded as the best available, although it has a number of disadvantages such as quantum yields which vary with the type and normality of acid concentration. O'Connor and Phillips (1982) have found that quinine exhibits a 2 component emission decay.

Velapoldi and Mielenz (1980) in a National Bureau of Standards publication recommended quinine sulphate in 0.1M Perchloric acid be used in certification measurements. In this solvent the quantum yield appears to be independent of acid concentration. A quantum yield of 0.59 is suggested at an excitation of 347 nm for a 1 $\mu g\, mL^{-1}$ solution. This compares with a value of 0.56 in 1.0 M sulphuric acid. When measuring quantum yields of aromatic compounds in organic solvents, 9,10-diphenylanthracene (9,10-DPA) in degassed cyclohexane has been proposed, Heinrich et al (1974). In this solvent the quantum yield is reported as being unity.

For biochemical applications, tryptophan has been suggested, Borreson and Parker (1966). However, there is great controversy in deciding what the quantum yield should be. Other disadvantages are photochemical instability, overlap of absorption and emission and a marked temperature dependence.

To determine quantum efficiency of powders Bril and De Jager-Veenis (1976 A/B) recommended sodium salicylate for the UV region and lunogen T red for the visible.

3.2.3 Corrected Emission

Emission spectra are uncorrected and hence a correction curve must be generated to compensate for the unique and non linear response of the detection system. The latter arises from the dispersion of the monochromator, the spectral response of the sample photomultiplier and any light losses, White et al (1960), Ritter et al (1981). The correction curve can be prepared by using:

a) a source of known spectral distribution

b) a thermopile or bolometer

c) a series of compounds of known emission spectra

d) a fluorescent quantum counter

Of these methods (a) is more widely used and can take two forms. Calibrated tungsten lamps of accurately measured spectral radiance are available from the National Bureau of Standards or the National Physical Laboratory. However, care has to be taken in the use of a standard lamp, Christensen and Ames (1961). As the excitation monochromator of the Model LS-5 gives corrected excitation spectra, it can be used as a light source of known spectral distribution, Parker (1962). Calibration curves obtained by this method agree very well with those obtained by the use of a standard lamp, Chen (1967B).

Over the region 250 nm to 410 nm light from the excitation monochromator is reflected into the emission monochromator using a diffuser and both monochromators scanned synchronously at the same wavelength. A fresh layer of M O has been proposed as a scatterer since, according to Drushel et al (1963), its

reflectivity does not vary by more than a few percent over the range 200 nm to 500 nm. Grum and Luckey (1967) proposed $BaSO_4$ as reflectance standard. Since the excitation and emission monochromators will not precisely pass the same wavelength as they are synchronously scanned, the bandwidth of the emission monochromator is set to be 4 times greater than that of the excitation, i.e. 20 nm and 5 nm respectively as recommended by Melhuish (1972).

In order to overcome errors associated with second order radiation and the fact that the sharp emission lines of xenon at approximately 470 nm, make precise correction difficult, the correction curve from 410 nm to 630 nm is generated by comparing the emission spectrum of quinine sulphate run under identical conditions with that published by Velapoldi and Mielenz (1980).

Both correction curves are merged using the PECLS II software to give an emission correction curve. Figure 16 A/B shows the correction curve for a red sensitive photomultiplier.

The shape of the curve is determined in part by the efficiency of the emission grating, the response of the photomultiplier and to a minor extent by the reflectivity of the various mirrors.

3.3 Results

A series of compounds in a variety of solvents were prepared and the UV absorption measured using the method described above. The solutions were prepared so that their absorbances ranged between 0.3A

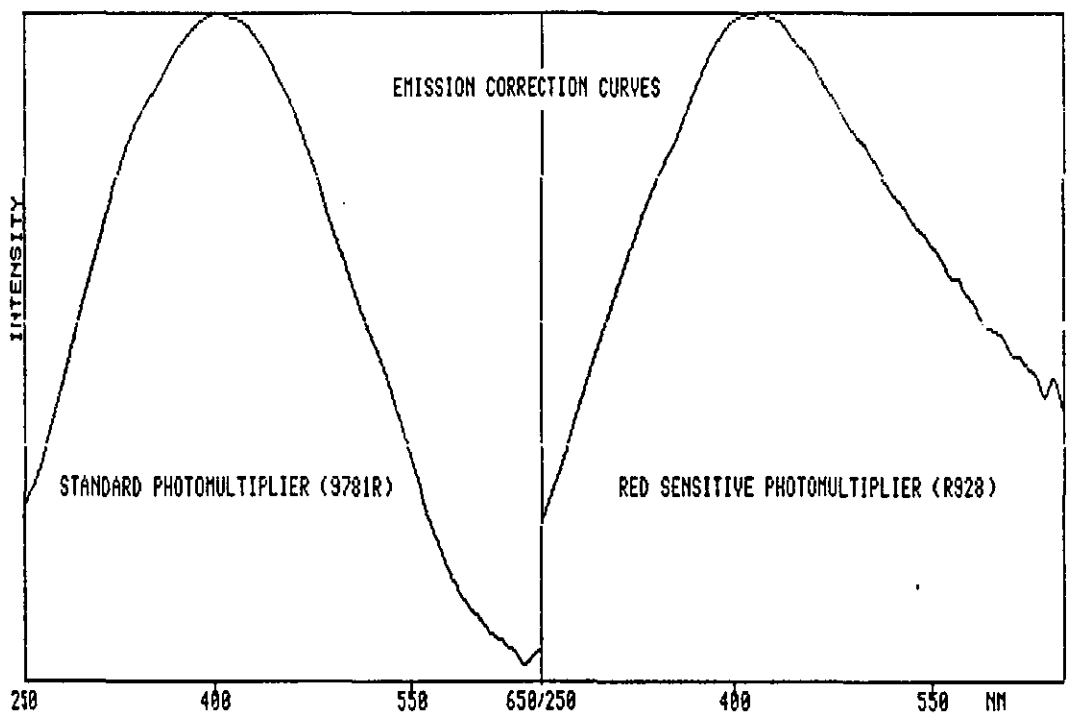

Figure 16. a) Correction curve for standard photomultiplier and

b) Correction curve for red sensitive photomultiplier

and 0.8A and were then accurately diluted to give absorbances in the range 0.005A to 0.01A, i.e. within the expected linear calibration range of fluorescence emission versus concentration.

The emisson spectra were measured using an instrumental bandwidth of 2.5 nm and corrected using the correction curve in Figure 16B. Solvent spectra were subtracted, the area under the corrected emission spectra measured and the fluorescence quantum yields calculated according to equation [21].

The results are shown in Table 5 compared with some literature values. Certain of the compounds, namely coronene and pyrene, showed a marked dependence upon the presence of oxygen, Melhuish (1961B). Their parent, phenanthrene, is also quenched by oxygen, Berlman (1971). Repeated measurements on 9,10-DPA gave an average fluorescent quantum yield of 0.96. This contrasts with the value given by Heinrich et al (1974) or Ware (1976) of 1.00, but is in agreement with the fact that the emission spectrum overlaps the absorption band, thus leading to reabsorption errors.

The variation in quantum yield of quinine sulphate with normality and acid type is shown in Table 6 and is in excellent agreement with the data published by Velapoldi and Mielenz (1980). The corrected excitation and emission spectra of quinine sulphate are shown in Figure 17. The corrected excitation and emission of 9,10-diphenyl anthracene in cyclohexane are shown in Figure 18.

TABLE 5

Experimentally obtained room temperature fluorescence quantum yields compared with some literature values

Compound	Solvent	Ex nm	Em Range nm	Standard Q_R	Q_F	Literature Values Q_F	Solvent	Reference
Anthracene	MCH	252	360-510	DPA (1.00)	0.31	0.33	H	Guilbault (1973)
Benzene	MCH	254	270-360	DPA (1.00)	0.03	0.05	H	Dawson (1968)
Coronene	MCH	303	400-500	DPA (1.00)	0.06 0.18	(before degassing) (degassed)		
Fluorene	MCH	265	280-400	DPA (1.00)	0.71	0.54	H	Weber (1957)
Pyrene	C	241	350-550	DPA (1.00)	0.16 0.31	(before degassing) 0.32	 C	Berlman (1965)
9,10-DPA	C	262	360-540	QS (0.59)	0.96	1.00	C	Heinrich (1976)
9-MA	C	256	300-500	DPA (1.00)	0.42	0.42	H	Lim (1966)
Naphthalene	H			DPA (1.00)	0.014			
TBP	C	346	360-580	DPA (1.00)	0.84	0.86	PA	Adams (1980)
Triphenylene	H			DPA (1.00)	0.015			

Table 5 contd.

Compound	Solvent	Ex nm	Em Range nm	Standard Q_R	Q_F	Literature Values Q_F	Solvent	Reference
Sodium salicylate	1M NaOH	302	340-550	QS (0.59)	0.25	0.25	NaOH	Inokuchi (1964)
Lucifer Yellow	W	430	460-630	QS (0.59)	0.20	0.24	W	Stewart (1980)
Fluorescein	1M NaOH	460	470-620	QS (0.59)	0.82	0.84	0.1M NaOH	Olmsted (1979)

The reproducibility of recovery and calculating the quantum efficiency of the same solution is within 3-6%.

9,10-DPA, 9,10-diphenylanthracene

9-MA, 9-methylanthracene

TPB, tetraphenylbutadiene

QS, quinine sulphate

C, cyclohexane

H, hexane

MCH, methylcyclohexane

PA, photoacoustic spectroscopy

W, water

TABLE 6

Relative fluorescence quantum yields of Quinine Sulphate 0.2 μg mL^{-1} in various acids using a value of 0.59 in 0.1 M $HClO_4$

	HNO_3	$HClO_4$	H_2SO_4
1M	0.51	0.59	0.58
.1M	0.57	0.59	0.55
.01M	0.58	0.58	0.53

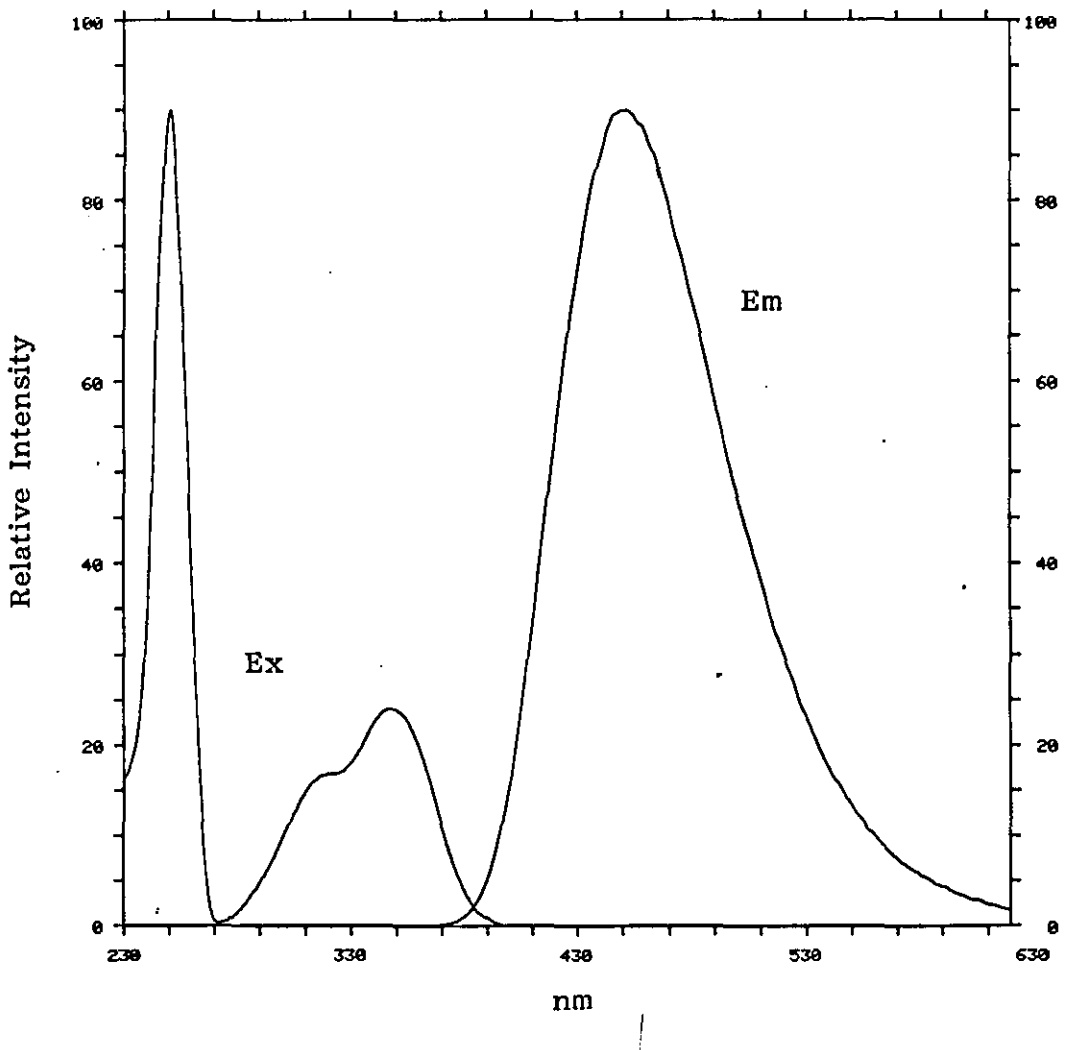

Figure 17. Corrected excitation and emission spectra of quinine sulphate, 0.2 μgmL^{-1} in 0.1M $HClO_4$, as measured on the Model LS-5.

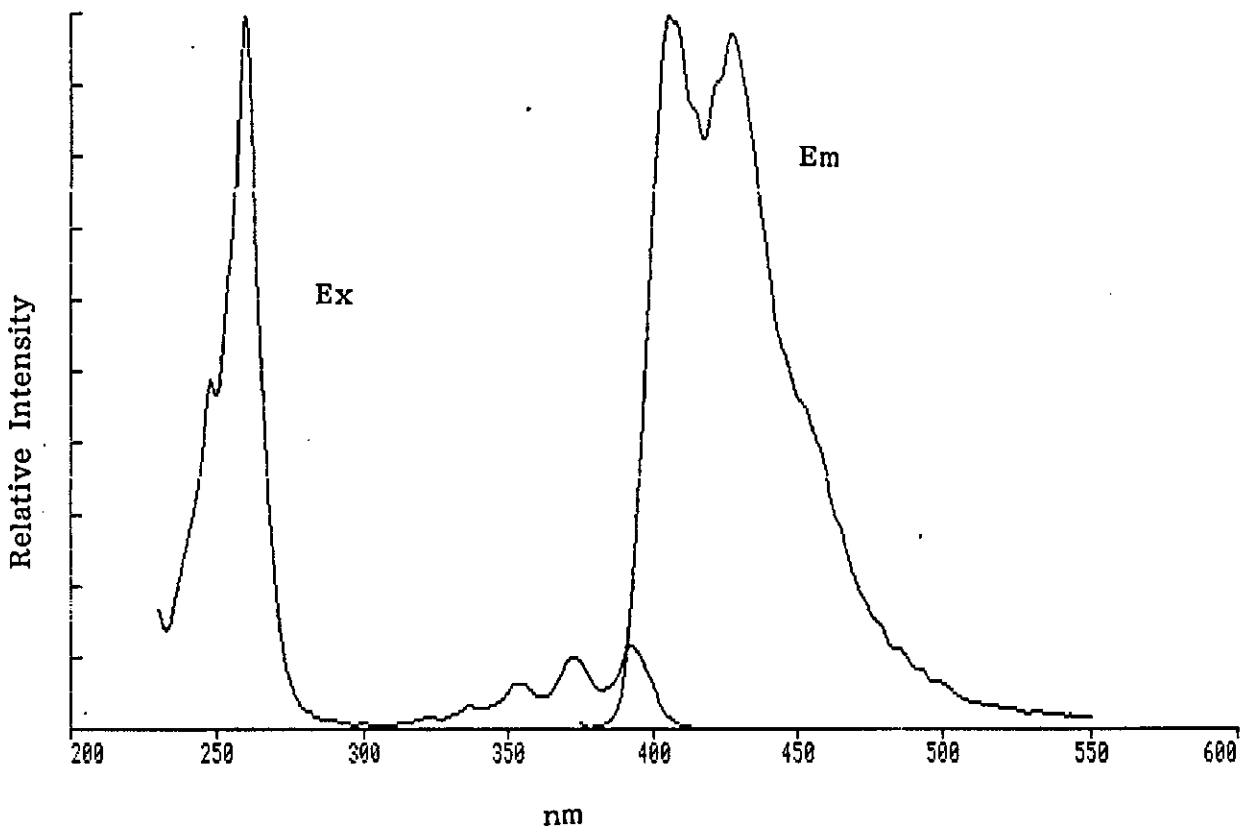

Figure 18. Room temperature corrected excitation and emission spectra of 9,10-diphenylanthracene in cyclohexane

CHAPTER FOUR

LOW TEMPERATURE LUMINESCENCE QUANTUM YIELDS

4.1 General

The majority of low temperature fluorescence and phosphorescence quantum yields are measured on a relative basis. The standard may either be a fluorophore such as 9,10-diphenylanthracene (DPA) or a phosphorescing compound such as benzophenone dissolved in CCl_4, Winnick and Lemire (1977).

A direct measure of quantum yields at low temperature has been proposed by Gilmore et al (1952, 1955) by means of measuring the luminescence from an EPA glass with light scattered by a magnesium oxide surface. Kellogg and Bennett (1964) proposed the use of triplet to singlet energy transfer. The latter depends upon the overlap of the donor emission with the acceptor absorption band. Measurements are made of the donor phosphorescence to fluorescence ratio in the absence and presence of the acceptor.

In this work the luminescence efficiencies are calculated on a relative basis using 9,10-DPA as the standard.

4.2 Conduction Cooling

Low temperature fluorescence and phosphorescence spectra and phosphorescence lifetimes were measured using the conduction cooling device as described in Chapter 2.1.3, Rhys Williams et al (1983C). Thermocouples placed in various points around the sample indicated that the temperature of that portion of the

sample tube which is in the optical window has a temperature between 79 - 81K. This compares with a figure of 92 - 97K found by Weinryb and Steiner (1970) for a sample immersed in liquid nitrogen in a conventional Dewar flask.

Experiments showed that samples cooled within 30 s of immersion in the accessory, Figure 19, and maintained a constant signal for 200 s. The reproducibility as determined by the repeated freezing, withdrawing and thawing, then freezing of a sample of 9,10-DPA in methylcyclohexane was better than 5%.

4.3 Relationship between the observed phosphorescence (P) and the total phosphorescence intensity (P_T)

The relationship between the observed phosphorescence and the total phosphorescence intensity is governed by the type, characteristics and geometry of the phosphoroscope and also the decay time, τ, of the phosphorescent species. Traditionally phosphorescence is measured using a mechanical system to discriminate between phosphorescent and fluorescent signals. Parker and Hatchard (1962) used two rotating discs, one in each of the excitation and emission beams. 16 slots were cut in each disc which were driven by synchronous motors at 3000 rpm. For this combination of speed and slot a chopping frequency of 800 hz is obtained, which is sufficient for measuring the intensity and spectra of long lived species. The diagrammatic relationship between chopper phase and phosphorescence intensity is shown in Figure 20. Assuming that the phosphorescence signals decay exponentially and that the cut off time of the exciting light by the first chopper is small compared with the frequency of the

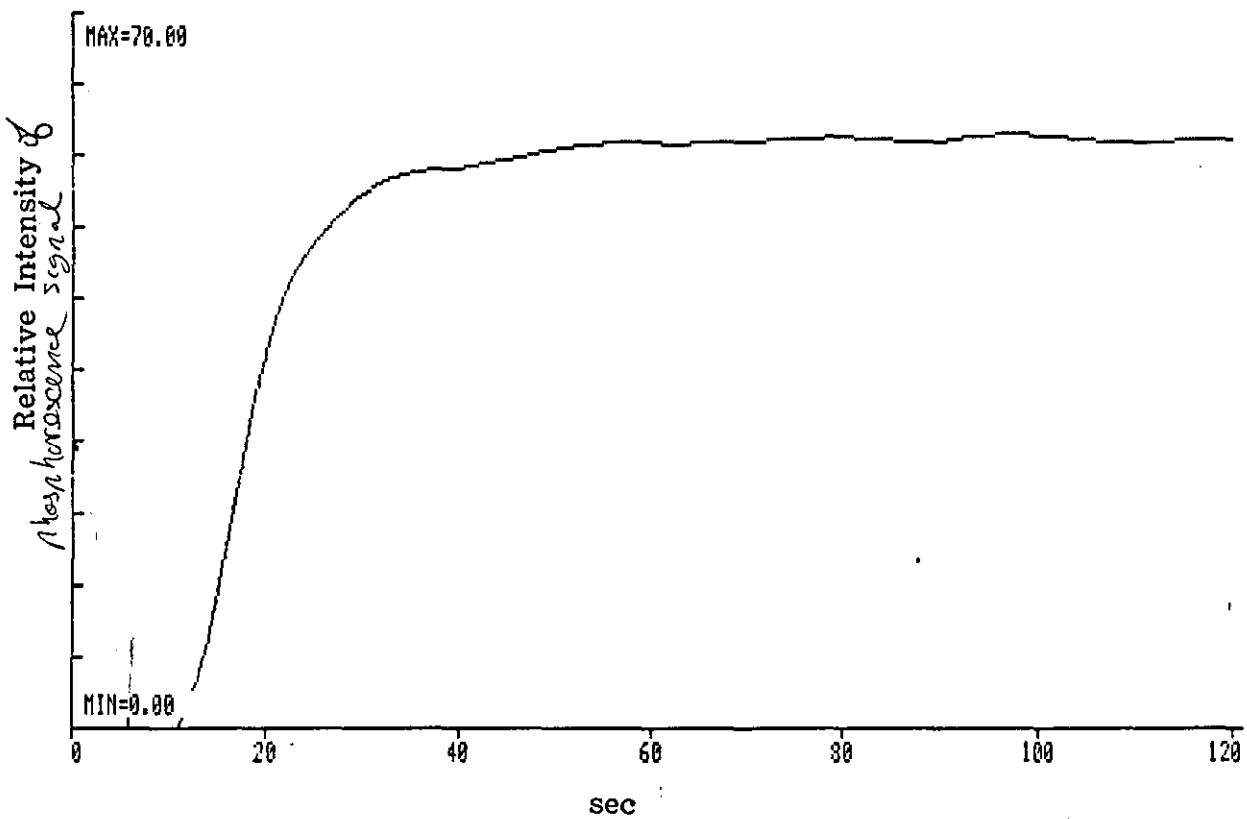

Figure 19. Rate of cooling of a sample of tryptophan in 50% ethanediol from room temperature to 77 K

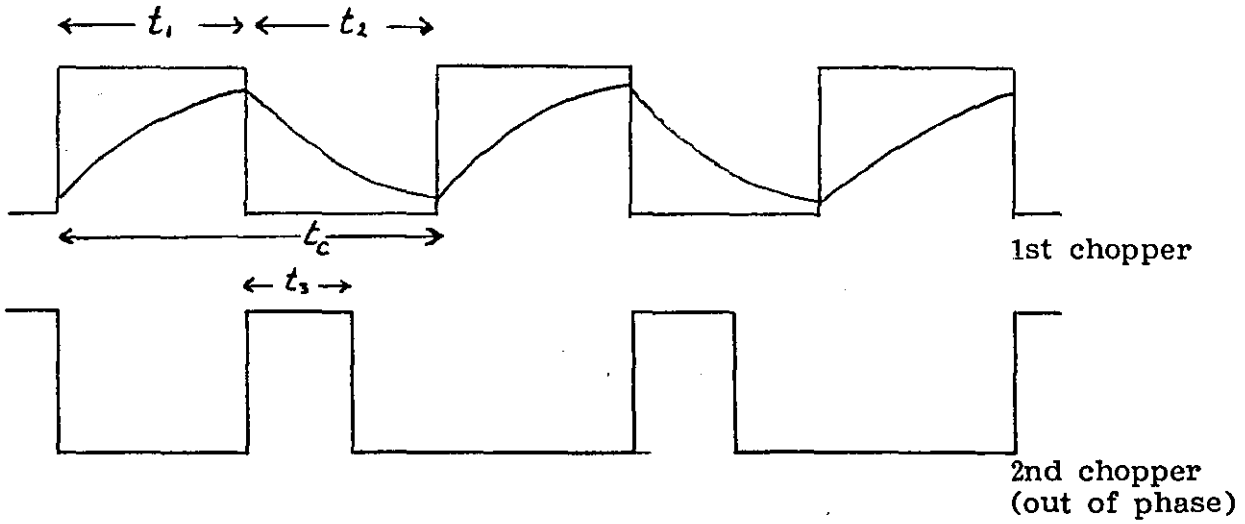

FIGURE 20. Diagrammatic relationship between chopper phase and phosphorescence intensity with respect to equation [22].

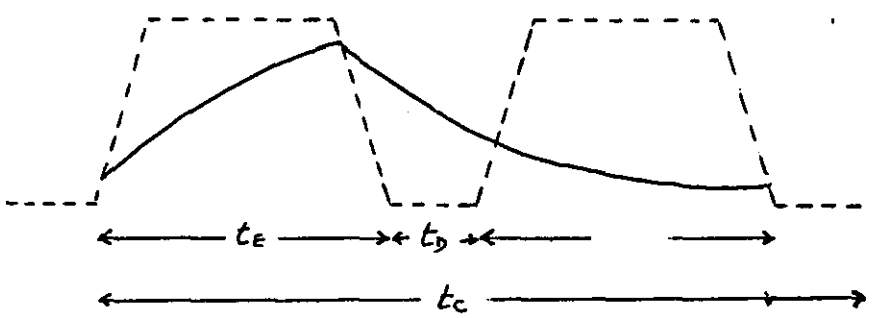

where t_E exposure time

t_D shutter delay time

t_c time for one cycle

FIGURE 21. Diagrammatic relationship between chopper phase and phosphorescence intensity with respect to equation]23].

cycle then the phosphorescent factor is given by:

$$\frac{P}{P_T} = \frac{\tau}{t_1}\left[\frac{1 - \exp^{(-t_1/\tau)}}{1 - \exp^{(-t_c/\tau)}}\right] X$$

$$\left[\exp^{(-(t_2 - t_3)/2\tau)} - \exp^{(-(-t_2 + t_3)/2\tau)}\right] \quad \ldots[22]$$

Thus, for $t_c = {}^1/800$ s and $t_1 = t_c/4$ and $t_3 = t_c/3$, the following values of P/P_T for various τ values are calculated:

τ ms	>5	1	0.5	0.10
P/P_T	0.33	0.32	0.27	0.02

For the conditions shown, if the lifetime is long compared with t_1, t_2 and t_3 the decay of the intensity during the time t_2 will be small, i.e. the intensity during one cycle will be virtually constant. The factor needed to multiply the observed phosphorescence to calculate the total phosphorescence will be relatively small. However, for fast decays the intensity will have reduced considerably between each cycle and the factor, therefore, would be large.

The expressions for a rotating can phosphoroscope and a rotating disc phosphoroscope derived by O'Haver and Winefordner (1966A), included a correction for the transit time of the shutter mechanism - a correction which Parker had assumed to be small. Figure 21 shows the diagrammatic relationship between chopper phase and phosphorescence intensity for a rotating can phosphoroscope.

$$\frac{P}{P_T} = \frac{\tau}{t_c} \times \frac{e^{\left(-t_d/\tau\right)}\left[1 - e^{\left(-t_E/\tau\right)}\right]^2}{1 - e^{\left(-tc/\tau\right)}} \qquad \ldots[23]$$

This equation can be extended to systems using a pulsed source and gated electronics, O'Haver and Winefordner (1966B). Figure 6 is the diagrammatic representation of the events taking place during one cycle of excitation and measurement with the Model LS-5. For the purposes of derivatising the equations, the excitation flash width t_f is considered to be very small compared with the decay time τ. For the Model LS-5 the flash halflife is less than 10 µsec and compares with phosphorescence lifetimes of 500 µs to 10's of seconds.

The total observed decay for a single exponential may be expressed by the following equation:

$$P_T = \int_0^\infty y_o e^{-t/\tau} dt \qquad \ldots[24]$$

where P_T is the total phosphorescence, y_o is the intensity at zero time and τ is the single exponential decay time. This may be evaluated as:

$$P_T = y_o/\tau \qquad \ldots[25]$$

The integrated phosphorescence intensity, P, during the line interval t_g, at a time t_d, after t_o, is given by the following expression:

$$P = y_o/\tau \left[\left[1 - e^{-\frac{(td + tg)}{\tau}}\right] - \left[1 - e^{-td/\tau}\right]\right] \qquad \ldots[26]$$

The fraction of light observed is then given by the ratio of equations [25] and [26]:

$$P_T/P = \frac{1}{\left(e^{-td/\tau}\right) - \left(e^{-\frac{(td+tg)}{\tau}}\right)} \qquad \ldots[27]$$

Equation [4] holds for a single pulse of excitation light and assumes that the source intensity immediately rises to its maximum value and also terminates instantaneously. Similarly, assumptions are made with regard to the opening and closing of the gate t_g. For a train of pulses with a cycle time of 20 msec, equation [4] becomes:

$$P_T/P = \frac{1 - e^{-20/\tau}}{(e^{-td/\tau}) - (e^{-(td+tg)/\tau})} \qquad \ldots[28]$$

where all times are in ms.

A plot of P_T/P for various lifetimes, with a fixed t_d and t_g is shown in Figure 22. The graph shows that almost all of the signal from short lived phosphors is measured whilst only a fraction of long lived phosphors are measured. For the same quantum efficiency short lived phosphors, τ ca. 10^{-3} sec will show an order of magnitude increase in intensity compared with long lived species τ ca. 10^{-1} sec.

Phosphorescence lifetimes in the range 60 µs to 250 ms are calculated by recording the intensity at various delay times using the program DECAY.OY. Lifetimes greater than 250 ms were measured by recording the decay of the luminescence signal after cutting off the exciting light. The data were recorded using the TDRIVE function with an instrumental response of 0.5 s and a data interval rate of 0.2 s. The standard deviation of measurements for short phosphors was found to be better than 10 µs and for long lived phosphors better than 0.1 s.

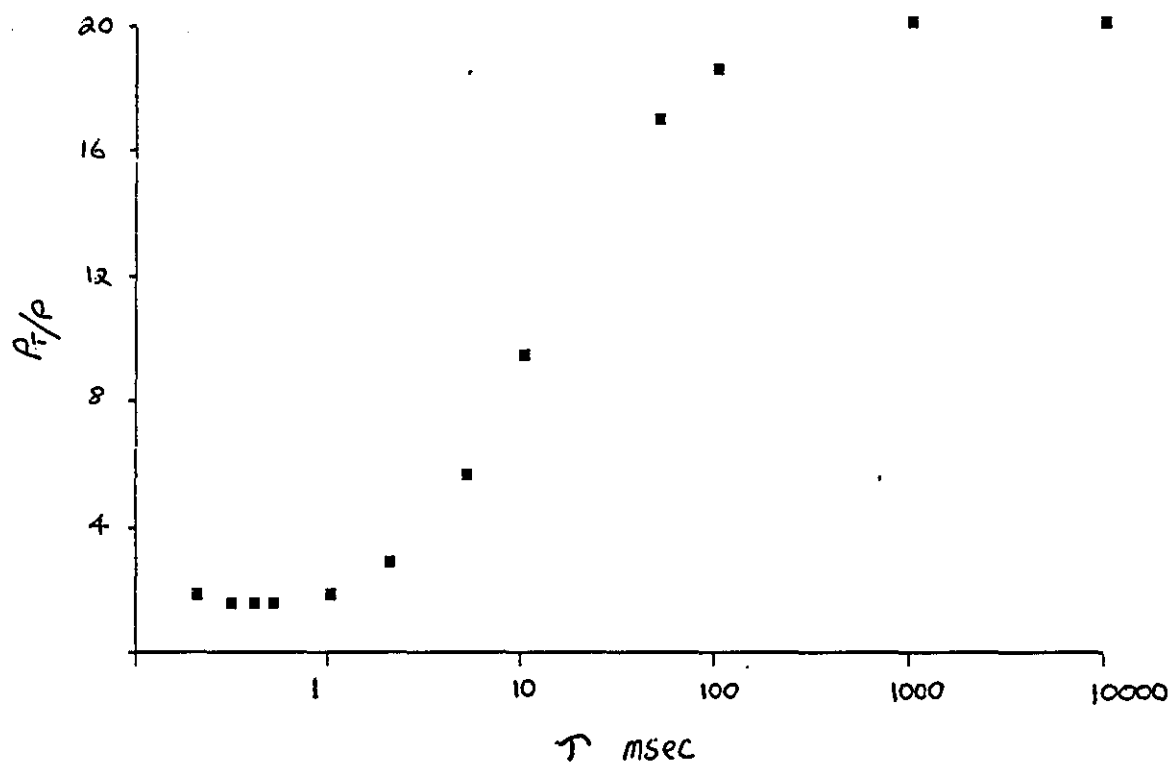

Figure 22. Variation of P_T/P (ratio of the total phosphorescence, P_T, to the integrated phosphorescence intensity, P), for different τ values (ms) measured with a t_d of 0.1 ms and a t_g of 1.0 ms

Confirmation of the equation for calculating the phosphorimeter factor was obtained by the following means. A terbium-transferrin complex was excited at 280nm and the area under the corrected emission spectrum of the terbium measured at various delay (t_d) and gate (t_g) times. The areas were multiplied by the appropriate factor to produce a mean result of 2513 with a coefficient of variation, 95% c.l., of 39.15, Table 7.

4.4 Results

Samples were degassed by passing a current of pure nitrogen through the solvent prior to detection and measurement. Certain aromatic hydrocarbons, for example, coronene and pyrene, exhibited a large difference in fluorescence quantum yields after degassing.

In a 2mm ID sample tube, up to 5 times, and in a 1mm ID, up to 10 times the standard solute concentrations can be used compared to a 10mm pathlength cuvette, Figure 22. This enables good signal to noise spectra and low background signals to be observed in the calculation of quantum yields. The observed peak intensity of the 9,10-DPA increased approximately 5 times on going from 293K to 77K. This increase is predominantly due to band sharpening, although an increase in the absorption coefficient cannot be ruled out, Figures 18 and 24.

The results of the quantum yield determinations are shown in Table 8, compared with some literature values. The reproducibility of measuring and calculating the quantum efficiency of the same solute at 77K is within 8 - 10%. Fluorescence quantum yields agreed within experimental error with those in the literature, with the exception of fluorene which Parker assumed to be a value of 0.54 at 298K and 77K.

TABLE 7

Determination of emission areas corrected for td, tg and τ

td ms	tg ms	Emission Area	Total phosphorescence emission
0.03	0.5	823	2508
0.1	0.5	791	2553
0.5	0.5	596	2570
1.0	0.5	359	2423
2.0	0.5	169	2589
3.0	0.5	78	2512
0.1	1.0	1286	2495
0.1	2.0	1851	2493
0.1	3.0	2087	2477
			2513

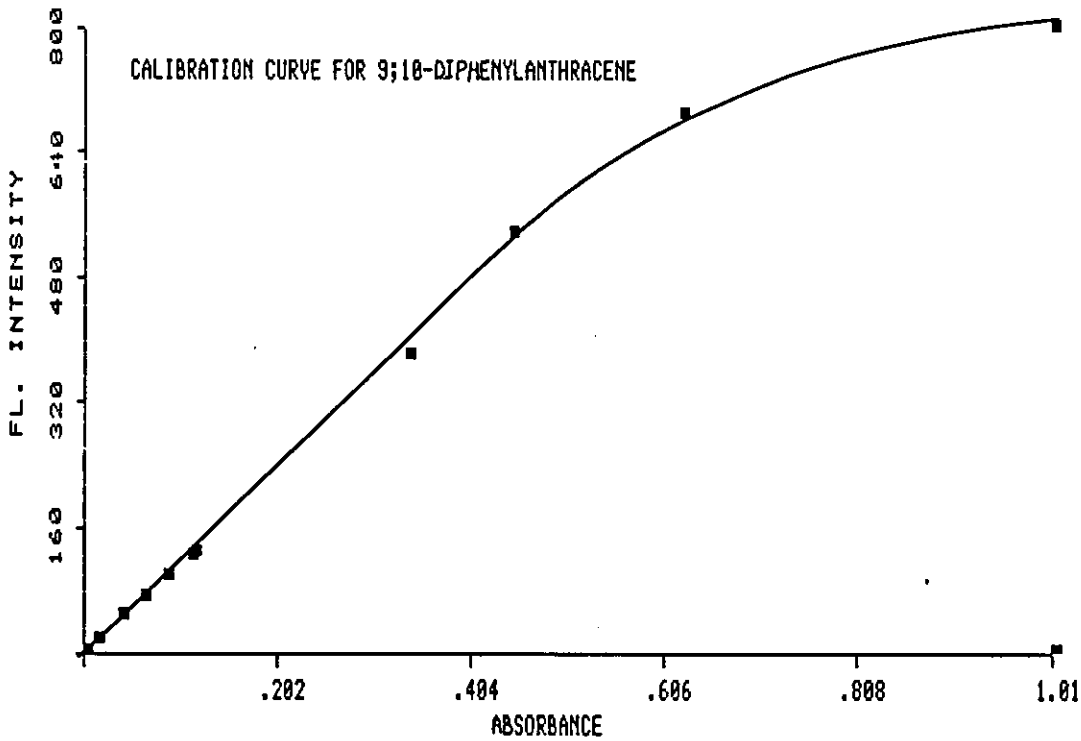

Figure 23. Relative fluorescence intensity versus absorbance values for 9,10-diphenyl anthracene in cyclohexane in a 1 mm ID sample tube. Linearity is observed up to approximately 0.45A.

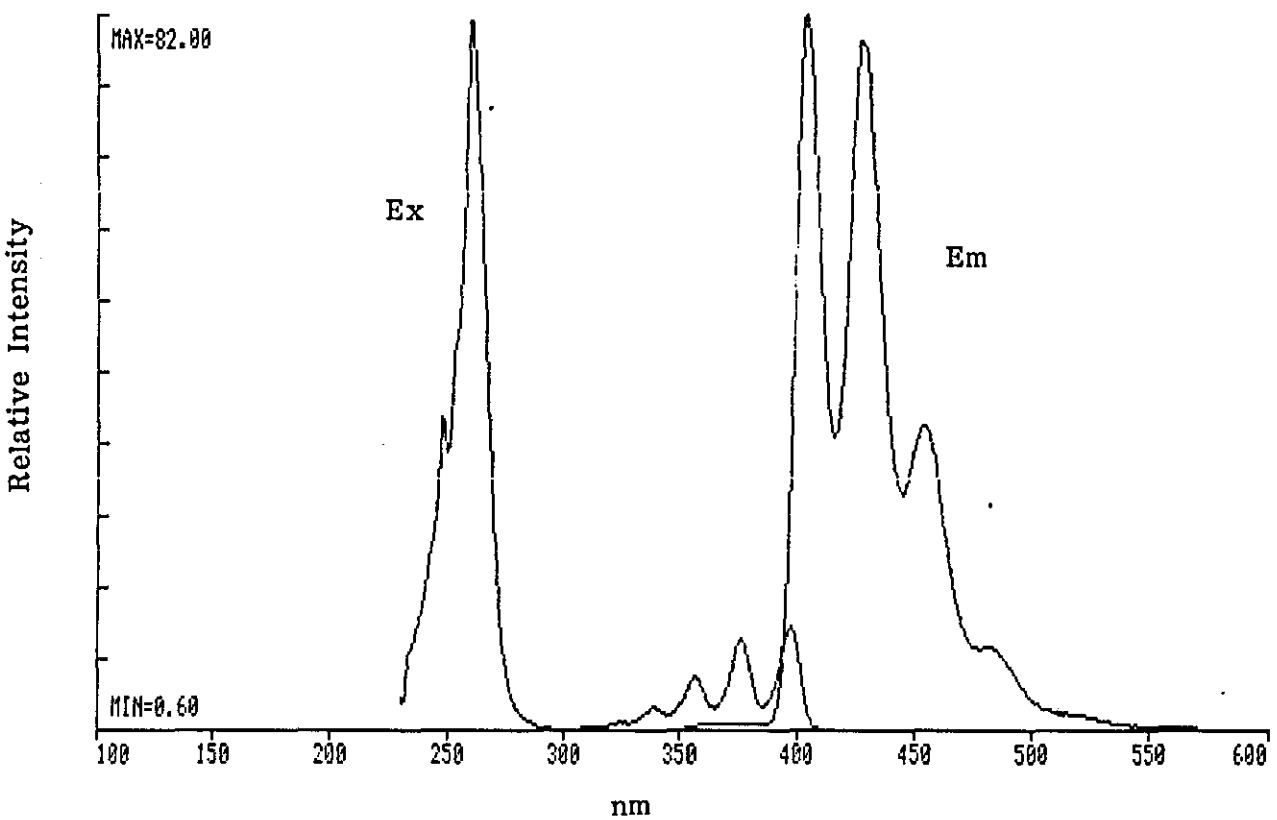

Figure 24. Low temperature corrected excitation and emission spectra of 9,10-diphenylanthracene in methylcyclohexane

TABLE 8

Experimentally obtained low temperature fluorescence and phosphorescence quantum yields relative to 9,10 diphenylanthracene at Q_f = 1.00

(Values in brackets are literature values)

Compound	Solvent	Ex nm	Em Range nm	Life Time sec	Observed Q_f	Observed Q_p	References
Anthracene	MCH	252	360-490	NR	0.29 (0.27)	NR	Parker (1962)
Benzene	MCH	254	265-340	5.8 (8)	0.20 (0.21)	0.31 (0.19)	Parker (1962)
Benzophenone	MCH	250	400-550	$6x10^{-3}$ ($8x10^{-3}$)	NR	0.89 (0.84)	Gilmore (1962)
Benzophenone	H	250	400-550	$3x10^{-3}$	NR	0.42	
Coronene	MCH	303	390-510	9	0.12	0.07	
Fluorene	MCH	265	275-380	NR	0.77 (0.54)	NR (.07)	Parker (1962)
Naphthalene	H	276	300-400	NR	0.35 (0.39)	NR (.008)	Parker (1962)
Tetraphenyl-butadiene	MCH	346	370-520	NR	0.90	NR	
Triphenylene	H	259	330-440	10.5 (17)	0.04 (0.06)	0.25 (0.28)	Parker (1962)
Room Temperature (25°C)							
$Eu(TTA)_3$	EtOH	275	550-630	$3.6x10^{-4}$	NR	0.13 (0.18)	Baumik (1964)

Phosphorescence quantum yields were also in good agreement with the exception of benzene. The latter was not purified before measurement. It should be noted that the value of 0.42 for the phosphorescence yield of triphenylene found by Kellogg and Bennett (1964) is inordinately high and can be attributed to the assumed quantum yield of rhodamine B of 1.0. The reproducibility of the quantum yield values at 77K is ±8–10%.

CHAPTER FIVE

THE LUMINESCENCE OF AMINO ACIDS

5.1 Tryptophan

The room temperature fluorescence characteristics of tryptophan are well documented with the corrected excitation and fluorescence emission maxima of aqueous samples occurring at 278 nm and 348 nm respectively. The shape of the fluorescence spectrum of tryptophan and the position of the maximum are determined by the indole ring of the molecule without any appreciable contribution from the substituent groups. The main reason for the lack of structure of the fluorescence band of tryptophan in aqueous solutions is its strong tendency to interact with the surrounding medium in the excited state. The amino group can form hydrogen bonds with solvent molecules and orientation solvation with relaxation of the solvate shell relative to the excited molecule leads to 3 effects: a) a long waveshift of the fluorescence emission b) band broadening and c) loss of structure.

The greater effect of interaction with the environment on the position of the levels of the excited state than on the ground state is due to the fact that the dipole moment of excited molecules becomes much greater and subsequently there is an increase in the strength of the interaction. Essentially the fluorescence wavelength is very variable, whilst the singlet excitation spectrum is constant. A reduction in temperature or an increase in viscosity causes a short waveshift in the fluorescence emission. The Stokes shift at 298 K is 0.76 μm^{-1} whilst at 77 K it is 0.43 μm^{-1}. This is well shown in Figure 25. The half bandwidth reduces from 55 nm to 39 nm.

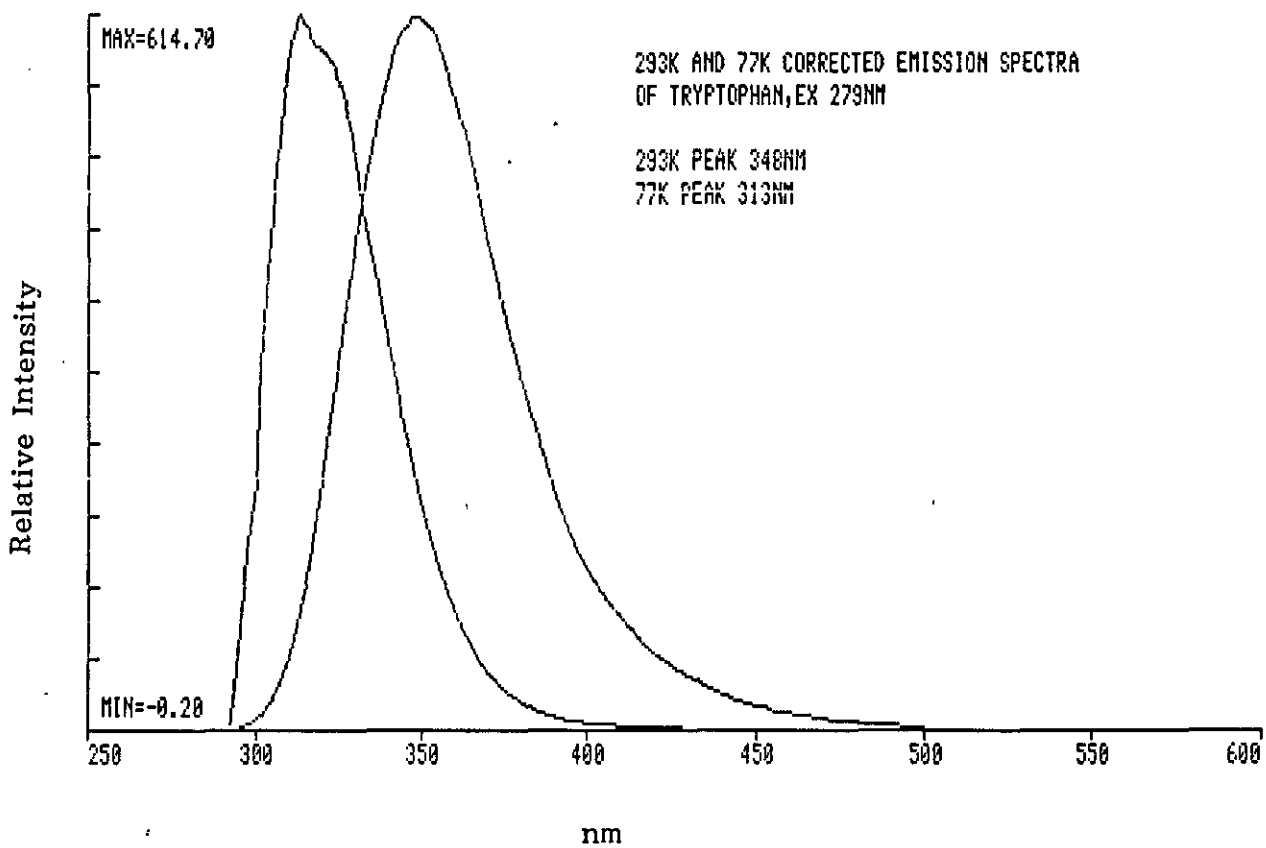

Figure 25. Corrected room temperature and low temperature fluorescence emission spectra of tryptophan at pH 8.0, excited at 279nm

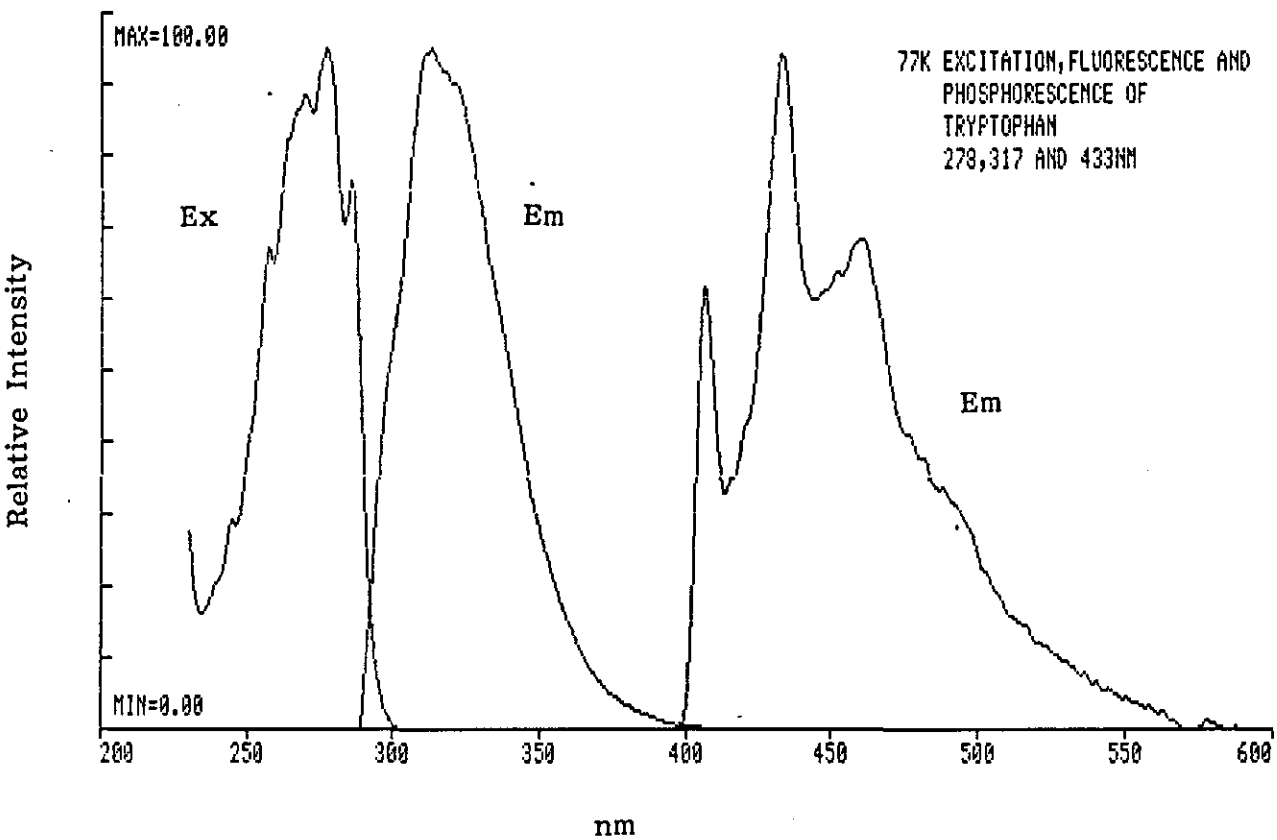

Figure 26. Corrected excitation, fluorescence and phosphorescence spectra of tryptophan at pH 8.0 at low temperature

TABLE 9

Luminescence characteristics of Tryptophan 1 x 10^{-5} M in 50% aqueous ethanediol at pH 8.0

Room Temperature (298 K)

Ex	Corrected Fluorescence	ϕ_f
278 nm	348nm	0.20

Low Temperature (77 K)

Ex	Corrected Fluorescence	ϕ_f	
279 nm	Peak 313nm, centre 321nm	0.70	
	Corrected Phosphorescence	ϕ_p	
	Peaks 407 nm, 433 nm	0.18	6.95 s

The corrected fluorescence and phosphorescence spectra of tryptophan at 77 K are shown in Figure 26. The phosphorescence decay was found to be exponential with a lifetime of 6.95 s. The relative quantum yields of fluorescence and phosphorescence of free tryptophan are shown in Table 9 and are in excellent agreement with those of Bishai et al (1967) and Longworth (1971). The total quantum yield of tryptophan ($\phi_f + \phi_P$) at 77 K was close to unity.

5.2 Tyrosine

The room temperature luminescence characteristics of tyrosine conformed with those documented in the literature with a maximum of the fluorescence band of aqueous solutions at 303 nm. At 77 K the fluorescence emission is at 312 nm with a phosphorescence emission at 396 nm. The fluorescence emission contrasts with that found by Bishai and other workers of a value of 296nm. The discrepancy can be accounted for by the fact that at pH 8.0 the tyrosine may be partially ionised, thus giving rise to a red shift. The decay time of the phosphorescence was found to be 1.8 s compared to 2.1 s found by Longworth (1971) and 2.7 to 2.8 s by Bishai. Ionisation of the hydroxyl group of tyrosine (pKa 10.0) produces a lifetime of 1.2 s with the fluorescence emission at 325 nm; the absorption also shifts to 293 nm.

The luminescence characteristics of tyrosine at pH 8.0 in 50% aqueous ethanediol are summarised in Table 10. The corrected fluorescence and phosphorescence spectra of tyrosine at 77 K are shown in Figure 27.

TABLE 10

Luminescence characteristics of Tyrosine 2.7×10^{-5} M in 50% aqueous ethanediol, pH 8.0

Room Temperature (298 K)

Ex	Corrected Fluorescence	Φ_f
274 nm	303 nm	0.22

Low Temperature (77 K)

Ex	Corrected Fluorescence	Φ_f	
283 nm	312 nm	0.35	
	Corrected Phosphorescence	Φ_p	
	396 nm	0.65	1.8 s

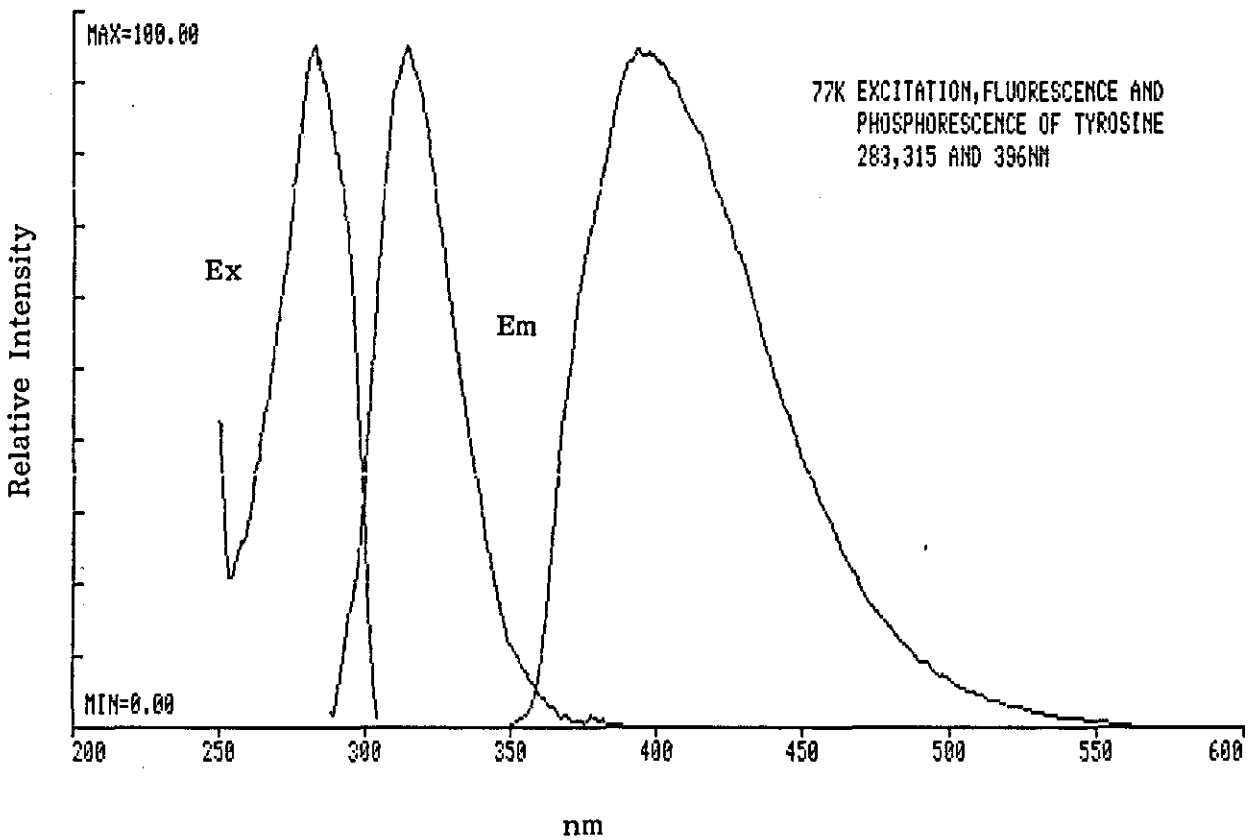

Figure 27. Corrected excitation, fluorescence and phosphorescence spectra of tyrosine at pH 8.0 at low temperature

5.3 Phenylalanine

In contrast to many works, it was relatively easy to obtain the characteristic luminescence of phenylalanine at 77 K. As can be seen from Figure 28, the fluorescence and excitation spectra are very similar, indicative of the fact that they are formed from one electronic transition. They are also very similar to that of benzene.

The fluorescence emission overlaps the absorption bands of tyrosine and tryptophan . The low ε of phenylalanine (200) compared with ε, 1510 for tyrosine and ε, 5400 for tryptophan, together with a moderate quantum yield is never compensated for by the large phenylalanine to tyrosine and tryptophan ratios in most proteins. Thus only tyrosine and tryptophan need be considered in proteins. The luminescence characteristics of phenylalanine at 77 K are summarised in Table 17 and compare favourably to that found in the literature.

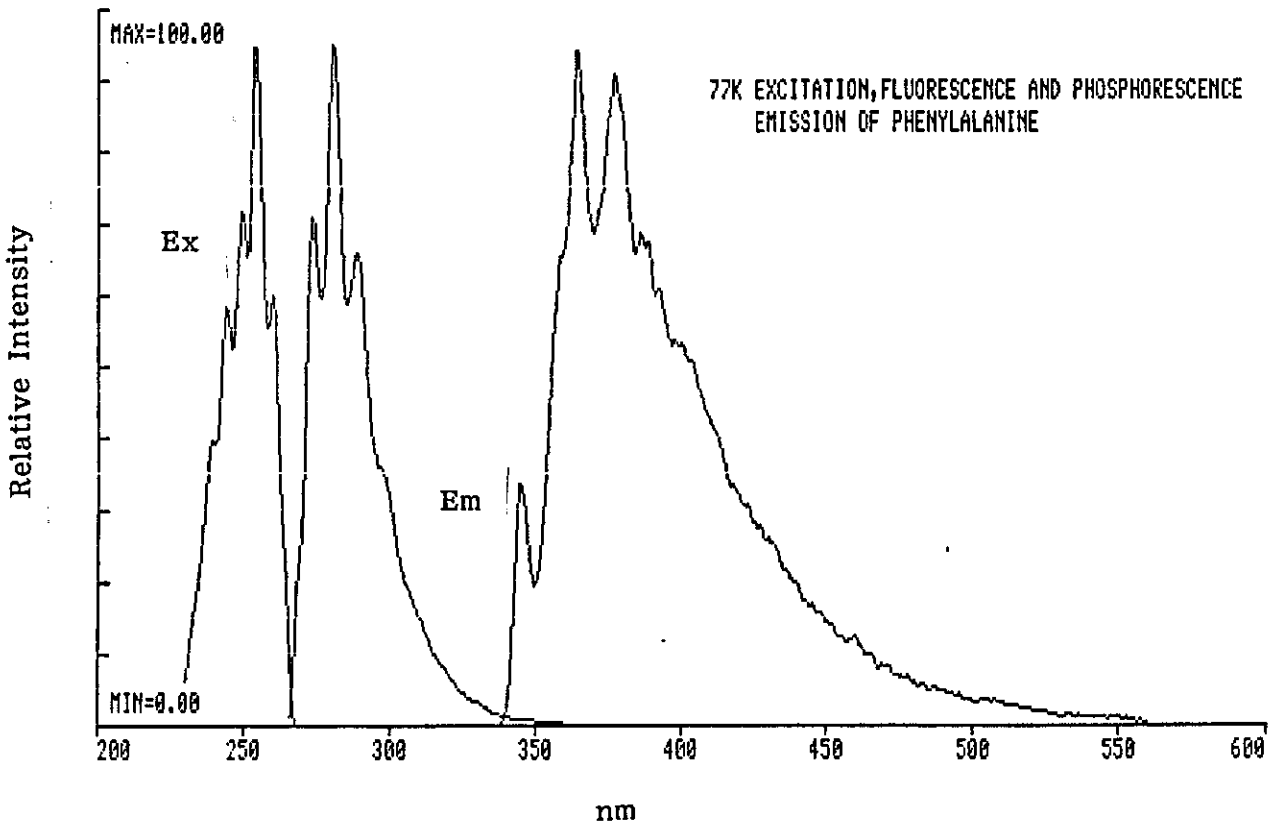

Figure 28. Corrected excitation, fluorescence and phosphorescence spectra of phenylalanine at pH 8.0 at low temperature

TABLE '11

Luminescence characteristics of Phenylalanine 3 x 10^{-4} M in 50% aqueous ethanediol, pH 8.0 at 77 K

Ex	Fluorescence	Φ_f	
253 nm	281 nm	0.30	
	Phosphorescence	Φ_p	—
	365 nm	0.34	7.5 s

CHAPTER SIX

LUMINESCENCE CHARACTERISTICS OF TERBIUM-TRANSFERRIN COMPLEXES

6.1 Fluorescence and Phosphorescence of Transferrin

As mentioned earlier the luminescence characteristics of Class B proteins such as transferrin are dominated by that of tryptophan. However, the fluorescence characteristics of the tryptophan residues are unlike those of the free amino acid in aqueous solutions. The Stokes shift is quite variable for different proteins and is dependent upon the local environment of the tryptophan residues, i.e. whether exposed, buried or partially exposed. Fluorescence emission < 335 nm is indicative of tryptophan in a hydrophobic environment, whilst emission > 340nm is found in aqueous solvents. The luminescence characteristics of transferrin at pH 8.0 are shown in Table 12 and the low temperature luminescence spectra in Figure 29. Lehrer (1969) found a value of 0.09 for the room temperature fluorescence quantum yield of transferrin. A comparison of the phosphorescence of tyrosine, tryptophan and transferrin is shown in Figure 30, which illustrates well that tyrosine does influence the shape of the transferrin phosphorescence emission.

A comparison of the excitation spectra taken at emission wavelengths corresponding to zero percent tryptophan (375 nm) and almost 100% tryptophan shows a difference which is attributed to the tyrosine component, Figure 31.

TABLE 12

Luminescence characteristics of Transferrin 9×10^{-7} M in 50% aqueous ethanediol, pH 8.0

Room Temperature (298 K)

Ex	Fluorescence	Φ_f
279 nm	325 nm	0.05

Low Temperature (77 K)

Ex	Fluorescence	Φ_f	
279 nm	320 nm	0.19	
	Phosphorescence	Φ_p	
	409 nm, 435 nm	0.07	1.3 s 5.2 s

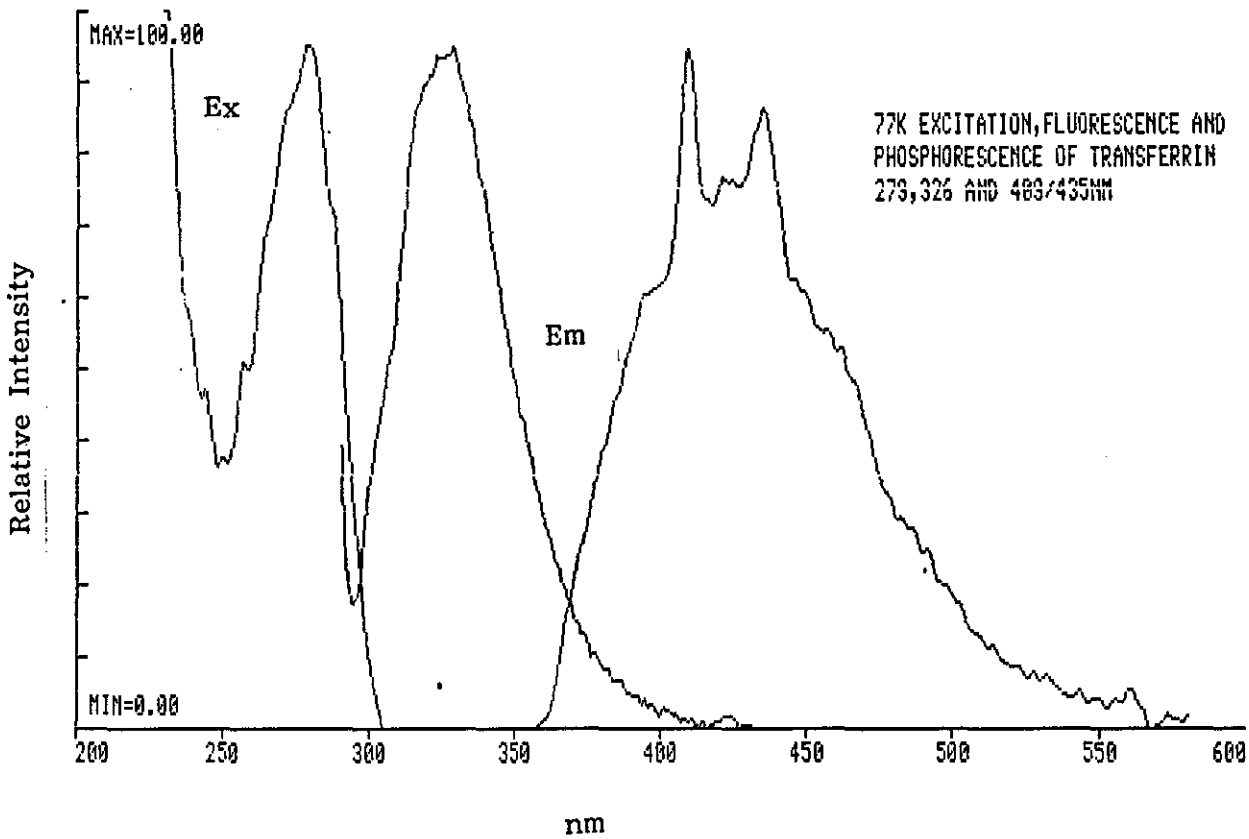

Figure 29. Corrected excitation, fluorescence and phosphorescence spectra of transferrin at pH 8.0 at low temperature

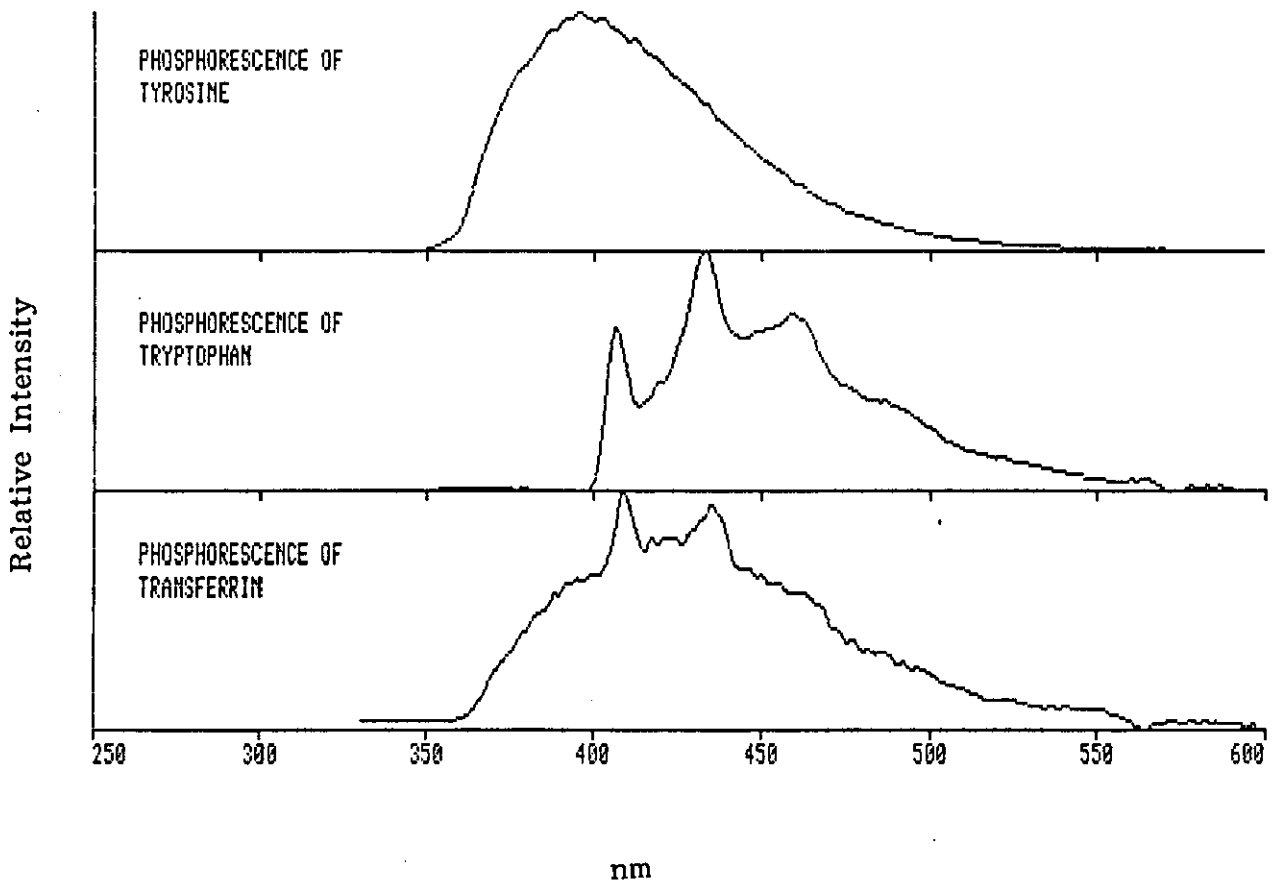

Figure 30. Comparison of the corrected phosphorescence emission of tyrosine, tryptophan and transferrin

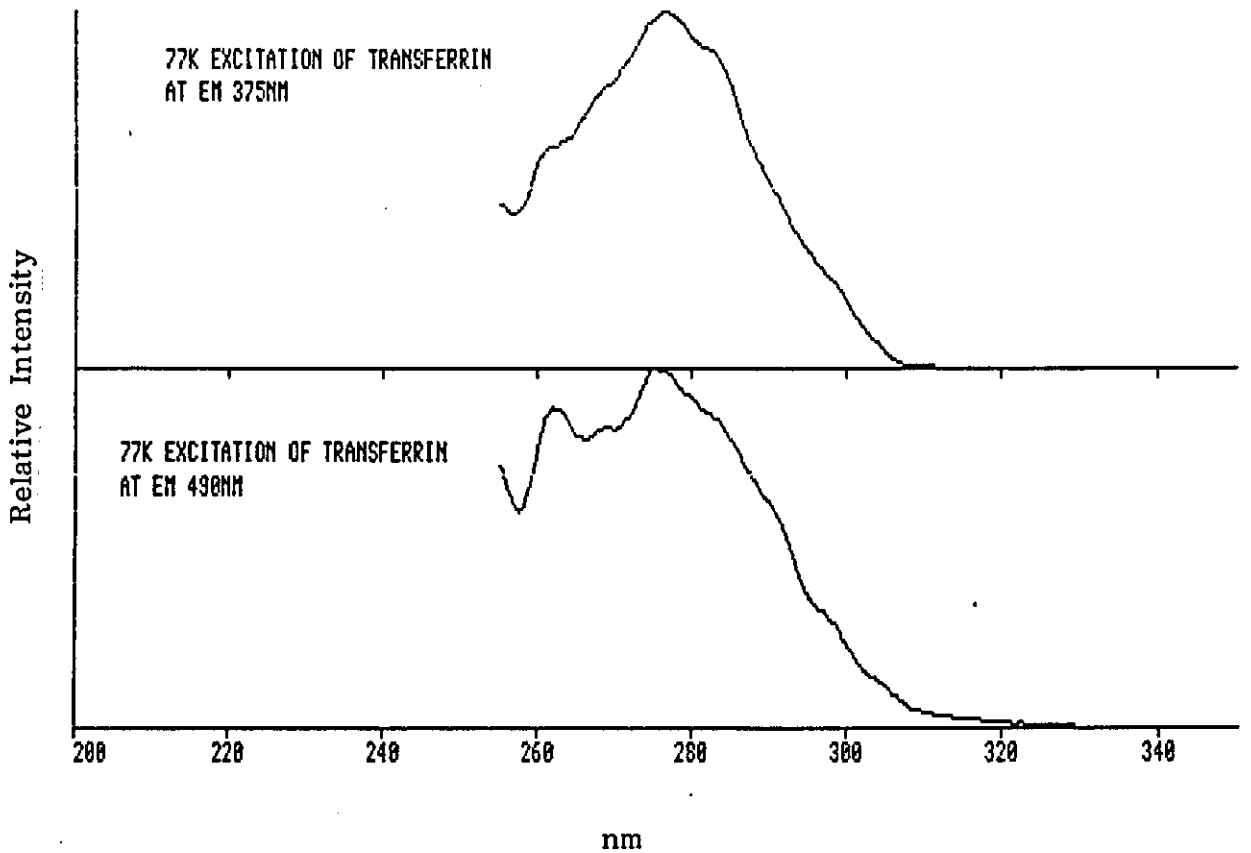

Figure 31. Comparison between the phosphorescence excitation spectra of transferrin with the emission monitored at 375nm and at 490nm

A feature of the absorption band of tryptophan is the presence of a fine structured shoulder on the long wavelength edge of the absorption spectrum. This feature is well defined at 77°K and is also present in the fluorescence excitation spectrum. A comparison of the latter with that of the excitation of transferrin monitored at 324 nm emission, also shows the presence of the shoulder, Figure 32. This confirms that the fluorescence emission of transferrin is due to the tryptophan residues.

6.2 Luminescence of Terbium-Transferrin Complexes

Rare earth ions incorporated in organic chelates by coordination through a donor atom such as O or N exhibit characteristic line spectra when excited at the ligand absorption maximum. Lanthanides such as Tb^{3+} have been used as probes for investigating the metal binding sites of a number of proteins, Brittain (1976), such as thermotysin, Berner et al (1975); nucleic acids, Mushrush and Yonuschot (1983) such as DNA, Yonuschot and Mushrush (1975).

In 1971 Luk used Tb^{3+} to investigate the nature of the metal binding sites of transferrin. Metal complexation to the phenolic oxygen of tyrosine residues perturbs the $\pi - \pi^*$ transitions of the aromatic ring. The resulting absorbance changes are easily observed in the difference spectra of metalloproteins versus apoproteins, since the absorbance for all non-binding groups in the protein are blanked out of the spectrum. Two tyrosine residues per metal is the general feature of almost all metallotransferrin complexes, Pecoraro and Harris (1981). A synergistic anion, such as carbonate, is also essential, Harris (1977) and Teuwisson et al (1972).

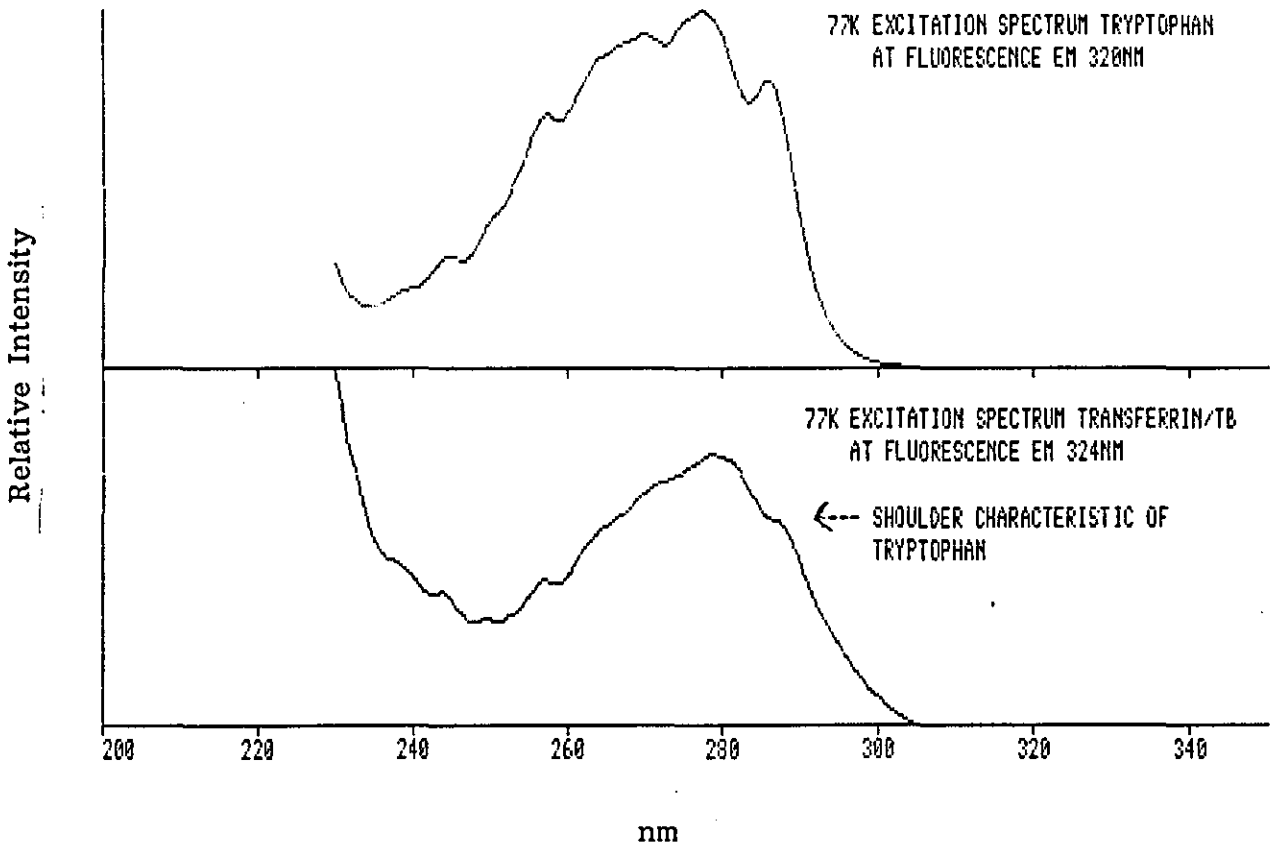

Figure 32. Comparison between the low temperature fluorescence excitation spectrum of tryptophan monitored at 320nm and the fluorescence excitation spectrum of transferrin monitored at 324nm

The excitation observed whilst monitoring the terbium emission at 550 nm serves to identify the chromophore engaged in energy transfer to the terbium ion, though this may not necessarily be the chromaphore coordinated to the lanthanide. The indirect excitation of Tb^{3+} can occur either by excitation of the coordinate tyrosinates or by excitation of nearby tryptophans, followed by radiationless energy transfer to Tb^{3+} coordinate tyrosinates. The latter route is possible as the critical distance R_o for energy transfer from tryptophan to tyrosinate ranges from 0.84, Eisinger et al (1969) to 1.33, Edelhoch et al (1967). The samples used by Luk (1971) had absorbance values of 0.9A. Severe distortion will occur at such high values leading to the incorrect assumption that the excitation spectrum was similar to that of tyrosinate residues. The effect of measuring the excitation spectra of amino acids and proteins at high absorbance values has been well documented by DeJersey et al (1981). When excitation spectra of protein samples with absorbances < 0.03A are measured they closely resemble that of tryptophan (λ max 280 nm), rather than tyrosinate (λ max 293 nm), Figure 33.

In a survey of a larger number of proteins, DeJersey et al (1981) found that the ratio of R of the excitation intensities at 292 to 276 nm is < 0.2 for tyrosine and 0.5 to 0.8 for tryptophan. From Figure 33 the ratio for the transferrin-terbium complex is 0.41, which points to the involvement of tryptophan residues in the energy transfer.

On binding to transferrin the room temperature quantum yield of Tb^{3+} increases from 0 to a maximum of 0.074 when the ratio of Tb^{3+} to transferrin is > 2.0, Figure 34. This compares with values of 0.02 for

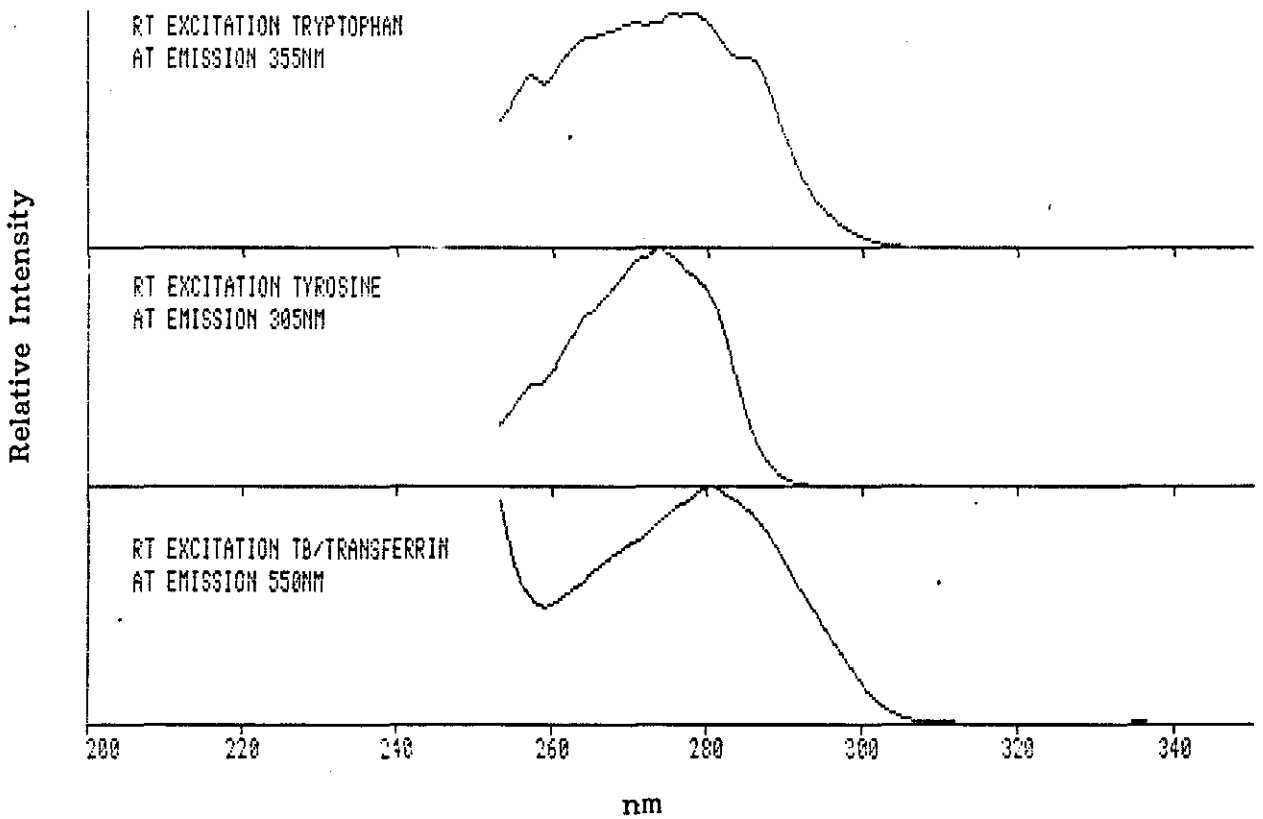

Figure 33. Comparison between the room temperature excitation spectra of tryptophan, tyrosine and terbium-transferrin

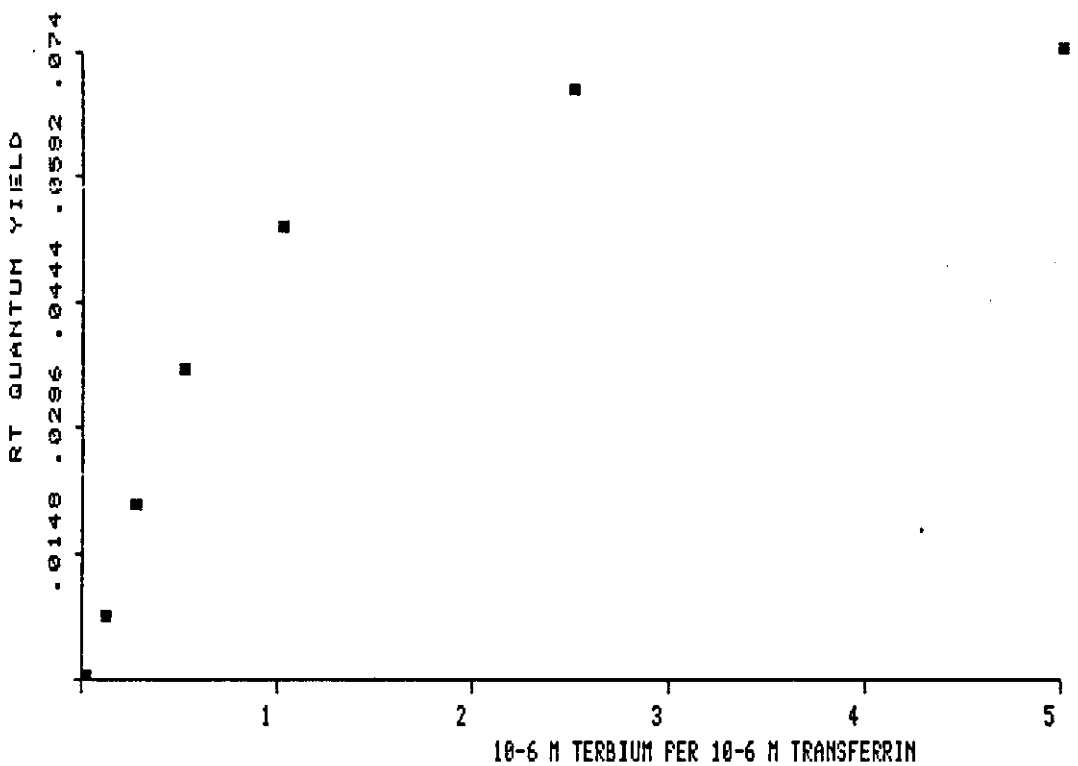

Figure 34. Increase in the relative quantum yield of the Tb^{3+} emission for increasing amounts of Tb^{3+} added to transferrin

Tb^{3+} - adenosine 5 phosphate and 0.196 for Tb^{3+} - guanosine 5 phosphate, Mushrush and Yonuschot (1983). The lifetime of the Tb^{3+} decay at 550 nm also increases from 0.460 ms to 1.240 ms. The shape and relative intensity of the various transitions change on binding, Figures 35 and 36. The relative fraction of photon distribution for the various transitions is shown in Table 13, compared with those found for Tb^{3+} - acetyl acetonate in ethanol, Dawson et al (1966). The asymmetric arrangement of the ligands around the terbium ion accounts for the splitting of the transitions. The natural radiative lifetime for Tb^{3+} is 4.75 ms and in D_2O the observed lifetime is 3.88 ms, Stein and Wurzberg (1975).

At low temperature the luminescence of the Tb^{3+} - transferrin complexes can be evaluated by using the variable delay and gate time of the Model LS-5. For a delay of 0.2 ms and a gate of 3.0 ms nearly all of the Tb^{3+} emission has decayed to zero so enhancing the observation of the protein phosphorescence, Figure 37. The phosphorescence of the transferrin was found to have a quantum yield of 0.07. For the Tb^{3+} the quantum yield is 0.19 with a decay time of 0.840 ms.

No significant change could be observed in the phosphorescence yield on addition of Tb^{3+}. This is probably due to the fact that the phosphorescence emission of the transferrin is the sum of the emission of $\sim$10 tryptophanyl residues.

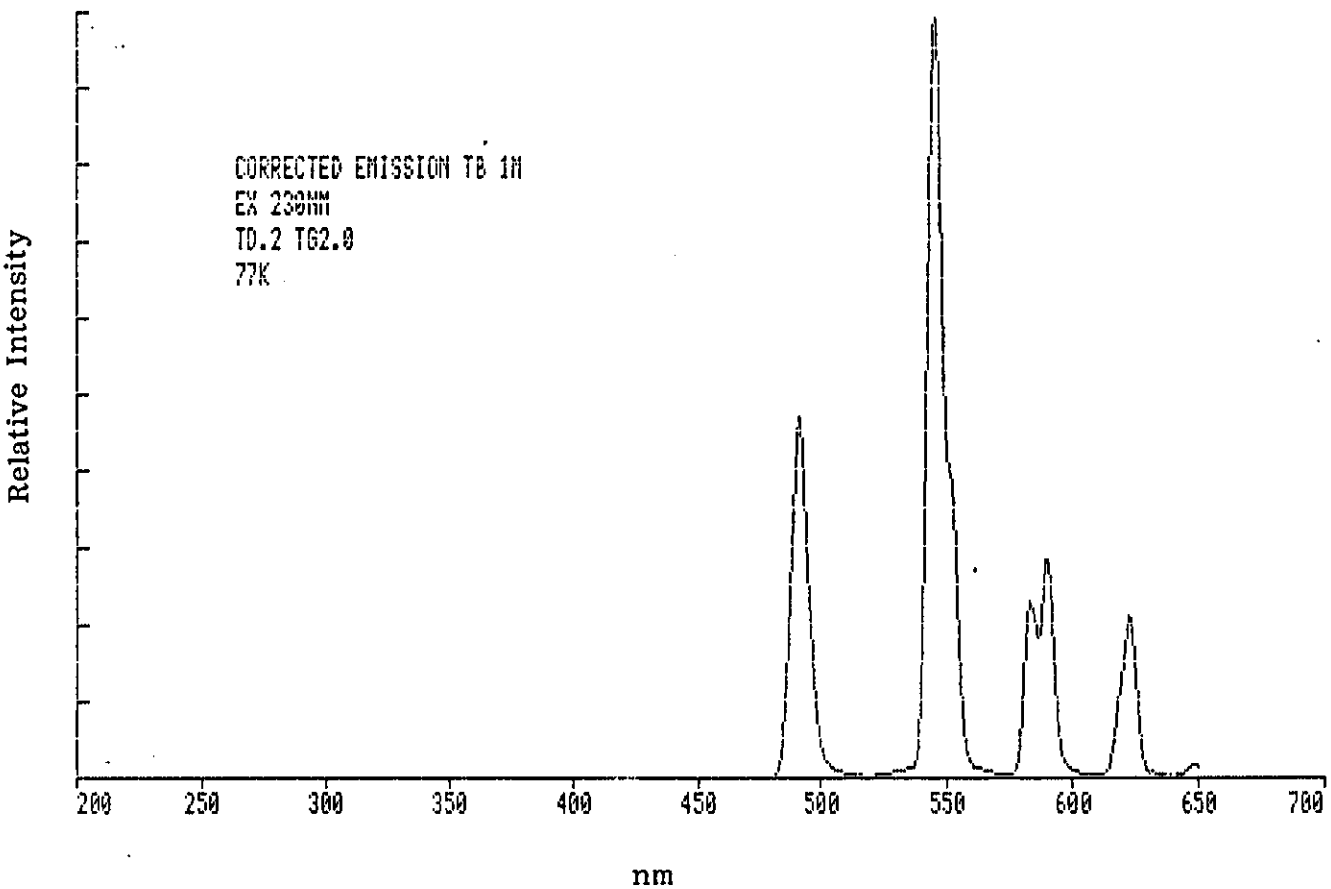

Figure 35. Corrected emission spectrum of Tb^{3+}, 0.1M, in water excited at 230nm.

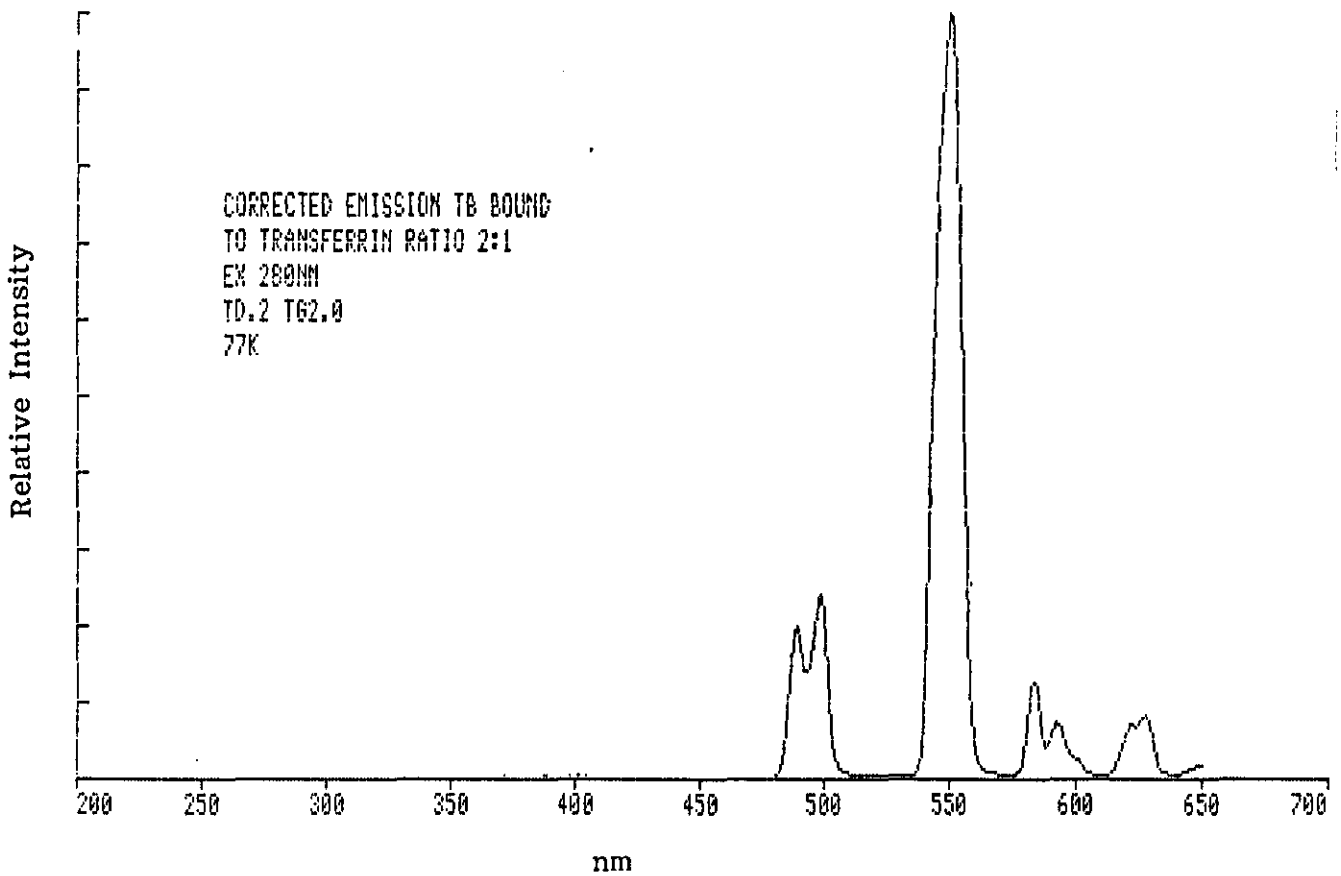

Figure 36. Corrected emission spectrum of Tb^{3+} shown bound to transferrin excited at 280nm

TABLE 13

Relative fraction of photon distribution for the various transitions of Tb^{3+}, free and bound to transferrin

Transition	nm	Free Tb^{3+}	Bound Tb^{3+}	TbA in ethanol Dawson et al (1966)
$^5D_4 - {}^7F_6$	480	22%	19%	11%
$^5D_4 - {}^7F_5$	543	49%	65%	79%
$^5D_4 - {}^7F_4$	582	19%	8.5%	3%
$^5D_4 - {}^7F_3$	620	9.3%	7.8%	7%

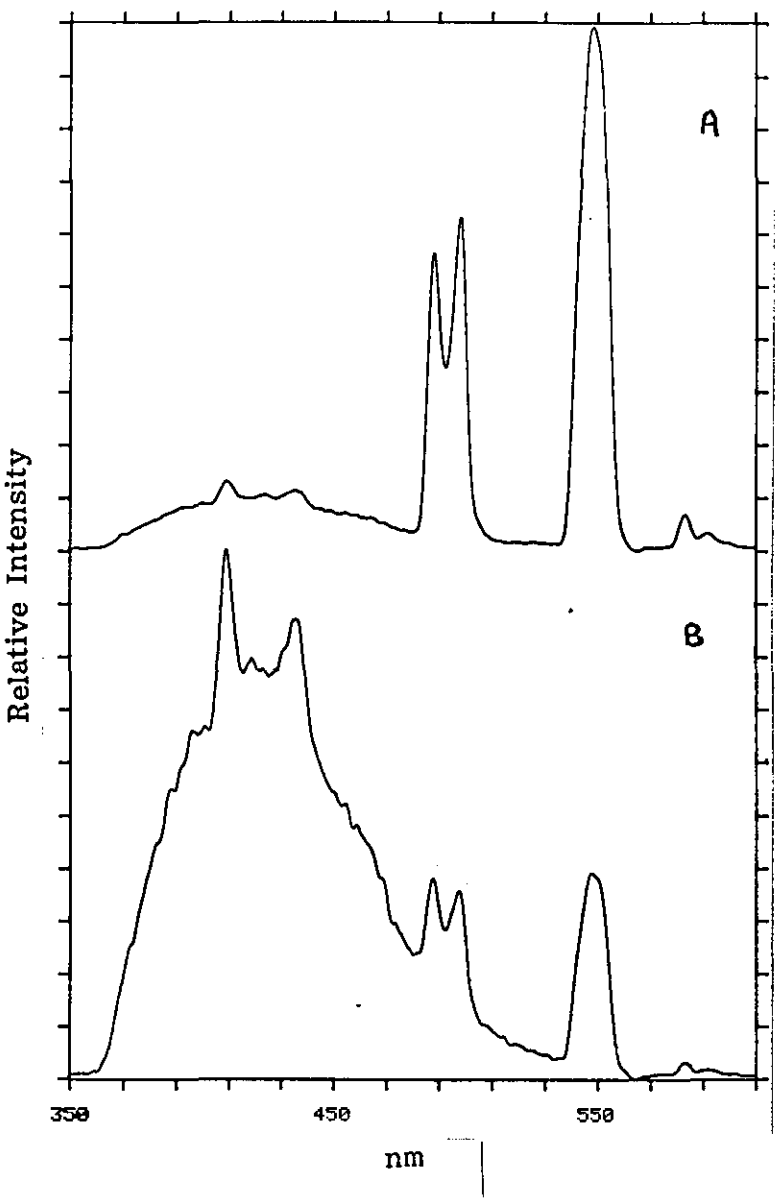

Figure 37. Comparison of the delayed emission from terbium-transferrin at low temperature excited at 279nm with a) t_d 0.2 ms, t_g 3.0 ms and b) t_d 3.0 ms and t_g 9.0 ms

CHAPTER SEVEN

LUMINESCENCE CHARACTERISTICS OF Eu^{3+}:Y_2O_3

The emission spectrum of a Y_2O_3:Eu^{3+} sample measured in a fluorescence spectrometer using a conventional 150 W Xe lamp is characterised by a relatively large peak at 611 nm compared with the other transitions. With a pulsed source spectrometer the emission spectrum is entirely different and depends upon the delay and gate time and the halflife of the Xe source, Rhys Williams and Fuller (1983).

When excited at 230 nm, i.e. into the change transfer band (CTB), the $^5D_{0-2}$ transitions show the characteristic build-up and decay shown in Figure 38. The observed lifetimes for these transitions are given in Table 14, together with those reported by other investigations. Although the emission from the $^5D_3$ excited state is observable, the lifetimes cannot be accurately measured as:

a) they are below the minimum level that is capable of being measured with the LS-5 and

b) they cannot be isolated from interfering $^5D_2$ transitions.

The lifetime of the $^5D_0$ excited states showed no variation with Eu^{3+} concentration, whereas the $^5D_1$ state varied from τ = 0.134 ms for 0.022 mole % Eu^{3+} to 0.066 ms for 5.05 mole % Eu^{3+}. This confirms the observation of Weber (1968) and is consistent with the observation that pairs of transitions suitable for ion-pair relaxation exist for the higher $^5D_3$ levels (J > 0), but not for the $^5D_0$ level.

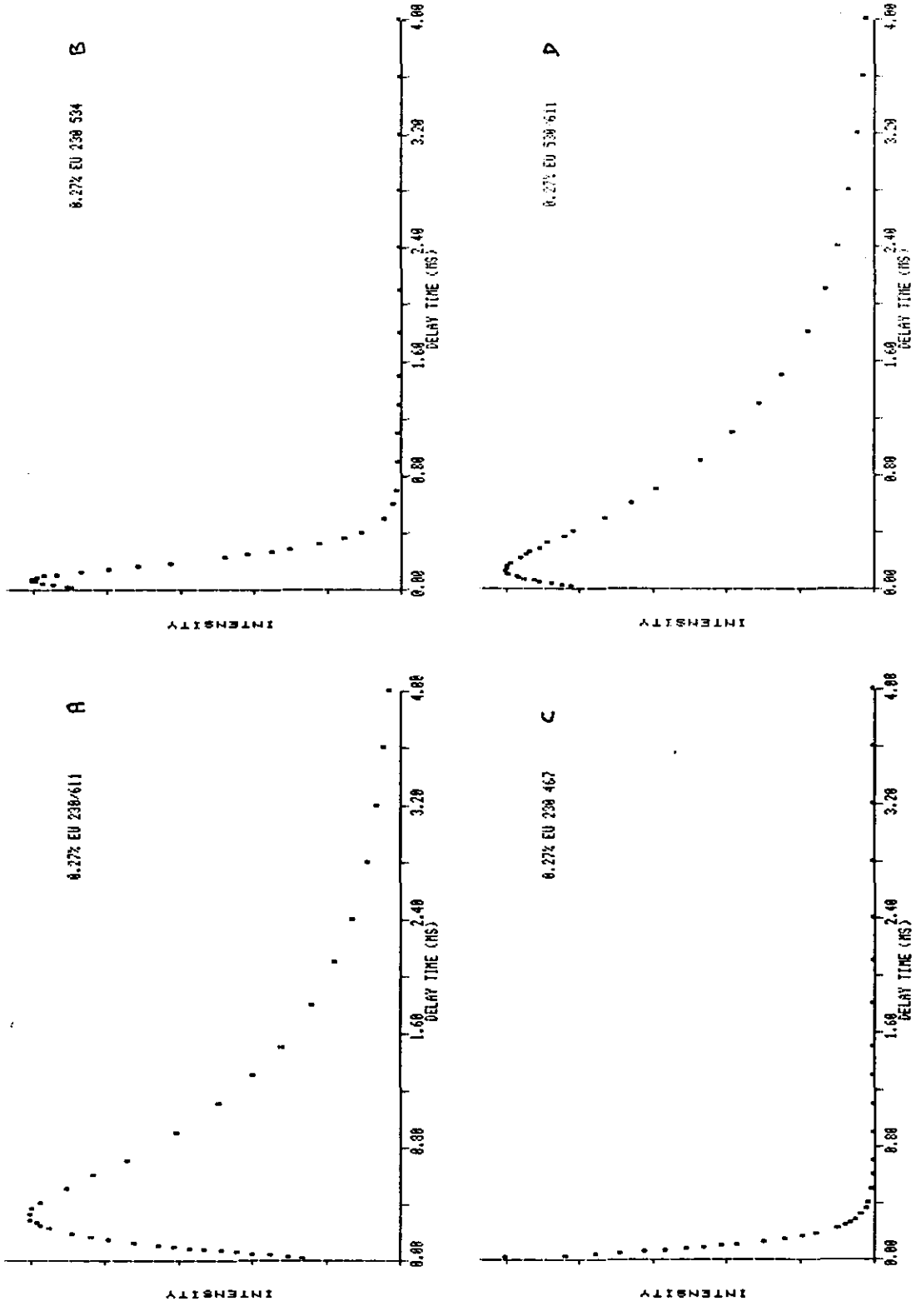

Figure 38. Plot of the relative intensity versus delay time for a) 611nm b) 534 and 467nm emission excited at 230nm and c) the 611nm emission excited at 530nm for 0.27% $Eu^{3+}.Y_2O_3$

TABLE 14

Excited state lifetimes of $Y_2O_3: Eu^{3+}$

at room temperature

Emitting level	Observed lifetime ms	Chang 1963	Axe 1964	Weber 1968	Blasse 1970
$^5D_0$	0.921 ± 0.018	0.870	0.960	0.860	0.895
$^5D_1$	0.120 ± 0.005	0.100	0.070	0.120	-
$^5D_2$	0.091 ± 0.003	-	-	0.095	-

The rise time for the $^5D_0$ transition decreases with increasing Eu^{3+} concentration as shown in Table 15. This is consistent with the fact that as Eu^{3+} increases the emission from the $^5D_{1-3}$ level decreases due to cross relaxation such as $^5D_1 \longrightarrow {}^5D_0 \nsim {}^7F_0 \longrightarrow {}^7F_3$. Direct excitation, Figure 38D,into the $^5D_5$ levels produces a decay curve for the 611 nm emission which has a shorter rise time, 0.22 ms but has the same lifetime compared with the charge transfer excitation at 230 nm. The difference in the two rise times obviously reflects both the rate at which the charge transfer state feeds the upper energy levels of Eu^{3+}, and the rate at which these cascade to the $^5D_0$ level.

Since the transitions from $^5D_{0-3}$ levels have different rise times and mean lifetimes, it should be possible to obtain emission spectra corresponding to the respective transitions using the following procedure.

Emission spectra were excited at 230 nm and measured with 3 delay times; 0, 0.1 and 1.0 ms, each with a gate time of 0.05 ms. The spectra corresponding to these times are shown in Figures 39, 40 and 41. Figure 41, with a delay time of 1.0 ms, has only transitions from the $^5D_0$ level. By normalising to the 611 nm line, the $^5D_0$ components are subtracted from Figures 39 and 40. The two intermediate spectra containing only the $^5D_1$, $^5D_2$ and $^5D_3$ transitions are then subtracted from each other, either normalised at 533 nm ($^5D_1$) or at 467 nm ($^5D_2$). The results are shown in Figure 42 which also contains the transitions from $^5D_3$ since these cannot be discriminated from the $^5D_2$ transitions because of the limiting resolution of the delay time (t_d) of 10 μs.

TABLE 15

Variation in rise time of the $^5D_0 \rightarrow {}^7F_2$ transition with Eu^{3+} concentrations in ms

Eu^{3+} mole %	Rise time ms
0.27	0.320
1.00	0.267
2.20	0.189
3.30	0.130
5.56	0.060
11.1	0.020

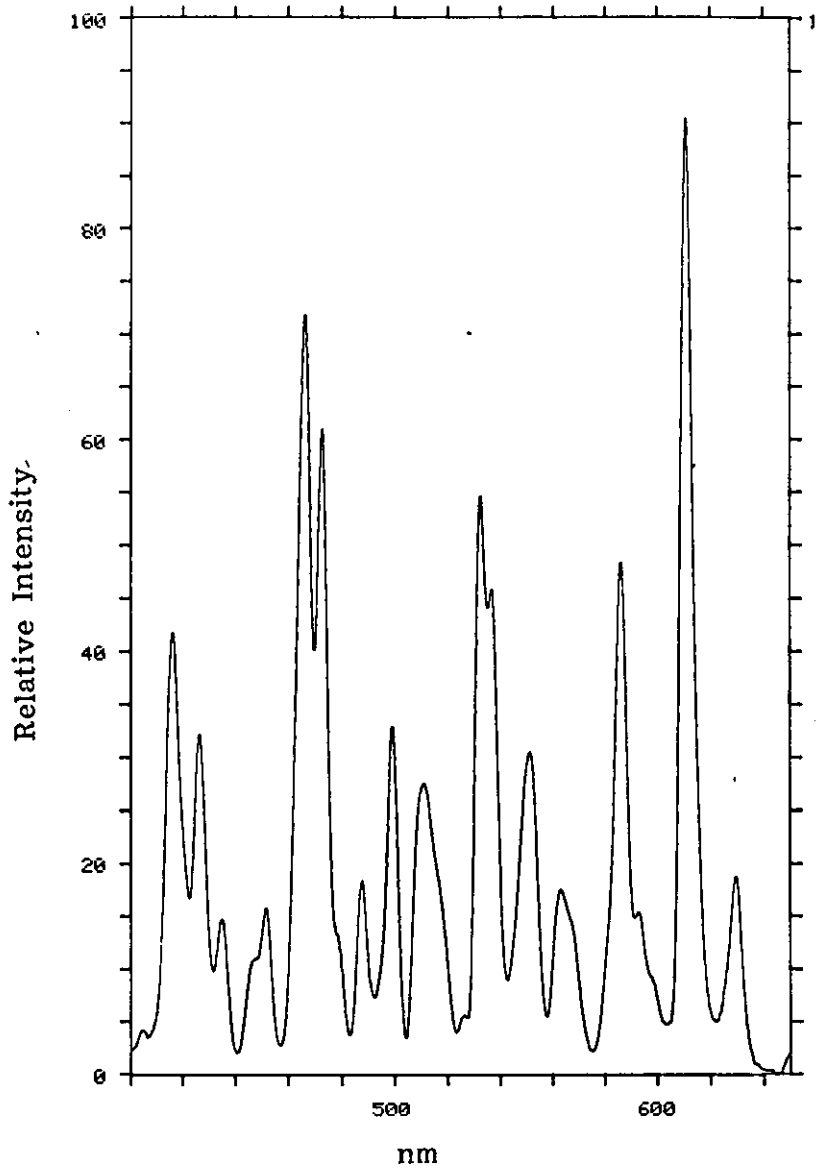

Figure 39. Corrected emission spectrum from 0.27% $Eu^{3+}.Y_2O_3$ excited at 230nm with a t_d of 0.0 (fluorescence mode)

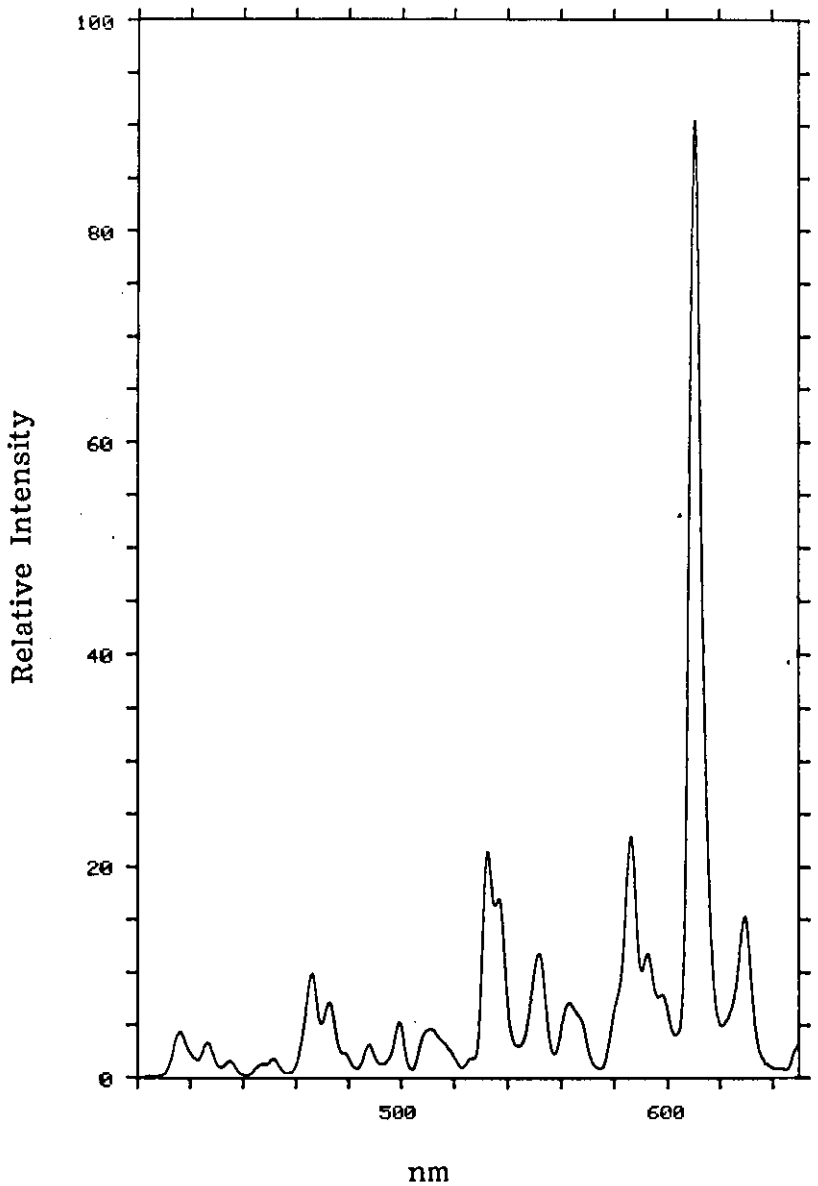

Figure 40. Corrected emission spectrum for 0.29% Eu^{3+} :Y_2O_3 excited at 230nm with a t_d of 0.1 ms and t_g of 0.05 ms

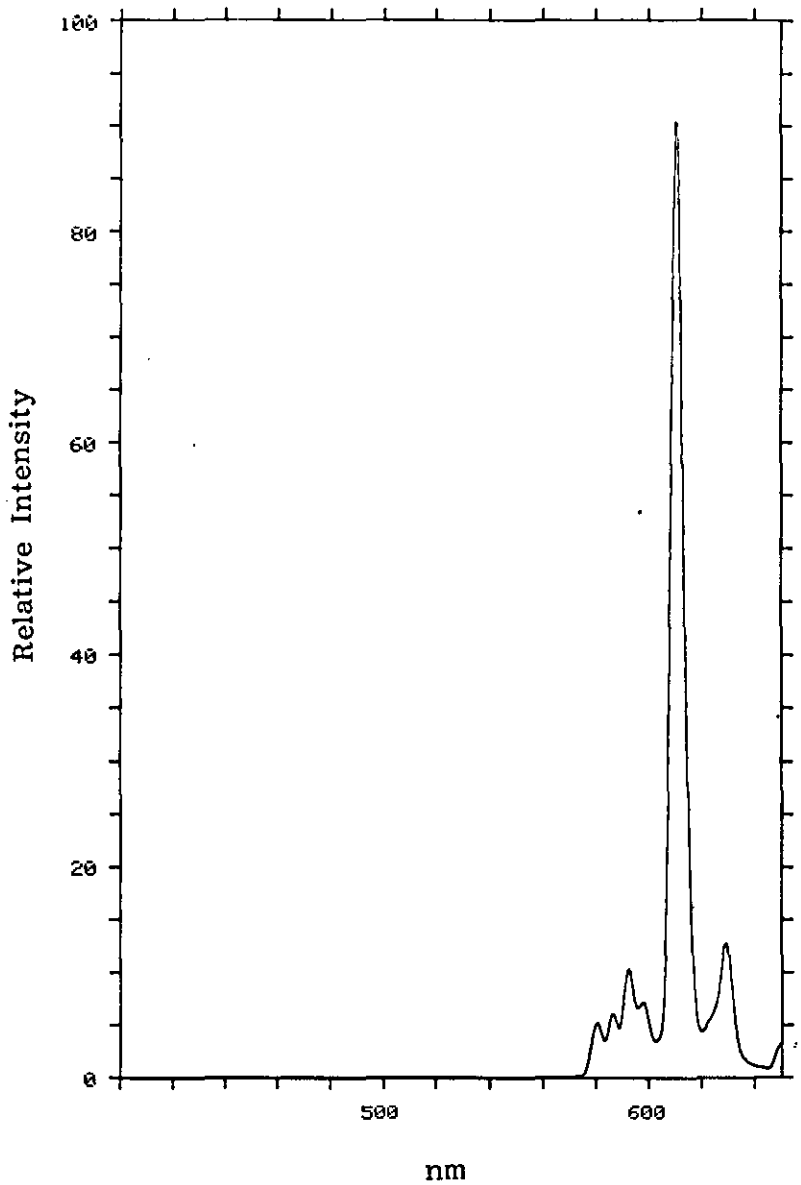

Figure 41. Corrected emission spectrum for 0.27% Eu^{3+}:Y_2O_3 excited at 230nm with a t_d of 1.0 ms and t_g of 0.05 ms

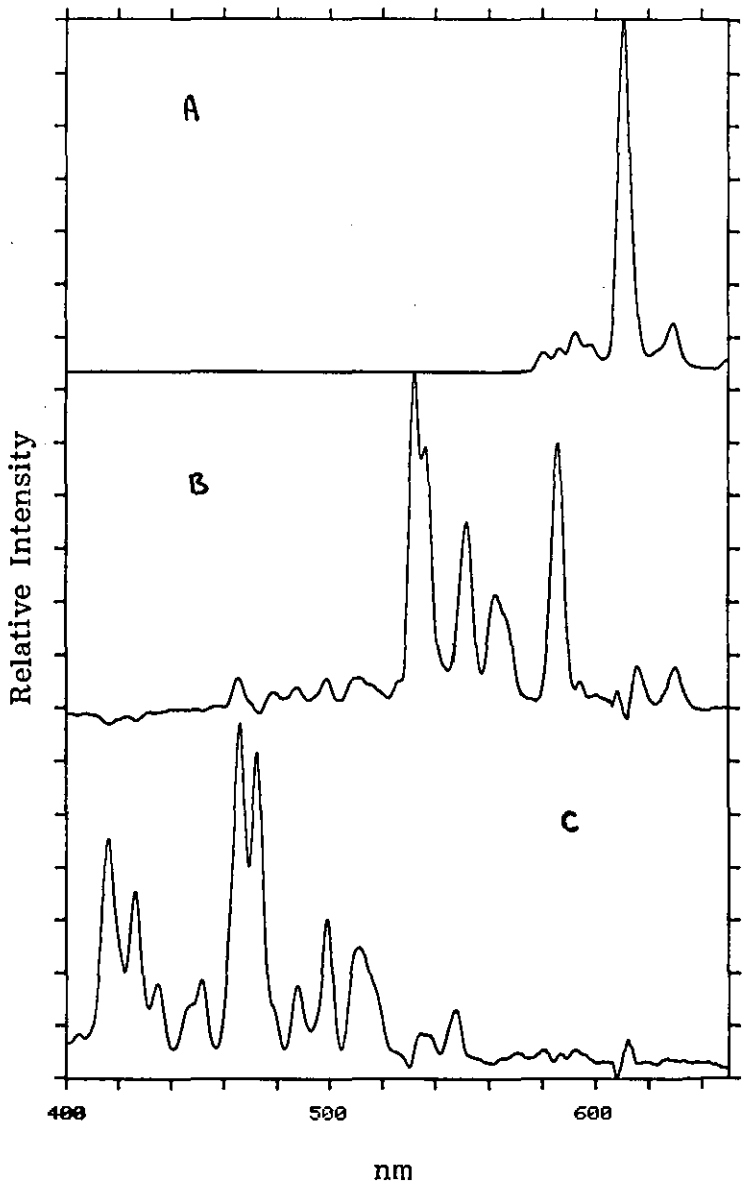

Figure 42. a) $^5D_0$ transitions b) $^5D_1$ transitions and c) $^5D_2$ and $^5D_3$ transitions from 0.27% Eu^{3+}:Y_2O_3

Table 15 compares the experimentally obtained energy levels of a 0.27 mole % Eu^{3+} with those obtained by other investigators. For the $^5D_{1-3}$ transitions the individual Stark components were not observed due to the limiting instrument resolution of 2.5 nm. Good agreement is obtained with the $^7F_{0-4}$ levels.

TABLE 16

List of identified levels of $Y_2O_3:Eu^{3+}$ observed in this work compared with experimentally obtained results from Chang 1963 and 1964

$^5L_3$ Levels	Observed Energy Levels cm^{-1}	Chang 1963	Chang 1964
$^7F_0$	0	0	0
$^7F_1$	343, 393, 570	203, 369, 546	371
$^7F_2$	904, 977, 1037	861, 919, 955	1120
$^7F_3$	1782, 1878, 1885 1902	1846, 1867, 1907 1997, 2017, 2129	2011
$^7F_4$	2820, 2937	2672, 2802, 2846 2960, 3014, 3080 3117, 3181	3007
$^5D_0$	17271	17224	17216
$^5D_1$	18797	18945, 18968, 19005 19021, 19095	18959
$^5D_2$	21529	21362, 21373, 21404 21497, 21514	21421
$^5D_3$	24125	-	24265

CHAPTER EIGHT

LUMINESCENCE CHARACTERISTICS OF AQUEOUS URANYL IONS

8.1 General

The photochemistry of the uranyl ion has been reviewed by Burrows (1974) amongst others. The shape and intensity of the absorption and emission spectra, together with the luminescent lifetime are greatly influenced by the environment surrounding the uranyl ion. For example, when the uranyl ion is incorporated into the sodium fluoride/lithium fluoride fusion mixture the emission spectrum appears as in Figure 43. The lifetime is very short (less than 50 μs) and could not be measured with the Model LS-5. In an aqueous environment the lifetimes can range from 10 μs to several hundred μs , depending upon the degree of radiationless deactivation via the O-H stretch modes of coordinated water molecules and/or paramagnetic ions such as Fe^{3+}. The emission spectrum displays considerable vibrational structure and is centred around 510 nm. The corrected and uncorrected emission spectra excited at 240 nm are shown in Figure 44. The solution contains 10% w/v orthophosphoric acid. Quantum yield measurement on a 1 μgmL^{-1} solution yielded a mean value of 0.105 with a relative standard deviation of ± 3.5%

8.2 Quantitative Analysis of Uranyl Ions in Aqueous Solutions

The combination of a solvent extraction procedure with a back extraction into dilute phosphoric acid for measurement provides an effective means of measuring uranyl ions in the presence of quenchers, Rhys Williams and Miller (1983). The solvent extraction procedure successfully

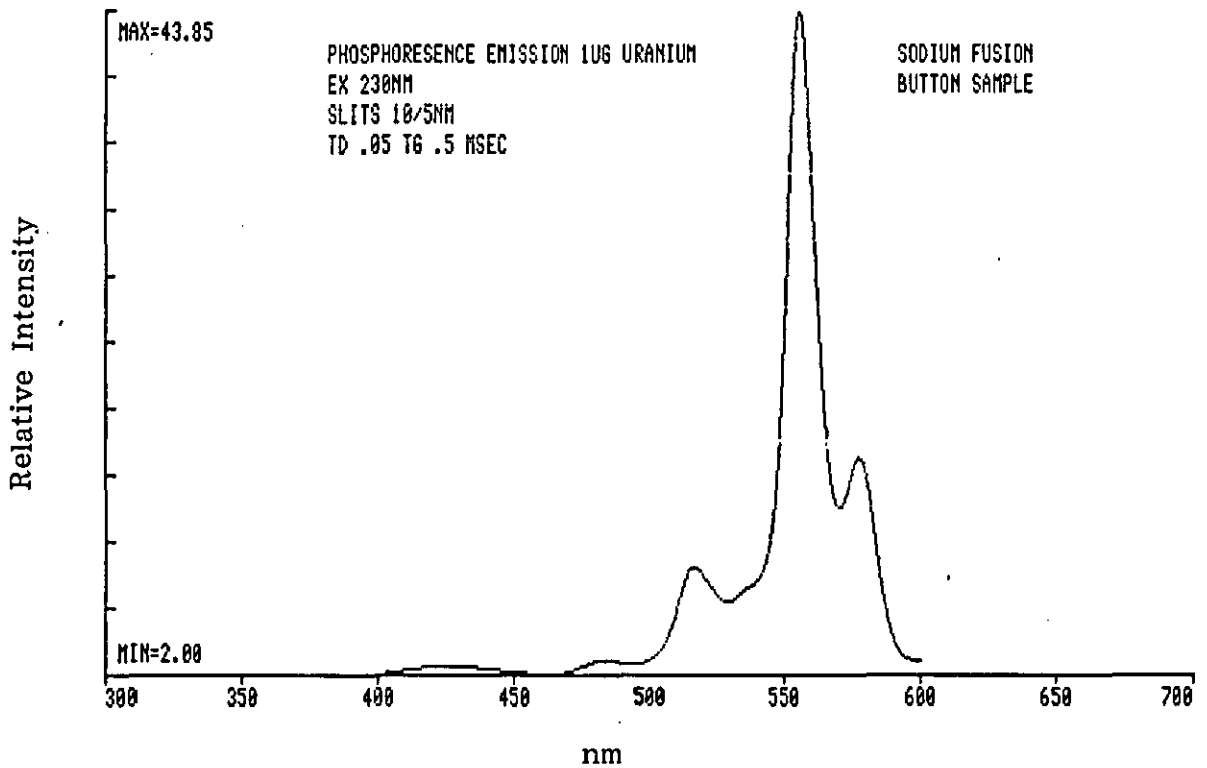

Figure 43. Emission spectrum of the uranyl ion incorporated in the sodium fluoride/

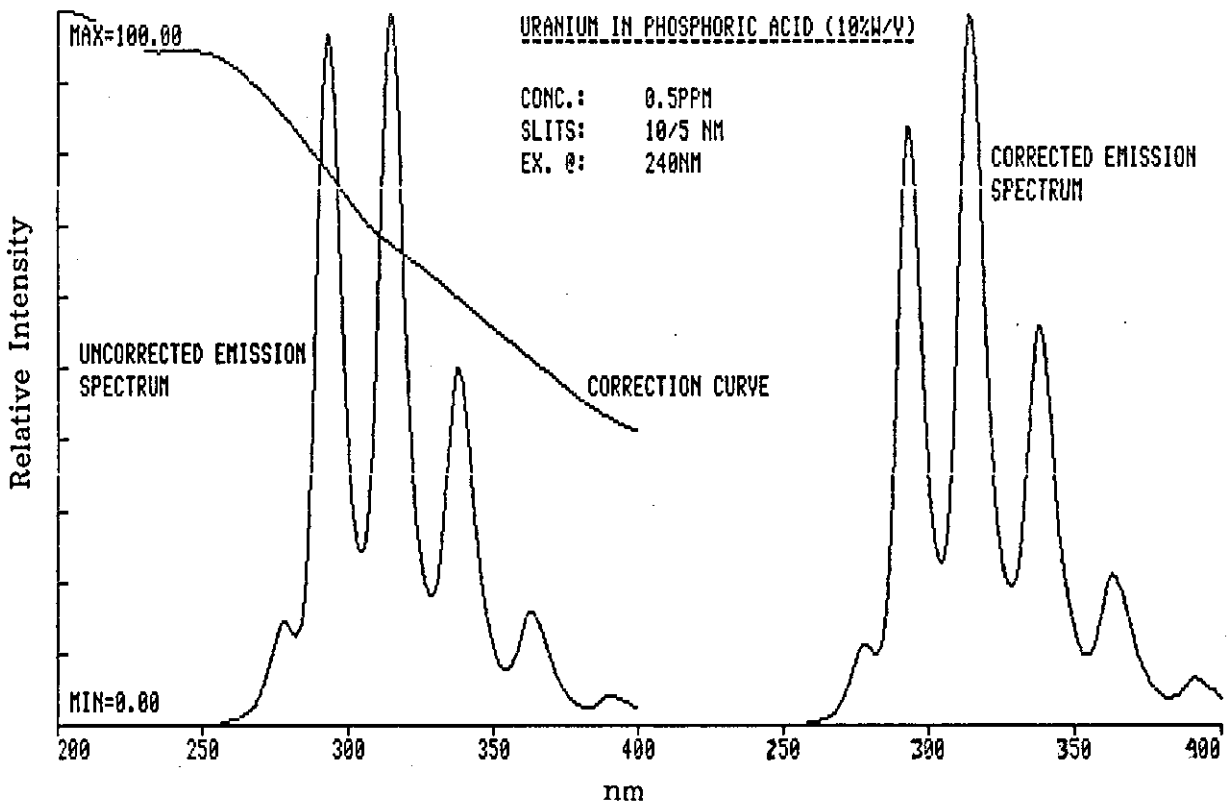

Figure 44. Uncorrected and corrected spectra of uranyl ion excited at 240nm in 10% w/v phosphoric acid

isolates the uranyl ions, whilst measurement in the dilute phosphoric acid enables the use of time discrimination to reduce the background fluorescence signal. Direct measurement of the uranium in the organic phase is not possible because the emission is totally suppressed. Tributyl phosphate (TBP) in hexane was found to be the most effective in extracting the uranyl ion compared with trioctylphosphate, trioctylphosphine oxide and ethyl acetate.

The optimum concentration of TBP was found to be 1%, Figure 45, whilst 10% w/v orthophosphoric acid gave the best efficiency for back extraction and measurement, Figure 46. The lifetime of a 1 μgmL^{-1} uranyl ion solution in phosphoric acid was found to be 170 µs, whilst the lifetime in the final extract was 85 µs. The decrease in lifetime shows that a little of the organic phase dissolves in the dilute acid and partly quenches the uranyl luminescence. A gate time t_g' of 250 µs and a delay t_d of 30 µs was chosen for the qualitative measurement. This ensured that approximately 96% of the emitted light was measured, yet at the same time ensured that any background fluorescence signal had decayed to zero. A comparison of a 50 $ngmL^{-1}$ uranyl ion solution measured in fluorescence and phosphorescence mode gave a signal to background ratio of 2.3 and 10.4 respectively, Figure 47. A salting agent is commonly employed when solvent extracting uranyl ion and the most efficient is aluminium nitrate. Calculations show that the latter contributes significantly to the blank value, since even AnalaR grade may contain up to 50 ng uranyl ion per 100 g of aluminium nitrate. In addition, phosphoric acid contains measureable quantities of uranium. Both these reagents were therefore washed with 1% v/v TBP in hexane to reduce the background signal. The analytical procedure is as follows:

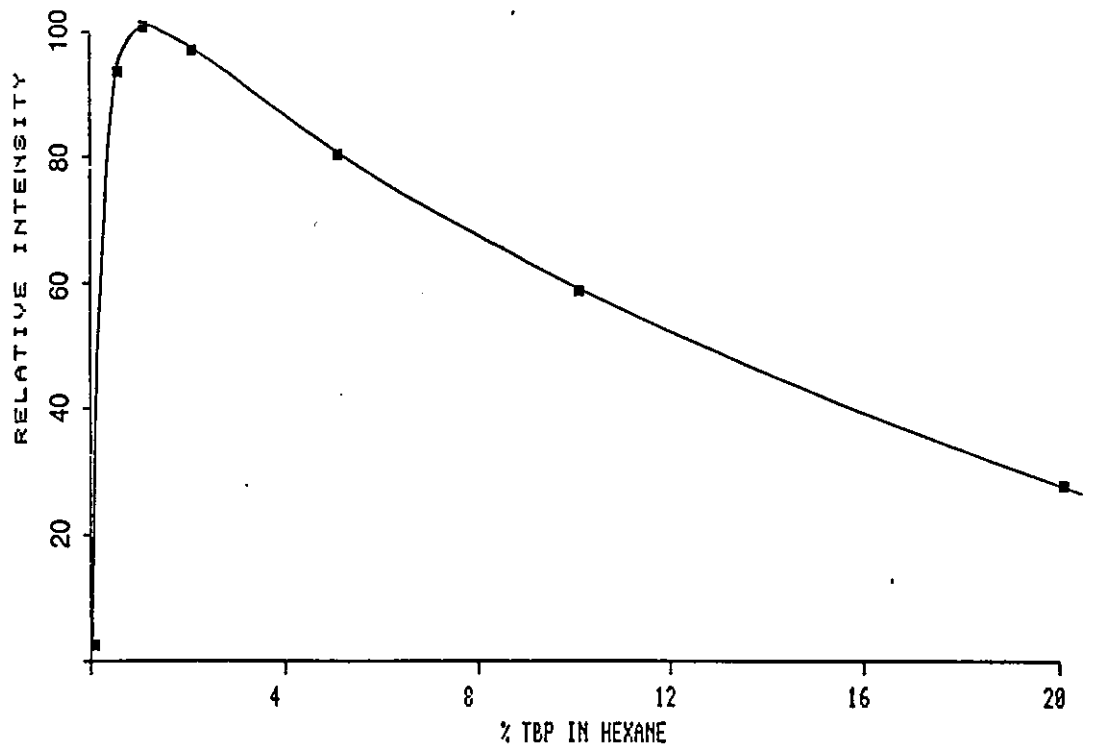

Figure 45. Variation in the relative intensity of the uranyl emission in the first aqueous phase with concentration of TBP in hexane

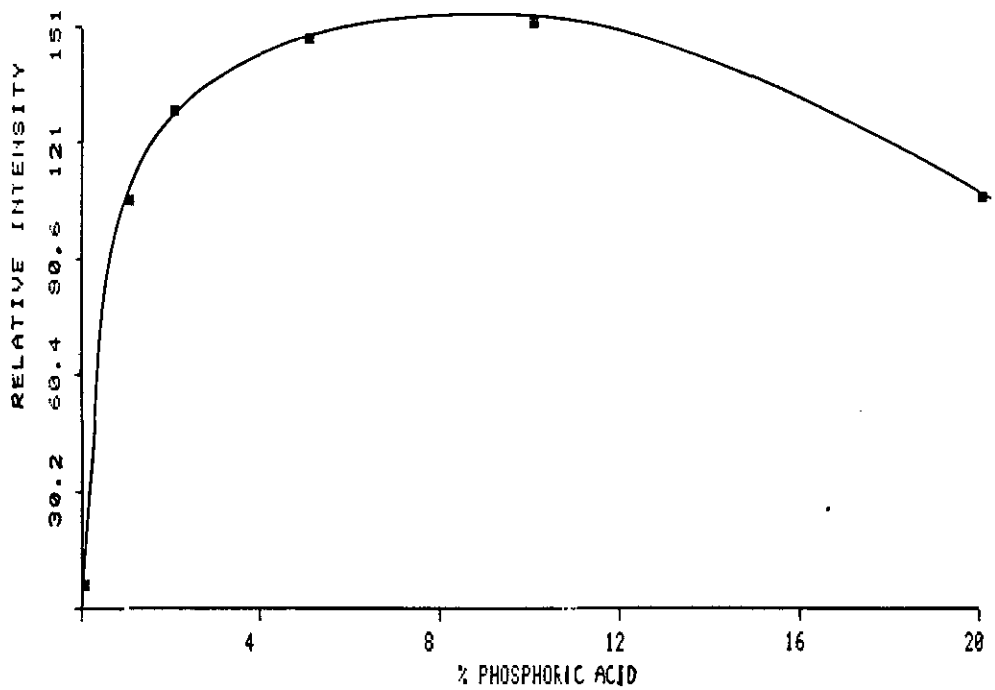

Figure 46. Variation in the relative intensity of the uranyl emission with varying concentrations of phosphoric acid

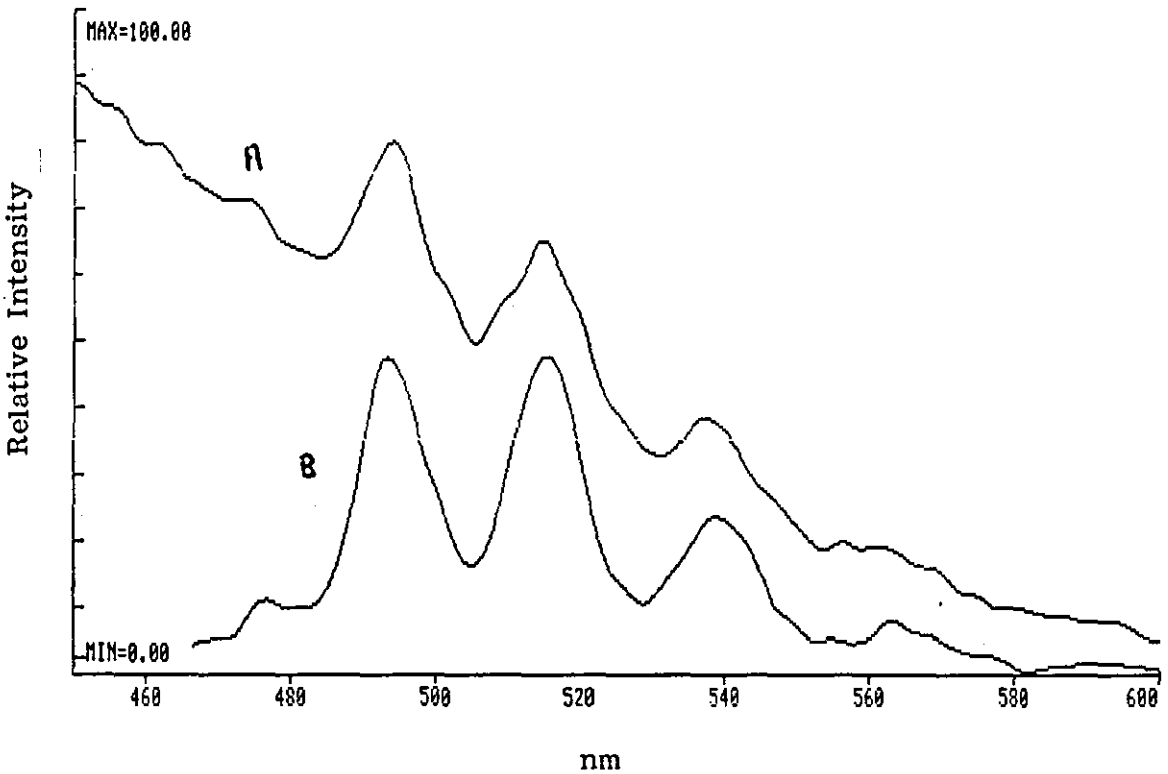

Figure 47. Comparison of a) the fluorescence and b) the phosphorescence mode emission of 50 ngmL^{-1} uranyl ion in 10% w/v ortho phosphoric acid saturated with 1% w/v TBP in hexane; excitation 245nm with t_d 30μs and t_g 2.50μs for the phosphorescence mode

To a 10 mL glass extraction tube containing 2 mL of the aluminium nitrate solution was added 1 mL of the sample of uranium standard. To this was added 3 mL of TBP in hexane, the tube sealed with a glass stopper and then shaken for two minutes. The tubes were centrifuged for 1 minute at 2000 rpm and 2 mL of the top organic layer removed and added to 3 mL of the phosphoric acid solution in a second 10 mL extraction tube. The latter was stoppered, shaken for two minutes, centrifuged as before, and the bottom aqueous layer transferred by Pasteur pipette to a cuvette for measurement.

The Model LS-5 was set at 245 nm excitation, and 515 nm emission, with the t_d and t_g, 30 µsec and 250 µsec respectively. A linear calibration curve with a slope of 80.7, intercept of 0.635 and a correlation coefficient of 0.98 was obtained for a 0 - 10 ugmL^{-1} uranyl ion solution, Figure 48. Eight standards were measured in triplicate. A calibration curve constructed from 0 - 200 ng mL^{-1} indicated that the minimum detection limit was approximately 5 ng mL^{-1} (2×background) At the 10 ng mL^{-1} level the relative standard deviation was ± 8%. The efficiency of the extraction procedure was found to be 81%.

Interference from quenchers such as Fe^{3+}, Mn^{2+} and Cl^- was examined by comparing the intensities of 0.25 µg mL^{-1} uranyl ion solutions containing from 0 - 100 µg mL^{-1} of the individual quenchers. The intensity of the extracted and unextracted solutions were compared. For Fe^{3+} the results are shown in Table 17. No significant difference was found up to 100 µg mL^{-1} Fe^{3+}. However, the unextracted solutions showed a rapid decrease in emission which obeyed the Stern-Volmer law, Figure 49. Similar results were obtained for Mn^{7+} and Cl^{-1}. A

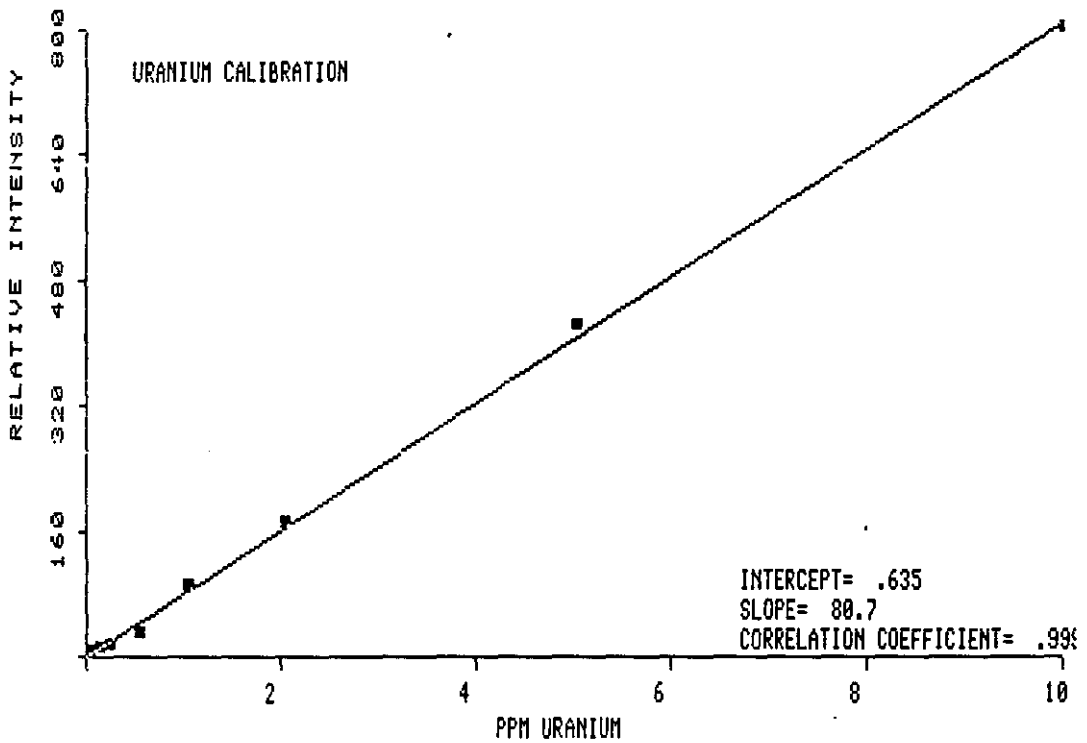

Figure 48. Relative intensity versus uranyl ion concentration (0 - 10 μgmL^{-1}) as measured by the solvent extraction procedure

TABLE 17

Fe^{3+} $\mu g\ mL^{-1}$	Uranyl emission intensity		(Ro/R)-1
	After extraction	Before extraction	
0	104.5	94.7	0.000
5	100.9	71.9	0.317
10	117.0	62.1	0.525
20	117.7	42.2	1.244
50	105.3	30.1	2.146
75	119.9	24.8	2.819
100	100.4	17.3	4.474

$\bar{x}$ = 109.5

δ = 8.0

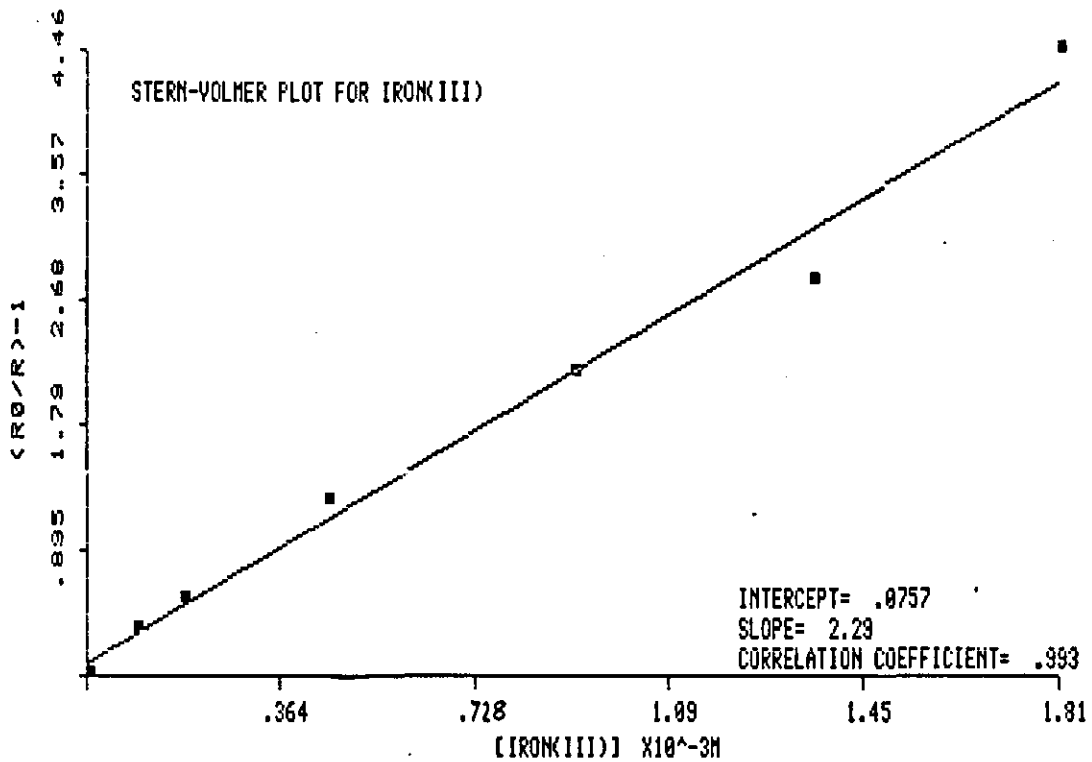

Figure 49. Stern-Volmer plot of increasing Fe^{3+} concentration on uranyl ion emission

comparison was made between a 100 μg mL^{-1} standard uranyl ion solution and a sample of river and drinking water to which an equivalent amount of uranium had been added. Again, no significant differences were observed, thus confirming the efficiency of the method in measuring uranium in the presence of quenchers.

CHAPTER NINE

CONCLUSIONS

The combination of a relatively fast optical system (f_3) with a pulsed 9 watt xenon source and gated electronics gave comparable performance in terms of sensitivity to conventional 150 watt xenon source instruments. Fluorescence and phosphorescence spectra were readily obtained by electronically measuring the emission signal either at the instant of the flash (fluorescence) or by delaying the measurement until the source energy has decayed to zero (phosphorescence). The delay, t_d, and gate time t_g, could be varied in 10 µs steps and with a minimum t_d of 10 µs and a maximum of 13 ms lifetimes between 60 µs and 600 ms can be accurately measured by recording the intensity at fixed delay times. Longer lived decays could be measured by monitoring the emission with respect to time after closing the excitation shutter. With the next generation of instruments it will be possible to decrease the source pulse rate so as to improve the accuracy of measuring lifetimes between 400 ms and 2 s. The intrinsic power of each flash will also be increased to maintain the same average power output per second.

Low temperature fluorescence and phosphorescence spectra were easily and rapidly obtained using the conduction cooling accessory. Sample temperatures were found to be ~74 K and reached this level 30 s after insertion in the accessory. A minimum sample volume of 20 µl is required using the 1 mm ID sample tube.

A major source of error in recording relative quantum yields - the measurement of absorbance values - was overcome by using the spectrometer to obtain both absorbance and excitation/emission data. A Rhodamine 101 quantum counter with a compensated beam splitter was used to give corrected excitation spectra. An emission correction curve was generated from a combination of the excitation monochromator used as a source of known spectral distribution and the corrected emission spectrum of quinine sulphate published by the NBS.

A desk top computer was used to control the spectrometer using a dedicated software program. Relative quantum yields were automatically calculated from a program called QYLDP.OY, using either quinine sulphate or 9,10-diphenylanthracene (9,10-DPA) as standard. Using a Φ_f value of 0.59 for quinine sulphate in 0.1 M $HClO_4$ resulted in a room temperature Φ_f value for 9,10-DPA of 0.96. This value contrasts with the value of 1.00 given by Heinrich et al (1974) or Ware (1976) but is in agreement with the fact that overlap of emission and excitation occurs leading to reabsorption errors.

The low temperature Φ_f and Φ_p values were not corrected for any polarisation errors because of the difficulty in positioning polarising filters in the sample area. These problems will be overcome in the next generation of spectrometers by positioning the polarising filter next to the entrance slits of the monochromators.

Both the room and low temperature Φ_f and Φ_p values agree well with those published by other workers. The differences that do exist are probably the result of using an incorrect value for the standard, the quenching effect of dissolved oxygen and also difference in the purity of both solute and solvent.

The Φ_f and Φ_p values for the amino acids agreed well with those published by Bishai et al (1967) and King (1972), but contrasted with those found by Chen (1967C).

The investigations of the luminescence of Tb^{3+} bound to transferrin indicated the probable involvement of tryptophanyl residues in energy transfer to the Tb^{3+}. Further work is required to confirm this theory and to establish the correct distance between the two binding sites of transferrin. In a recent paper, O'Hara et al (1981) have questioned the value found by Luk (1971).

The ability to discriminate between phosphors on a time basis was well demonstrated in the emission spectrum of the Tb^{3+}-transferrin complex, and further amplified in the evaluation of the luminescence of Eu^{3+} in yttrium oxide. The various transitions were isolated on a time basis rather than by direct excitation at the appropriate levels. The observed transition agreed well with those published by other workers. The minimum resolution of 2.5 nm was a limiting factor in being able to resolve the splitting of the various transitions.

Uranyl emission is readily quenched by ions such as Fe^{3+}, Ma^{2+} and Cl^{-}. Extraction with TPB in hexane was found to be very effective in isolating the uranyl ion from these interfering ions. Following back extraction from the organic phase into phosphoric acid solution, the uranyl emission was measured in phosphorescence mode. This effectively reduced the background fluorescence signal from the solvent. A detection limit of 5 ng mL^{-1} was obtained with a linear calibration range of 0 - 10 μg mL^{-1}. This compares well with the 1 ng mL^{-1} detection limit observed using laser excitation.

References

Adams, J.A.S., Maeck, W.J., Anal. Chem., 26, 1635 (1954).

Adams, M.J., Highfield, J.G., Kirkbright, G.F., Anal. Chem., 49, 1850 (1977).

Adams, M.J., Highfield, J.G., Kirkbright, G.F., Anal. Chem., 52 1260 (1980).

Adams, M.J., Highfield, J.G., Kirkbright, G.F., Analyst 106, 850 (1981).

Almgren, M., Photochem. Photobiol., 8 231 (1968).

Araki, T., Uchida, T., Minami, S., Japan J. Appl. Phys., 15 2421 (1976).

Arbeloa, I.L., J. Photochem., 14 97 (1980).

Axe, J.D., Weller, P.F., J. Chem. Phys., 40 3066 (1964).

Azumi, T., McGlynn, S.P., J. Chem. Phys., 52 1364 (1970).

Baker, H.G., King, T.A., J. Phys. E., 8 219 (1975).

Barel, A.O., Glazer, A.W., J. Biol. Chem., 244 268 (1969).

Bauer, R., Baczinski, A., Bull. Acad. Polon. Sci., 6 113 (1958).

Baumik, M.L., Clark, G.L., Snell, L., Fender, L., Rev. Sci. Inst., 36 37 (1965).

Baumik, M.L., Telk, C.L., J. Opt. Soc. Am., 54 1211 (1964).

Becquerel, E., Anal. Chim. Phys., 27 539 (1971).

Bendig, J., Kreysig, D., Schoneich, R., Opt. Spectrosc. USSR, 49 29 (1980).

Benson, P., Cox, A., Kemp, T.J., Sultana, Q., Chem. Phys. Lett., 35 195 (1975).

Berlman, I.B., Handbook of Fluorescence Spectra of Aromatic Molecules. Academic (1965) 2nd Ed. (1971).

Berner, V.G., Darnall, D.W., Birnbaum, E.R., Biochim. Biophys. Res. Com., 66 763 (1975).

Birks, J.B., J. Res. Natl. Bur. Stnd., 80A 389 (1976).

Bishai, F., Kuntz, E., Augenstein, L., Biochim. Biophys. Acta., 140 318 (1967).

Blasse, G., J. Lumin., 1,2 766 (1970).

Bodo, Z., Acta. Phys. Acad. Sci. Hung., 3 23 (1963).

Borreson, H.C., Parker, C.A., Anal. Chem., 38 1073 (1963).

Boutilier, G.D., Bradshaw, J.D., Weeks, S.J., Winefordner, J.D., Appl. Spec., 31 307 (1977).

Brannon, J.H., Magde, D., J. Phys. Chem., 82 705 (1978),

Breyesse, M., Faure, L., J. Lumin., 26 107 (1981).

Bridges, J.W., "Standards in FL Spec", Miller, J.N., Ed., Chapman & Hall (1981).

Bril, A., De Jager-Veenis, A.W., J. Electrochem. Soc., 123 396 (1976 A).

Bril, A., De Jager-Veenis, A.W., J. Res. Natl. Bur. Stnd., 80A 401 (1976 B).

Brittain, H.G., Richardson, F.S., Martin, R.B., J. Am. Chem. Soc., 98 8225 (1976).

Britten, A., Archer-Hall, J., Lockwood, G., Analyst, 103 928 (1978).

Bromba, M.V.A., Ziegler, H., Anal. Chem., 53 1583 (1981).

Buck, A., Erickson, R., Barnes, F., J. App. Phys. 34 2115 (1963).

Burrows, H.D., Kemp, T.G., Chem. Soc. Rev., 3 139 (1974).

Busselle, F.J., Haig, N.D., Lewis, C., Chem. Phys. Lett., 72 533 (1980).

Callis, J.B., J. Res. Nat. Bur. Stand., 80A 413 (1976).

Cehelnik, E.D., Mielenz, K.D., Velapoldi, R.A., J. Res. Nat. Bur. Std., 79A, 1 (1975).

Centanni, F.A., Ross, A.M., Desassa, M.A., Anal. Chem., 25 1651 (1956).

Chang, N.C., J. App. Phys., 34 3500 (1963).

Chang, N.C., Gruber, J.B., J. Phys. Chem., 41 3227 (1964).

Charles, R.G., Riedel, E.P., J. Inorg. Nucl. Chem., 28 527 (1966).

Chen, R.F., in Fluorescence, Ed. Guilbault, G.G., Arnold (1967 A).

Chen, R.F., Anal. Biochem., 20 339 (1967 B).

Chen, R.F., Anal. Lett., 1 35 (1967 C).

Chen, R.F., Anal. Lett., 14 1591 (1981).

Chen, R.F., J. Res. Nat. Bur. Stand., 76A, 593 (1972).

Christensen, R.L., Ames, I., J. Opt. Soc. Am., 51 224 (1961).

Crosby, G.A., Luminescent Organic Complexes of Rare Earths in Molecular Crystals, 1 37 (1966).

Crosby, G.A., Demas, J.N., Callis, J.B., J. Res. Nat. Bur. Std., 76A, 561 (1972).

Crosby, G.A., Whan, R.E., Alire, R.M., J. Chem. Phys., 34 743 (1961).

Cundall, R.B., Pereira, L.C., J.C.S. Faraday II 1152 (1972).

Dawson, W.R., Kropp, J.L., Windsor, M.W., J. Chem. Phys., 45 2410 (1966).

Dawson, W.R., Windsor, M.W., J. Phys. Chem., 72 3251 (1968).

Dejersey, J., Morley, P.J., Martin, R.B., Biophys. Chem., 13 233 (1981).

Demas, J.N., Blumenthal, B.H., J. Res. Natl. Bur. Stnd., 80A 409 (1976).

Demas, J.N., Bowman, W.D., Zalewski, E.F., Velapoldi, R.A., J. Phys. Chem., 85 2766 (1981).

Demas, J.N., Crosby, G.A., J. Phys. Chem., 75 991 (1971).

Dexter, D.L., J. Chem. Phys., 21 836 (1953).

Drexhage, K.H., J. Res. Nat. Bur. Stand., 80A 421 (1976).

Drexhage, K.H., Topics in Appl. Phys., 1 144 (1973).

Drushel, H.V., Sommers, A.L., Cox, R.C., Anal. Chem., 35 2166 (1963).

Duggan, D., Udenfriend, S., J. Biol. Chem., 223 313 (1956).

Edelhoch, H., Brand, L., Wilchek, M., Biochem., 6 547 (1969).

Eisinger, J., in Molecular Luminescence Ed. Lim, E.C., (1969).

Eisinger, J., Feuer, B., Lamola, A.A., Biochem., 8 3908 (1969).

Eisinger, J., Lamola, A.A., Biochim. Biophys. Acta, 240 299 (1971).

Ermolaev, V.L., Svitashev, K.K., Opt. Spectroscop., 7 399 (1959).

Filipescu, N., Mushrush, G.W., J. Phys. Chem., 72 3516 (1968).

Fisher, R.P., Winefordner, J.D., Anal. Chem., 44 948 (1972).

Forster, Th., Fluoreszenze Organischer Verbindungen, Vandenhoek & Ruprecht (1951).

Francois, C.A., Anal. Chem., 30 50 (1958).

Freed, S., Turnbull, J.H., Salmre, W., Nature 181 1731 (1958).

Gains, N., Dawson, A.P., Analyst, 104 481 (1979).

Galley, W.C., Stryer, L., Biochem., 8 1831 (1969).

Galley, W.C., Stryer, L., Proc. N.A.S.Am., 60 108 (1968).

Gelernt, B., Findeisen, A., Poole, J., J. Chem. Soc. Faraday Trans., 70 939 (1974).

Gifford, L.A., Hayes, W.P., King, L.A., Miller, J.N., Burns, D.T., Bridges, J.W., Anal. Chim. Acta., 62 214 (1972).

Gilmore, E.H., Gibson, G.E., McClure, D.S., Analyst 87 664 (1962).

Gilmore, E.H., Gibson, G.E., McClure, D.S., J. Chem. Phys., 20 829 (1952).

Gilmore, E.H., Gibson, G.E., McClure, D.S., J. Chem. Phys., 23 399 (1955).

Grum, F., Luckey, G.W., Appl. Optics, 7 2289 (1968).

Guilbault, G.G., Practical Fluorescence. Marcel Dekker (1973).

Hamilton, T.D.S., Naqvi, K.R., Anal. Chem., 45 1581 (1973).

Harris, D.C., Biochem., 16 560 (1977).

Haugen, G.R., Lytle, F.E., Anal. Chem., 53 1554 (1981).

Heinrich, G., Schoof, S., Gusten, H., J. Photochem., 3 315 (1974).

Heller, A., Wasserman, E., J. Chem. Phys., 42 949 (1965).

Hendee, C.F., Brown, W.B., Philips Tech. Rev., 19 50 (1957).

Hermans, J.J., Levinson, S., J. Opt. Soc. Am., 41 460 (1951).

Hinton, E.R., White, L.E., Anal. Lett., 14 947 (1981).

Holland, E.R., Teets, R.E., Timmick, A., Anal. Chem., 45 145 (1973).

Holland, J.F., Teets, R.E., Kelly, R.M., Timmick, A., Anal. Chem., 49 706 (1977).

Hollifield, H.C., Winefordner, J.D., Anal. Chem., 40 1759 (1968).

Horton, C.A., White, J.C., Anal. Chem., 30 1779 (1958).

Inokuchi, H., Harada, Y., Kondow, T., J. Opt. Soc. Am., 54 842 (1964).

Kaminski, R., Purcell, F.J., Russavage, E., Anal. Chem., 53 1093 (1981).

Kellogg, R.E., Bennett, R.G., J. Chem. Phys., 41 3042 (1964).

King, L.A., PhD. Loughborough (1972).

Kojima, T., Shigetomi, Y., Kamba, H., Iwashiro, H., Analyst, 107 519 (1982).

Konev, S.V., Bobrovich, V.P., Biophysics 10 813 (1965).

Kubin, R.F., Fletcher, A.N., J. Lumin., 27 455 (1982).

Kuntz, I.D., J. Am. Chem. Soc., 93 514 (1971).

Lamola, A.A., Eisinger, J., Biochim. Biophys. Acta, 240 313 (1971).

Lehrer, S.S., J. Biol. Chem., 244 3613 (1969).

Lewis, G.N., Kasha, M., J. Am. Chem. Soc., 66 2100 (1944).

Lim, E.C., Laposa, J.D., Yu, J.M.H., J. Mol. Spec., 19 412 (1966).

Lipsett, F.R., Progress in Dielectrics 7 217 (1967).

Longworth, J.W., Biochem., 81 23 (1961).

Longworth, J.W., in Excited States of Proteins and Nucleic Acids, Ed. Steiner, R.F., Weinryb, I., Plenum (1971).

Luk, C.K., Biochem., 10 2838 (1971).

Lukasiewcz, R.J., Mousa, J.J., Winefordner, J.D., Anal. Chem., 44 1339 (1972).

Mantulin, W.W., Huber, J.R., Photochem. Photobiol., 17 139 (1973).

Marcantonatos, M.D., Inorg. Chim. Acta., 25 2101 (1977).

Mardelli, M., Olmsted, J., J. Photochem., 7 277 (1977).

Moriyasu, M., Yokoyama, Y., J. Inorg. Nucl. Chem., 39 2199 (1977).

McAvoy, N., Filipescu, N., Kagan, M.R., Serafin, F.A., J. Phys. Chem., 25 261 (1964).

McCarville, M., Hauxwell, R., Biochim. Biophys. Acta. 251 285 (1971).

McElhaney, R.J., Y-2111 NTIS (1978).

Melhuish, W.H., J. Phys. Chem., 65 229 (1961).

Melhuish, W.H., J. Opt. Soc. Am., 52 1256 (1962).

Melhuish, W.H., J. Res. Nat. Bur. Stand., 76A 547 (1972).

Melhuish, W.H., Zander, M., Pure Appl. Chem., 53 1953 (1981).

Mielenz, K.D., Applied Optics 18 4134 (1979).

Morris, J.V., Mahaney, M.A., Huber, J.R., J. Phys. Chem., 80 969 (1976).

Mousa, J.J., Winefordner, J.D., Anal. Chem., 46 1195 (1974).

Mushrush, G.W., Yonuschot, G., J. Lumin., 28 233 (1983).

O'Connor, D., Phillips, D., Chem. Phys. Lett., 88 222 (1982).

O'Haver, T.C., Winefordner, J.D., Anal. Chem., 38 602 (1966 A)

O'Haver, T.C., Winefordner, J.D., Anal. Chem., 38 1258 (1966 B).

O'Hara, P., Yeh, S.M., Meares, C.F., Bersohn, R., Biochem., 20 4074 (1981).

Ohba, Y., Mizuta, M., Kukimoto, H., J. Lumin., 28 111 (1983).

Olmsted, J., J. Phys. Chem., 83 2581 (1979).

Ozawa, L., J. Electrochem. Soc., 126 106 (1979).

Paloetti, J., Lapecq, J.B., Anal. Biochem., 31 33 (1969).

Pant, D.D., Tripathi, H.B., J. Lumin., 8 492 (1974).

Parker, C.A., Nature 182 1002 (1958).

Parker, C.A., Anal. Chem., 34 502 (1962).

Parker, C.A., Photoluminescence of Solutions Elsevier N.Y., (1968).

Parker, C.A., Hatchard, C.G., Analyst 87 664 (1962).

Parker, C.A., Rees, W.T., Analyst 85 587 (1960).

Pecoraro, W.L., Harris, W.R., Biochem., 20 7033 (1981).

Perry, D.L., Bowman, H.R., Millanovitch, H., Miller, S., Anal. Chem., 53 1048 (1981).

Peterson, G.E., Bridenbaugh, P.M., J. Opt. Soc. Am., 53 1129 (1963).

Poole, J.A., Findeisen, A., J. Chem. Phys., 67 5338 (1977).

Rhys Williams, A.T., Int. Lab., 11 90 (1981).

Rhys Williams A.T., Fuller, M., Comp. Enhanc. Spectr., 1 145 (1983).

Rhys Williams, A.T., Miller, J.N., Anal. Chim. Acta., 154 341 (1983 A).

Rhys Williams, A.T., Winfield, S.A., Miller, J.N., Analyst 108 1067 (1983 B)

Rhys Williams, A.T., Winfield, S.A., Miller, J.N., Analyst 108 1471 (1983 C).

Ritter, A.W., Tway, P.C., Cline Love, L.J., Ashworth, H.A., Anal. Chem., 53 280 (1981).

Robbins, J.C., Kinrade, J.D., Canada Pat., 1064726 Oct (1979).

Savitzki, A., Golay, M., Anal. Chem., 36 1627 (1964).

Schmidt-Ott, A., Meier, F., Rev. Sci. Inst., 48 524 (1977).

Schulman, E.M., Walling, C., J. Phys. Chem., 77 902 (1973).

Seybold, P.J., Gouterman, M., Callis, J.B., Photochem. Photobiol., 9 229 (1969).

Shinitzky, M., J. Chem. Phys., 56 5979 (1972).

Stein, G., Wurzberg, E., J. Chem. Phys., 62 208 (1975).

Steiner, R.F., Kolinski, R., Biochem., 7 1014 (1968).

Stewart, W.W., Nature 292 17 (1981).

Strambini, G.B., Galley, W.C., Can. J. Spectrosc., 21 1 (1976).

Strickland, E.H., Horwitz, J., Billups, C., Biochem., 8 3205 (1969).

Taylor, D.G., Demas, J.N., Anal. Chem., 51 717 (1979).

Teale, F.W.G., Weber, G., Biochem., 65 476 (1956).

Teuwissen, B., Masson, P.L., Osinski, P., Heremans, J.F., Eur. J. Biochem., 31 239 (1972).

Thatcher, L.L., Barker, F.B., Anal. Chem., 29 1575 (1957).

Truong, T., J. Biol. Chem., 242 2979 (1967).

Turro, N.G., Kou-Chang, L., Ming-Fea, C., Lee, P., Photochem. Photobiol., 27 523 (1978).

Udenfriend, S., Fluorescence Assay in Biology and Medicine, Vol.1,2 Academic (1970).

UKAEA Report PG 186 (CA) 1962.

Upton, L.M., Cline Love, L.J., Anal. Chem., 51 1941 (1979).

Vavilov, S.I., Z. Phys., 42 311 (1927).

Velapoldi, R.A., J. Res. Nat. Bur. Stand., 76A 641 (1972).

Velapoldi, R.A., Mielenz, K.D., NBS Special Pub., 260 (1980).

Veselsky, J.C., Ratismandresy, Y., Anal. Chim. Acta., 104 345 (1979).

Vladimirov, Y.A., Litvin, F.F., Biofizika 5 127 (1960).

Ward, J.L., Bateh, R.P., Winefordner, J.D., Appl. Spec., 34 15 (1980 A).

Ward, J.L., Walden, G.L., Bateh, R.P., Winefordner, J.D., Appl. Spec., 34 348 (1980 B).

Ware, W.R., Rothman, W., Chem. Phys. Lett., 39 449 (1976).

Weber, G., Daniel, E., Biochem., 5 1900 (1966).

Weber, G., Teale, F.W.J., Trans. Faraday Soc., 53 646 (1957).

Weber, M.J., Phys. Rev., 171 283 (1968).

Weinryb, I., Steiner, R.F., 7 2488 (1968).

Weinryb, I., Steiner, R.F., Biochem., 9 135 (1970).

Weissman, S.I., J. Chem. Phys., 10 214 (1942).

West, M.A., Photochemistry 10 (1979).

White, C.E., Ho, M., Weimer, E., Anal. Chem., 32 438 (1960).

Whitkop, P.J., Anal. Chem., 54 2475 (1982).

Winefordner, J.D., Accounts Chem. Res., 2 361 (1969).

Winefordner, J.D., J. Res. Nat. Bur. Std., 76A 579 (1972).

Winnick, M.A., Lemire, A., Chem. Phys. Lett., 46 283 (1977).

Yokoyama, Y., Ikeda, S., J. Inorg. Nucl. Chem., 38 1329 (1976).

Yonuschot, G., Mushrush, G.W., Biochem., 14 1677 (1975).

APPENDIX I

Printout of the results from the OBEY program DECAY.OY in the calculation of the decay time of free Tb^{3+} in H_2O.

```
=% Sample name:   TB                  Solvent: RTP
=%
=% Concentration: .1M                 EX Slit: 2.5  , EM Slit: 2.5
=%
=% Values for Log(Intensity) are as Follows (Gate Time= .1 ms):
=%
=%        Delay Time (ms)       Intensity (I)        Log(I)
=%              0.10              99.800              1.999
=%              0.30              62.700              1.797
=%              0.50              39.000              1.591
=%              0.70              24.400              1.387
=%              0.90              15.300              1.185
=%              1.10               9.600              0.982
=%
=% The Average Lifetime for the Decay (EX 221 nm, EM 543 nm) is:
=%
=%                                        0.426 ms
=%
=% The Correlation Coefficient is:        1.000
=% The Standard Error of Estimate is:     0.002
```

APPENDIX II

A typical long lived phosphorescence decay curve obtained by recording the signal after cutting off the exciting light with the shutter. The data is recorded in TDRIVE mode with an instrumental response of 0.5 s and a data interval of 0.2 s.

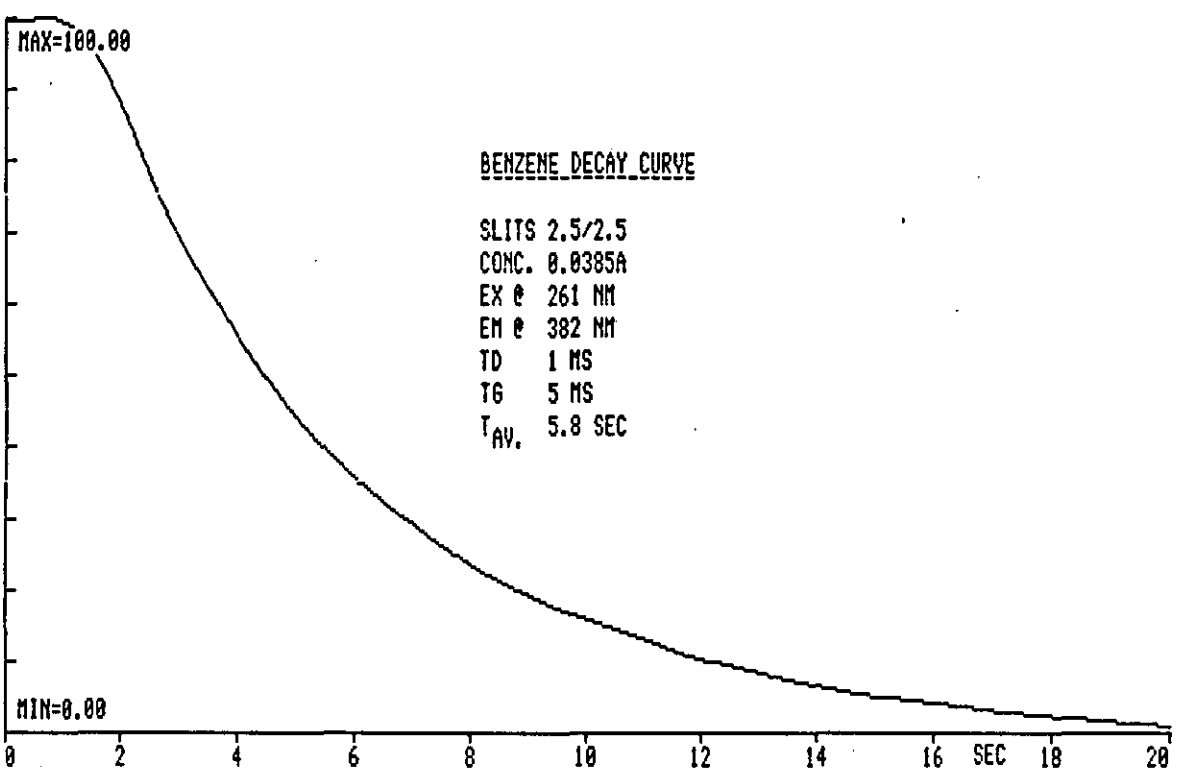

APPENDIX III Program listing of OBEY file QYLDP.OY

```
DO DISPLAY OFF
SET WAIT OFF
DO SCLEAR
DO VCLEAR
OUTPUT CLEAR V0
DO DISPLAY ON
*  QUANTUM YIELD DETERMINATION
*  ===========================
*
*    This program calculates quantum yields by
*    the comparative method.Phosphorescence quantum
*    yields are calculated using a FL standard.
*
*    If calculating phosphorescence quantum yields
*    ensure that that the DELAY and GATE times give
*    a reasonable signal compared to fluorescence standard.
*     The LIFE TIME of the phosphor must be found
*     before continuing.

*
*
* An EMISSION CORRECTION CURVE must be obtained
* before calculation of the QUANTUM YIELD. This is
* stored on a disk in DRIVE 1 under the filid CORRF.
*
* This file is derived from the OBEY program CORRC.OY.
*
* Press!RETURN!when ready to continue:
DO DISPLAY OFF
DO PAUSE
DO SCLEAR
DO DISPLAY ON
* Set the EXCITATION and EMISSION SLITS to 2.5nm
*
* Enter the QUANTUM EFFICIENCY of the STANDARD:
&ENTER A2
* &A2
*
DO SCLEAR
* Place the STANDARD in the CELL HOLDER
*
* Press!RETURN!to continue:
DO DISPLAY OFF
DO PAUSE
DO SCLEAR
&L10 *
PHOS DELAY 0 GATE 0
&ERROR L15
&GOTO L20
&L15 *
DO DISPLAY ON
* ***** INSTRUMENT ERROR *****
*
* Press!RETURN!when ready to continue:
DO DISPLAY OFF
DO PAUSE
DO SCLEAR
&GOTO L10
&L20 *
DO DISPLAY ON
```

```
* Enter the analytical EXCITATION WAVELENGTH for the STANDARD:
&ENTER A3
* &A3 nm.
*
* Enter the WAVELENGTH of MAXIMUM EMISSION for the STANDARD:
&ENTER A4
* &A4 nm.
*
* Enter the START WAVELENGTH for the EMISSION scan:
&ENTER A5
* &A5 nm.
*
* Enter the FINISH WAVELENGTH for the EMISSION scan:
&ENTER A6
* &A6 nm.
*
DO SCLEAR
*!SCANNING!  STANDARD EMISSION
DO DISPLAY OFF
CALC V22= &A2
CALC V23= &A4
CALC V24= &A3
MODE 240 2.5
&ERROR L15
GOTO &A3 &A4
ORD AC 90.0
SCAN X EM &A5 &A6 &V24
DO DISPLAY ON
DO VCLEAR
DO SCLEAR
* Place the STANDARD SOLVENT in the CELL HOLDER
*
* Press!RETURN!to continue:
DO DISPLAY OFF
DO PAUSE
DO SCLEAR
DO DISPLAY ON
*!SCANNING!  STANDARD SOLVENT
DO DISPLAY OFF
SCAN Y EM &A5 &A6 &V24
DIFF X Y
COPY Z X
&CHECK BLNK.SP
&ERROR L35
CNTENT DELETE BLNK
&L35 *
SAVE Y BLNK
RETRVE Y CORRF
CALC V2=XSTRT
CALC V3=XFIN
COPY Y Y &V2 &V3
CORR D
DO DISPLAY ON
DO VCLEAR
&L40 *
DO DISPLAY ON
DO SCLEAR
*
* Enter a FILID to SAVE the CORRECTED EMISSION of the STANDARD:
&ENTER A10
```

```
* &A10
*
DO DISPLAY OFF
SAVE Z &A10
&ERROR L40
AREA Z &V2 &V3
CALC V4=V19
&L45 *
OUTPUT CLEAR V1,V15
DO SCLEAR
DO DISPLAY ON
* Place the SAMPLE in the CELL HOLDER
*
* Press!RETURN!to continue:
DO DISPLAY OFF
DO PAUSE
DO SCLEAR
DO DISPLAY ON
* Enter the DELAY TIME
&ENTER A3
* &A3
* Enter the GATE TIME
&ENTER A4
* &A4
*
DO DISPLAY OFF
PHOS DELAY &A3 GATE &A4
DO DISPLAY ON
*
*!CHECK ZERO!*
*
* Press!RETURN!when ready to continue:
DO DISPLAY OFF
MANUAL
DO PAUSE
DO SCLEAR
DO DISPLAY ON
* Enter the analytical EXCITATION WAVELENGTH for the SAMPLE:
&ENTER A3
* &A3
*
* Enter the WAVELENGTH of MAXIMUM EMISSION for the SAMPLE:
&ENTER A4
* &A4 nm.
*
* Enter the START WAVELENGTH for the EMISSION scan:
&ENTER A5
* &A5 nm.
*
* Enter the FINISH WAVELENGTH for the EMISSION scan:
&ENTER A6
* &A6 nm.
*
DO SCLEAR
*!SCANNING! SAMPLE EMISSION
DO DISPLAY OFF
CALC V24= &A3
CALC V23= &A4
SCAN X EM &A5 &A6 &V24
SAVE X EM
```

```
DO SCLEAR
DO VCLEAR
DO DISPLAY ON
* Enter 1 to scan the EXCITATION SPECTRUM, press!RETURN!if not:
&ENTER A1
DO DISPLAY OFF
OUTPUT CLEAR V15
CALC V15= &A1
&IF V15 L50 L50 L48
&L48 *
DO SCLEAR
DO DISPLAY ON
* Enter the START WAVELENGTH for the EXCITATION scan:
&ENTER A7
* &A7 nm.
*
* Enter the FINISH WAVELENGTH for the EXCITATION scan:
&ENTER A8
* &A8 nm.
*
DO SCLEAR
*!SCANNING!  SAMPLE EXCITATION
DO DISPLAY OFF
SCAN Z EX &A7 &A8 &V23
DO VCLEAR
SAVE Z EX
&L50 *
DO SCLEAR
DO DISPLAY ON
* Place the SAMPLE SOLVENT in the CELL HOLDER
*
* Press!RETURN!to continue:
DO DISPLAY OFF
DO PAUSE
DO SCLEAR
DO DISPLAY ON
*!SCANNING!  SAMPLE SOLVENT EMISSION
DO DISPLAY OFF
SCAN Y EM &A5 &A6 &V24
SAVE Y EMB
DO VCLEAR
DO SCLEAR
&IF V15 L60 L60 L55
&L55 *
RETRVE X EX
CNTENT DELETE EX
DO DISPLAY ON
*!SCANNING! SAMPLE SOLVENT EXCITATION
DO DISPLAY OFF
SCAN Y EX &A7 &A8 &V23
DIFF X Y
&L56 *
DO SCLEAR
DO VCLEAR
DO DISPLAY ON
*
* Enter a FILID to SAVE the CORRECTED EXCITATION of the SAMPLE:
&ENTER A9
* &A9
*
```

```
DO DISPLAY OFF
SAVE Z &A9
&ERROR L56
RETRVE X EM
RETRVE Y EMB
&L60 *
CNTENT DELETE EM
CNTENT DELETE EMB
DIFF X Y
COPY Z X
RETRVE Y CORRF
CALC V2=XSTRT
CALC V3=XFIN
COPY Y Y &V2 &V3
CORR D
&L65 *
DO SCLEAR
DO DISPLAY ON
* Enter a FILID to SAVE the CORRECTED EMISSION of the SAMPLE:
&ENTER A8
* &A8
DO DISPLAY OFF
SAVE Z &A8
&ERROR L65
DO DISPLAY ON
*
DO SCLEAR
DO VCLEAR
* Enter the ABSORBANCE value of the STANDARD:
&ENTER A2
* &A2 A
*
* Enter the ABSORBANCE value of the SAMPLE:
&ENTER A3
* &A3 A
*
* Enter the CONCENTRATION of the STANDARD (NG/ML):
&ENTER A4
* &A4
*
* Enter the CONCENTRATION of the SAMPLE (NG/ML):
&ENTER A5
* &A5
*
* Enter the REFRACTIVE INDEX of the STANDARD solvent:
&ENTER A6
* &A6
*
* Enter the REFRACTIVE INDEX of the SAMPLE solvent:
&ENTER A7
* &A7
*
DO DISPLAY OFF
DO SCLEAR
AREA Z &V2 &V3
CALC V6=&A2
CALC V7=&A3
CALC V10=&A4
DO DISPLAY ON
* Enter the DELAY TIME td
```

```
&ENTER A2
* &A2
* Enter the GATE TIME tg
&ENTER A3
* &A3
* Enter the LIFE TIME in msec.
&ENTER A4
* &A4
DO DISPLAY OFF
CALC V1=&A2
CALC V2=&A3
CALC V3=&A4
OUTPUT CLEAR V11,V13,V14
CALC V13=EXP(-V1/V3)
&ERROR L68
&GOTO L69
&L68 *
CALC V13=0
&L69 *
CALC V11=EXP(-20/V3)
&ERROR L70
&GOTO L71
&L70 *
CALC V11=0
&L71 *
CALC V14=EXP(-(V1+V2)/V3)
&ERROR L72
&GOTO L73
&L72 *
CALC V14=0
&L73 *
CALC V13=(1-V11)/(V13-V14)
&ERROR L74
&GOTO L75
&L74 *
CALC V13=1
&L75 *
CALC V5=V19*V13
CALC V19=V13
CALC V11= &A5
CALC V13= &A6
CALC V14= &A7
CALC V8=V13*V13
CALC V9=V14*V14
CALC V12=V22*(V5/V4)*(V6/V7)*(V9/V8)
CALC V4=V1
DO VCLEAR
DO SCLEAR
DO DISPLAY ON
*
* The CORRECTED EMISSION of the STANDARD is in REGION X
*
* The CORRECTED EMISSION of the SAMPLE is in REGION Y
*
* The CORRECTED EXCITATION of the SAMPLE is in REGION Z (if SCANNED)
*
* Enter 1 to PRINT the CORRECTED SPECTRA of the SAMPLE
*
* or!RETURN! if not:
*
```

```
&ENTER A1
DO SCLEAR
DO DISPLAY OFF
OUTPUT CLEAR V1
CALC V1= &A1
RETRVE Y &A8
RETRVE X &A10
GOTO &V24 &V23
&IF V15 L79 L79 L78
&L78 *
RETRVE Z &A9
VIEW Z AUTE 200 650
AXIS
LABEL 500 200 EXCITATION SPECTRUM
LABEL 500 180 FILID: &A9
DO VPRNT
&L79 *
DO VCLEAR
DO SCLEAR
&IF V1 L85 L85 L84
&L84 *
VIEW Y AUTE 200 650
AXIS
LABEL 10 200 EMISSION SPECTRUM
LABEL 10 180 FILID: &A8
DO VPRNT
&L85 *
DO VCLEAR
DO SCLEAR
DO DISPLAY ON
* ============QUANTUM YIELD DETERMINATION============
&OUTPUT DATE
*                                    SAMPLE                  STANDARD
&IF V15 L87 L87 L86
&L86 *                                    ======                  ======
* SPECTRAL FILID:                  (EX- &A9  EM- &A8 )       &A10
&GOTO L88
&L87 *                                    ======                  ======
* SPECTRUM FILID:                         &A8                    &A10
&L88 *
* CONCENTRATION (NG/ML):       &V11.3          &V10.3
* ABSORBANCE VALUES:           &V7.5         &V6.5
* SOLVENT REFRACTIVE INDICES: &V14.3          &V13.3
*
* QUANTUM EFFICIENCY:          &V12.3          &V22.3
*
* ------------------------------------------------------
INST STATUS
*
* SAMPLE ANALYTICAL WAVELENGTHS: EX- &V24.0 nm  EM- &V23.0 nm
*
* SLITS:   2.5/2.5
* Td: &V4.2 ms  Tg: &V2.2 ms  Phosphorimeter Factor: &V19.3
DO PRNT
*
* For another SAMPLE determination press!RETURN!.
* To EXIT the program enter 1.
&ENTER A1
DO DISPLAY OFF
OUTPUT CLEAR V1
```

```
CALC V1= &A1
&IF V1 L45 L45 L90
&L90 *
DO DISPLAY OFF
OUTPUT CLEAR V0
SET WAIT ON
```

APPENDIX IV

Printout of the results from the OBEY program QYLDP.OY in the calculation of the Φ_f yield for anthracene using 9,10-DPA as standard. The corrected excitation and emission spectra of anthracene obtained during the run are shown overleaf.

```
=X ============QUANTUM YIELD DETERMINATION============
DATE: 82/07/14
=X                                    SAMPLE                STANDARD
=X                                    ======                ========
=X SPECTRAL FILIO:                 (EX- ANEX  EM- ANEM )      DPAEM
=X
=X CONCENTRATION (NG/ML):             7.000                 7.000
=X ABSORBANCE VALUES:                 0.00882               0.00873
=X SOLVENT REFRACTIVE INDICES:        1.427                 1.427
=X
=X
=X QUANTUM EFFICIENCY:                0.31                  1.00
=X
=X ------------------------------------------------
=INST STATUS
 F  EX250 EM400  SPEED 240  RESP 0     A/C  102.1
=X
=X SAMPLE ANALYTICAL WAVELENGTHS: EX-    250. nm  EM-    400. nm
=X
=X SLITS:                  2.5 / 2.5
```

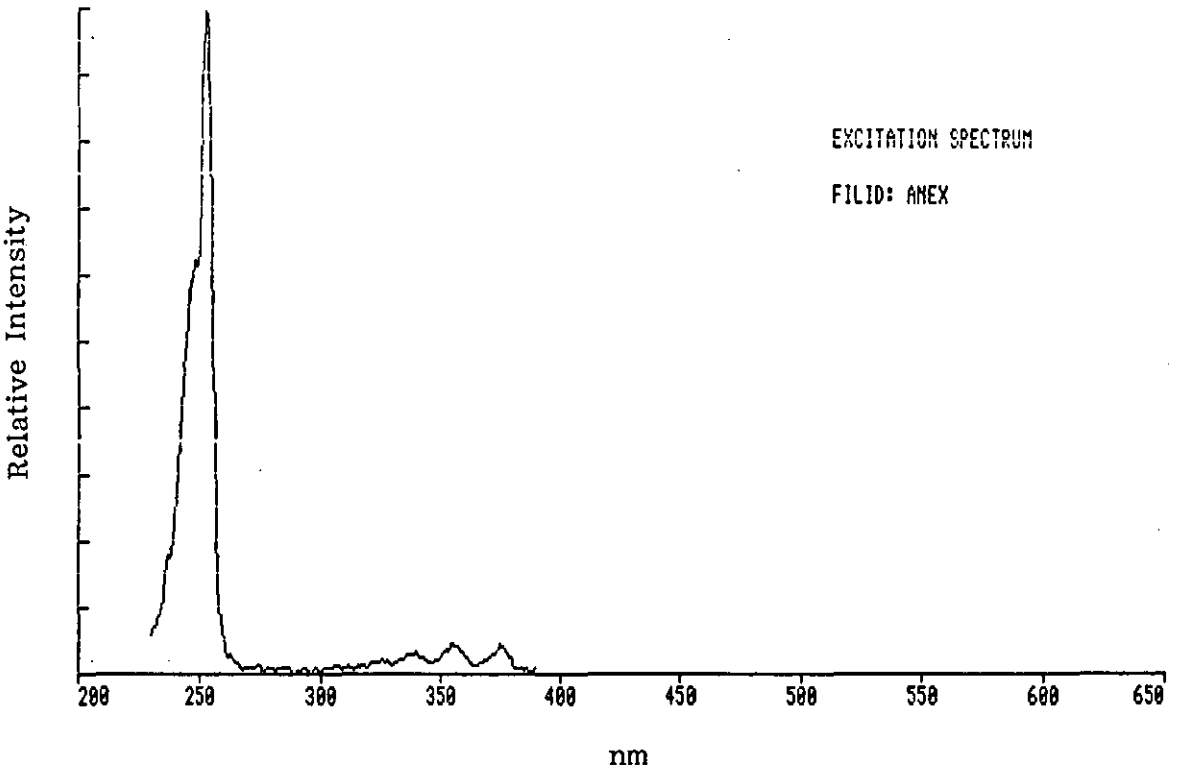
EXCITATION SPECTRUM
FILID: ANEX
Relative Intensity
200
250
300
350
400
450
500
550
600
650
nm

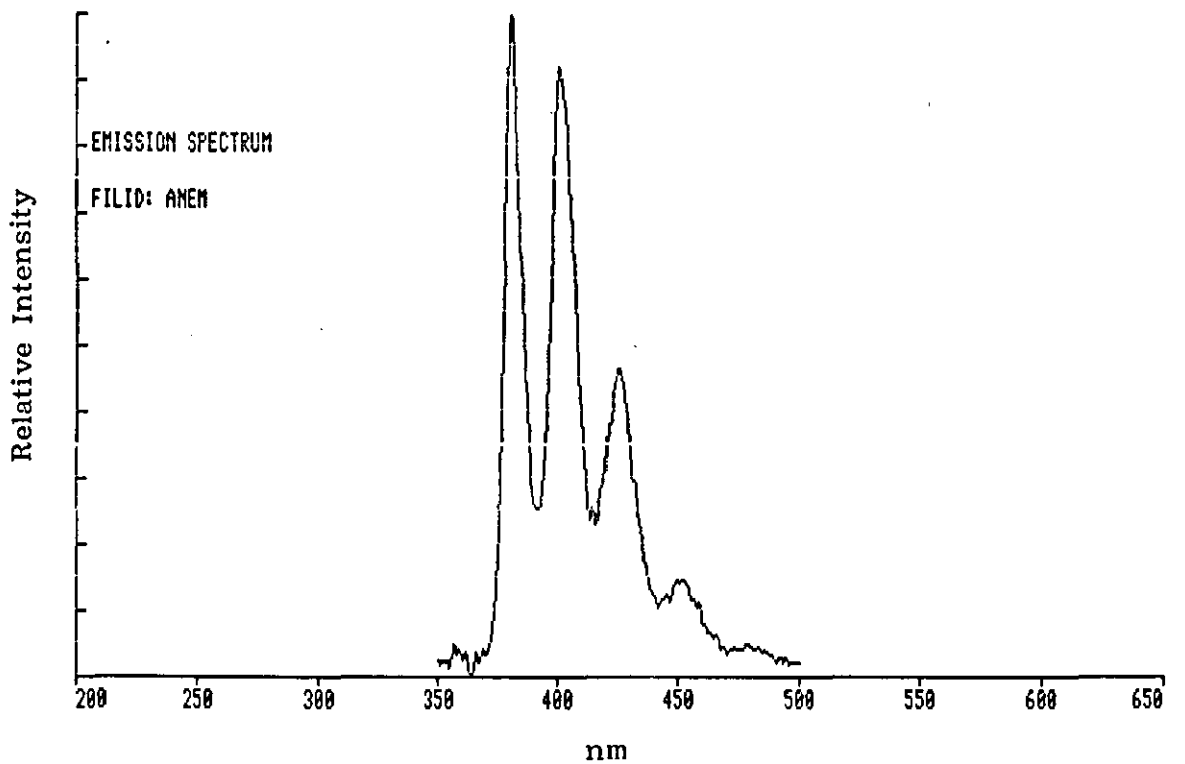
EMISSION SPECTRUM
FILID: ANEM
Relative Intensity
200
250
300
350
400
450
500
550
600
650
nm